Supplementary Information

for

Bis(trimethylsilyl)amide Complexes of the s-Block Metals with Bidentate Ether and Amine Ligands

Philipp Schüler,[a] Helmar Görls,[a] Matthias Westerhausen,*[,a] Sven Krieck*[,a]

Content

Table S1: Crystal data and refinement details for the X-ray structure determinations.

Compound	**1b**	**2a**	**2b**	**2c**
formula	$C_{11}H_{31}LiN_2OSi_2$	$C_{24}H_{68}N_6Na_2Si_4$	$C_{16}H_{44}N_3NaO_2Si_2$	$C_{14}H_{38}NNaO_4Si_2$
fw ($g \cdot mol^{-1}$)	270.50	599.18	389.71	363.62
T/°*C*	-140(2)	-140(2)	-140(2)	-140(2)
crystal system	monoclinic	monoclinic	monoclinic	triclinic
space group	P 2_1/n	P 2_1/n	C 2/c	P $\bar{1}$
a/ Å	9.2104(2)	11.1441(3)	16.133(3)	9.559(3)
b/ Å	12.9407(4)	11.4784(4)	10.266(2)	14.979(4)
c/ Å	16.0186(4)	31.0449(9)	17.076(3)	17.510(6)
α/°	90	90	90	71.634(9)
β/°	101.408(2)	99.178(1)	116.86(3)	85.046(9)
γ/°	90	90	90	78.137(9)
V/$Å^3$	1871.52(8)	3920.3(2)	2523.1(9)	2328.0(12)
Z	4	4	4	4
ρ ($g \cdot cm^{-3}$)	0.960	1.015	1.026	1.037
μ (cm^{-1})	1.79	1.95	1.7	1.84
measured data	15714	24609	8384	46642
data with I > 2σ(I)	3122	6636	2415	12399
unique data (R_{int})	3540/0.0328	8784/0.0783	2865/0.0432	18961/0.0668
wR_2 (all data, on F^2)[a)]	0.1836	0.1380	0.1455	0.1662
R_1 ($I > 2\sigma(I)$) [a)]	0.0660	0.0783	0.0558	0.0572
s [b)]	1.061	1.166	1.061	1.018
Res. dens./$e \cdot Å^{-3}$	0.938/-0.444	0.320/-0.345	0.512/-0.398	0.780/-0.583
absorpt method	multi-scan	multi-scan	multi-scan	multi-scan
absorpt corr $T_{min}/_{max}$	0.6145/0.7456	0.6701/0.7456	0.6891/0.7456	0.6529/0.7456
CCDC No.	1907118	1907119	1907120	1907121

Contd. Table S1: Crystal data and refinement details for the X-ray structure determinations.

Compound	**3b**	**3c**	**4a**	**4b**	**4c**
formula	$C_{22}H_{62}K_2N_4O_2Si_4$	$C_{20}H_{56}K_2N_2O_4Si_4$	$C_{24}H_{68}N_6Rb_2Si_4$	$C_{22}H_{62}N_4O_2Rb_2Si_4$	$C_{20}H_{56}N_2O_4Rb_2Si_4$
fw ($g \cdot mol^{-1}$)	605.32	579.23	724.14	698.06	671.97
°*C*	-140(2)	-140(2)	-140(2)	-140(2)	-140(2)
crystal system	triclinic	triclinic	monoclinic	triclinic	triclinic
space group	P $\bar{1}$	P $\bar{1}$	C 2/c	P $\bar{1}$	P $\bar{1}$
a/ Å	9.7712(3)	8.9461(3)	22.5359(18)	10.0974(3)	8.5102(3)
b/ Å	10.4930(4)	10.7526(4)	9.0412(7)	10.2990(3)	11.0496(3)
c/ Å	11.0190(4)	10.9069(4)	21.0299(16)	10.9912(4)	11.1416(3)
α/°	70.532(2)	106.864(2)	90	72.113(2)	108.386(2)
β/°	65.430(2)	102.532(1)	92.682(4)	65.759(1)	108.706(2)
γ/°	73.177(2)	109.884(2)	90	72.496(2)	101.031(1)
V/Å^3	953.62(6)	884.21(5)	4280.2(6)	971.55(5)	890.44(5)
Z	1	1	4	1	1
ρ ($g \cdot cm^{-3}$)	1.054	1.088	1.124	1.193	1.253
μ (cm^{-1})	3.96	4.27	24.18	26.63	29.06
measured data	10927	10528	11214	12096	7116
data with I > 2σ(I)	3758	3717	2557	3665	3763
unique data (R_{int})	4327/0.0320	4002/0.0219	3954/0.0616	4388/0.0275	4038/0.0196
wR_2 (all data, on F^2)[a)]	0.0901	0.0839	0.1783	0.1363	0.0588
R_1 ($I > 2\sigma(I)$) [a)]	0.0390	0.0328	0.0796	0.0529	0.0263
s [b)]	1.041	1.054	1.158	1.054	1.109
Res. dens./e·Å^{-3}	0.284/-0.279	0.644/-0.404	0.596/-0.532	0.877/-0.820	0.304/-0.442
absorpt method	multi-scan	multi-scan	multi-scan	multi-scan	multi-scan
absorpt corr $T_{min}/_{max}$	0.6829/0.7456	0.6802/0.7456	0.4438/0.7456	0.6768/0.7456	0.5858/0.7456
CCDC No.	1907122	1907123	1907124	1907125	1907126

Contd. Table S1: Crystal data and refinement details for the X-ray structure determinations.

Compound	**5b**	**5c**	**6a**	**6b**	**6c**
formula	$C_{22}H_{62}Cs_2N_4O_2Si_4$	$C_{20}H_{56}Cs_2N_2O_4Si_4$	$C_{18}H_{52}MgN_4Si_4$	$C_{17}H_{49}MgN_3OSi_4$	$C_{16}H_{46}MgN_2O_2Si_4$
fw ($g \cdot mol^{-1}$)	792.94	766.85	461.31	448.26	435.22
°*C*	-140(2)	-140(2)	-140(2)	-140(2)	-140(2)
crystal system	triclinic	triclinic	monoclinic	monoclinic	monoclinic
space group	P $\bar{1}$	P $\bar{1}$	P 2_1/n	C 2/c	P 2_1/c
a/ Å	8.6707(2)	10.9375(3)	8.6988(2)	8.8108(2)	8.3703(2)
b/ Å	11.8156(2)	11.4382(4)	17.5010(4)	16.9986(4)	34.2576(7)
c/ Å	20.4375(4)	16.0225(7)	19.7454(3)	19.5944(5)	19.6484(4)
α/°	106.144(1)	101.900(2)	90	90	90
β/°	95.431(1)	99.249(2)	102.331(1)	101.657(1)	100.452(1)
γ/°	101.977(1)	108.487(2)	90	90	90
V/Å^3	1941.43(7)	1804.14(11)	2936.65(11)	2874.15(12)	5540.6(2)
Z	2	2	4	4	8
ρ ($g \cdot cm^{-3}$)	1.356	1.412	1.043	1.036	1.043
μ (cm^{-1})	20.23	21.77	2.35	2.4	2.49
measured data	24697	16971	21032	10702	36137
data with I > 2σ(I)	7998	5970	5868	2867	10134
unique data (R_{int})	8854/0.0276	7216/0.0680	6711/0.0365	3303/0.0360	12416/0.0428
wR_2 (all data, on F^2)[a)]	0.0578	0.2247	0.0883	0.1090	0.1042
R_1 ($I > 2\sigma(I)$) [a)]	0.0264	0.0837	0.0361	0.0444	0.0474
s [b)]	1.054	1.114	1.076	1.088	1.100
Res. dens./e·Å^{-3}	0.570/-0.521	2.543/-2.462	0.318/-0.221	0.400/-0.371	0.423/-0.274
absorpt method	multi-scan	multi-scan	multi-scan	multi-scan	multi-scan
absorpt corr $T_{min}/_{max}$	0.6376/0.7456	0.4738/0.7456	0.7122/0.7456	0.6931/0.7456	0.6995/0.7456
CCDC No.	1907127	1907128	1907129	1907130	1907131

Contd. Table S1: Crystal data and refinement details for the X-ray structure determinations.

Compound	**7b**	**8a**	**8b**	**9b**
formula	$C_{17}H_{49}CaN_3OSi_4$	$C_{18}H_{52}N_4Si_4Sr$	$C_{17}H_{49}N_3OSi_4Sr$	$C_{22}H_{62}BaN_4O_2Si_4$
fw ($g \cdot mol^{-1}$)	464.03	524.62	511.57	664.46
°*C*	-140(2)	-140(2)	-140(2)	-140(2)
crystal system	monoclinic	monoclinic	monoclinic	monoclinic
space group	C 2/c	C 2/c	C 2/c	C 2/c
a/ Å	8.5730(2)	8.5757(1)	8.5565(3)	23.5555(4)
b/ Å	17.0814(6)	17.6605(2)	17.3552(5)	10.2892(2)
c/ Å	20.3873(7)	20.4099(3)	20.6264(6)	17.2253(3)
α/°	90	90	90	90
β/°	100.288(2)	101.900(1)	100.138(1)	118.317(1)
γ/°	90	90	90	90
V/Å^3	2937.49(16)	3024.67(7)	3015.19(16)	3675.27(11)
Z	4	4	4	4
ρ ($g \cdot cm^{-3}$)	1.049	1.152	1.127	1.201
μ (cm^{-1})	3.88	19.52	19.58	12.33
measured data	10364	6799	16826	14325
data with $I > 2\sigma(I)$	2910	3224	3006	4076
unique data (R_{int})	3336/0.0346	3471/0.0289	3446/0.0349	4201/0.0225
wR_2 (all data, on F^2)[a)]	0.0930	0.0549	0.0817	0.0398
R_1 ($I > 2\sigma(I)$) [a)]	0.0405	0.0233	0.0366	0.0163
s [b)]	1.076	1.050	1.105	1.060
Res. dens./$e \cdot$Å^{-3}	0.383/-0.274	0.446/-0.378	0.509/-0.440	0.316/-0.229
absorpt method	multi-scan	multi-scan	multi-scan	multi-scan
absorpt corr $T_{min}/_{max}$	0.7032/0.7456	0.6239/0.7456	0.6706/0.7456	0.6958/0.7456
CCDC No.	1907132	1907133	1907134	1907135

[a)] Definition of the *R* indices: $R_1 = (\Sigma ||F_o| - |F_c||)/\Sigma|F_o|$;
$wR_2 = \{\Sigma[w(F_o^2-F_c^2)^2]/\Sigma[w(F_o^2)^2]\}^{1/2}$ with $w^{-1} = \sigma^2(F_o^2) + (aP)^2+bP$; $P = [2F_c^2 + Max(F_O^2]/3$;
[b)] $s = \{\Sigma[w(F_o^2-F_c^2)^2]/(N_o-N_p)\}^{1/2}$.

Molecule representations

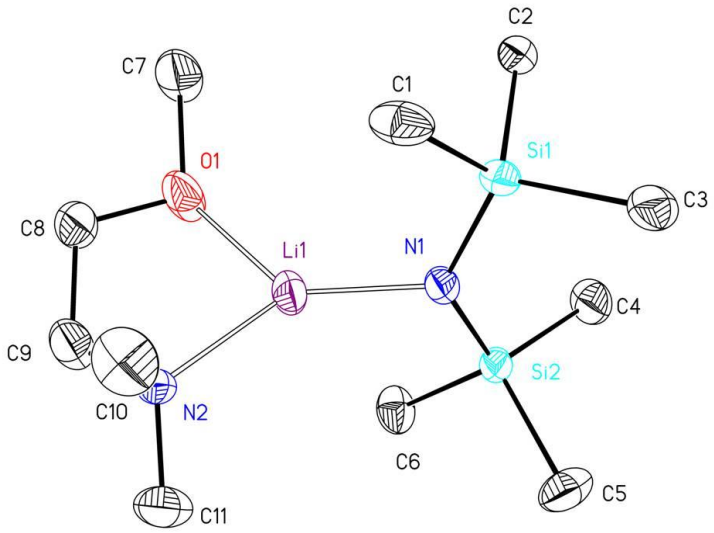

Figure S1. Molecular structure and numbering scheme of [(dmmea)LiN($SiMe_3$)$_2$]$_2$ (**1b**). The ellipsoids represent a probability of 30 %, H atoms are omitted for clarity reasons. Selected bond lengths (pm): Li1-N1 189.1(5), Li1-N2 204.4(5), Li1-O1 194.5(6), N1-Si1 167.3(2), N1-Si2 167.4(2), Li1⋯Si1 305.4(5), Li1⋯Si2 293.8(5); angles (deg.): N1-Li1-N2 139.6(3), N1-Li1-O1 134.3(3), N2-Li1-O1 85.0(2), Li1-N1-Si1 117.8(2), Li1-N1-Si2 110.9(3).

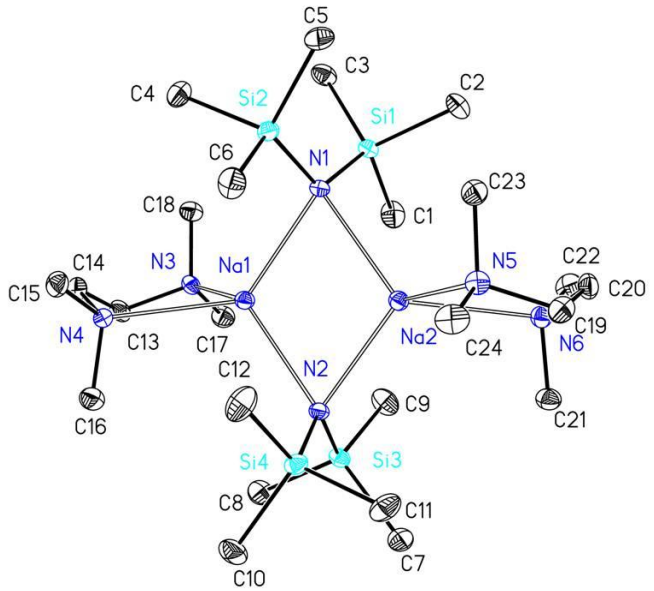

Figure S2. Molecular structure and numbering scheme of [(tmeda)NaN($SiMe_3$)$_2$]$_2$ (**2a**). The ellipsoids represent a probability of 30 %, H atoms are omitted for clarity reasons. Selected bond lengths (pm): Na1-N1 252.5(3), Na1-N2 250.4(3), Na1-N3 258.3(3), Na1-N4 260.7(3), Na2-N1 254.2(3), Na2-N2 253.0(3), Na2-N5 259.6(3), Na2-N6 260.7(3), N1-Si1 170.0(3), N1-Si2 170.0(3), N2-Si3 169.7(3), N2-Si4 169.7(3), Na1⋯Na2 308.73(17), Na1⋯Si2 346.30(15), Na1⋯Si3 349.31(15), Na2⋯Si1 341.89(15), Na2⋯Si4 341.07(15); angles (deg.): N1-Na1-N2 105.26(9), N1-Na2-N2 103.99(9), Na1-N1-Na2 75.09(8), Na1-N2-Na2 75.66(8), Si1-N1-Si2 118.7(2), Si3-N2-Si4 117.1(2), N3-Na1-N4 73.75(9), N5-Na2-N6 72.19(9).

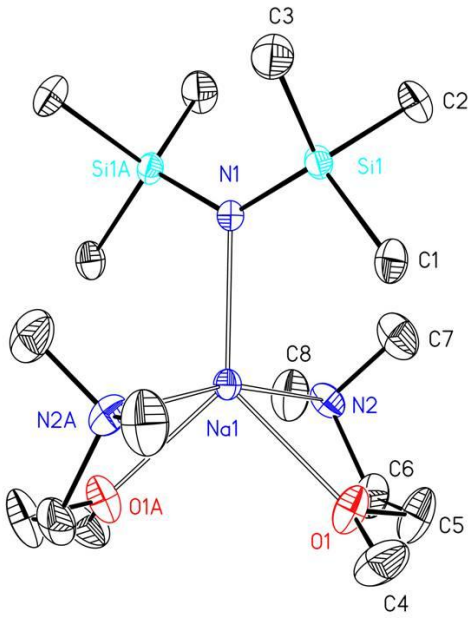

Figure S3. Molecular structure and numbering scheme of $[(dmmea)_2NaN(SiMe_3)_2]$ (**2b**). The ellipsoids represent a probability of 30 %, H atoms are omitted for clarity reasons. Symmetry-related atoms (-x+1, y, -z+1.5) are marked with the letter "A". Selected bond lengths (pm): Na1-N1 234.2(3), Na1-N2 252.6(14), Na1-O1 241.98(19), N1-Si1 166.62(12), Na1⋯Si1 339.40(13); angles (deg.): Na1-N1-Si1 114.68(8), Si1-N1-Si1A 130.63(15), N2-Na1-O1 66.7(4), N2-Na1-N2A 166.0(2).

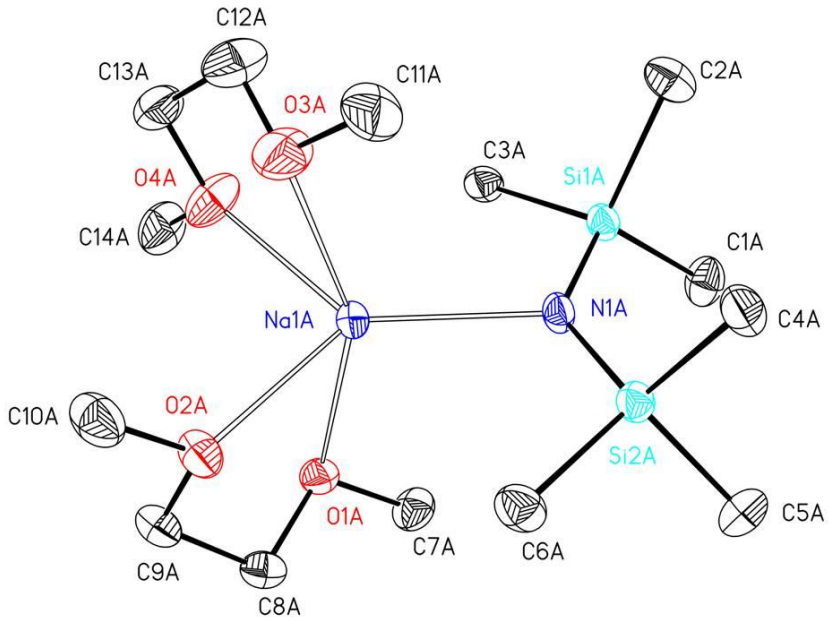

Figure S4. Molecular structure and numbering scheme of $[(dme)_2NaN(SiMe_3)_2]$ (**2c**). The ellipsoids represent a probability of 30 %, H atoms are omitted for clarity reasons. The two molecules of the asymmetric unit are distinguished by the letters "A" and "B". Selected bond lengths of molecules A [and B] (pm): Na1-N1 230.22(18) [230.91(18)], Na1-O1 235.56(18) [243.05(19)], Na1-O2 246.48(17) [237.03(19)], Na1-O3 245.41(17) [236.33(17)], Na1-O4 237.05(17) [244.59(16)], N1-Si1 166.10(17) [166.93(18)], N1-Si2 167.09(17) [166.04(17)], Na1⋯Si1 337.17(11) [337.89(14)], Na1⋯Si2 334.07(14) [331.16(11)]; angles (deg.): Na1-N1-Si1 115.63(9) [115.33(9)]; Na1-N1-Si2 113.50(9) [112.04(9)], Si1-N1-Si2 130.86(10) [132.54(10)]; O1-Na1-O2 69.78(6) [69.29(6)]; O3-Na1-O4 70.27(6) [70.76(5)].

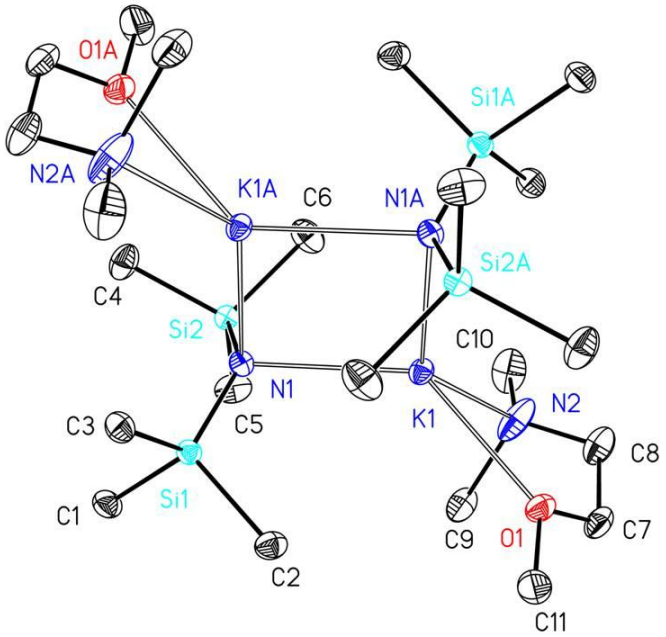

Figure S5. Molecular structure and numbering scheme of $[(dmmea)KN(SiMe_3)_2]_2$ (**3b**). The ellipsoids represent a probability of 30 %, H atoms are omitted for clarity reasons. Symmetry-related atoms (-x+1, -y+1, -z+1) are marked with the letter "A". Selected bond lengths (pm): K1-N1 278.53(15), K1-N1A 282.77(15), K1-O1 271.19(13), K1-N2 289.81(18), N1-Si1 167.57(14), N1-Si2 167.67(15), K1⋯K1A 372.56(7), K1⋯Si1 370.08(6), K1⋯Si2 373.27(6), K1⋯Si1A 365.31(6), K1⋯Si2A 373.60(6); angles (deg.): N1-K1-N1A 96.83(4), O1-K1-N2 61.15(5), K1-N1-Si1 109.59(7), K1-N1-Si2 111.11(7), Si1-N1-Si2 128.45(9).

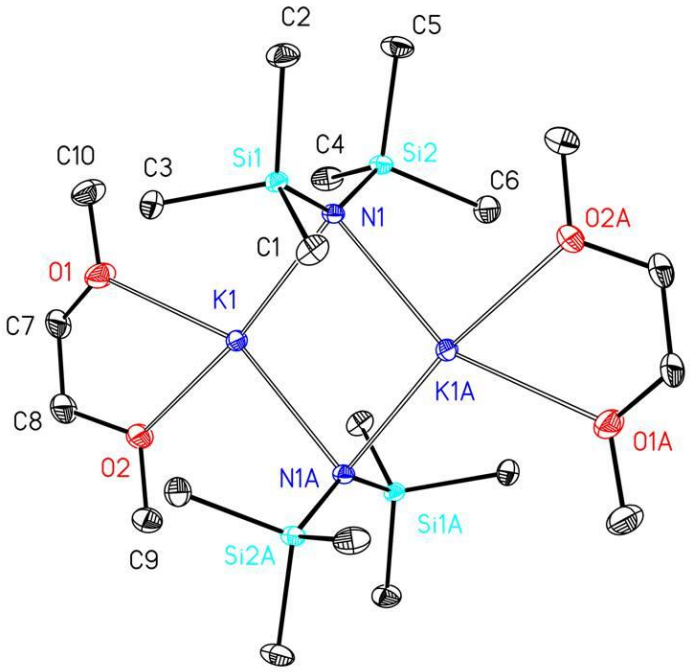

Figure S6. Molecular structure and numbering scheme of $[(dme)KN(SiMe_3)_2]_2$ (**3c**). The ellipsoids represent a probability of 30 %, H atoms are omitted for clarity reasons. Symmetry-related atoms (-x+1, -y+1, -z+1) are marked with the letter "A". Selected bond lengths (pm): K1-N1 281.87(12), K1-N1A 281.07(12), K1-O1 275.53(13), K1-O2 278.07(13), N1-Si1 167.18(12), N1-Si2 166.97(12), K1⋯K1A 384.78(6), K1⋯Si1 363.81(5), K1⋯Si2 365.79(5), K1⋯Si1A 363.54(5), K1⋯Si2A 365.57(5); angles (deg.): N1-K1-N1A 93.76(3), K1-N1-Si1 105.36(5), K1-N1-Si2 106.33(5), Si1-N1-Si2 135.75(8), O1-K1-O2 60.62(4).

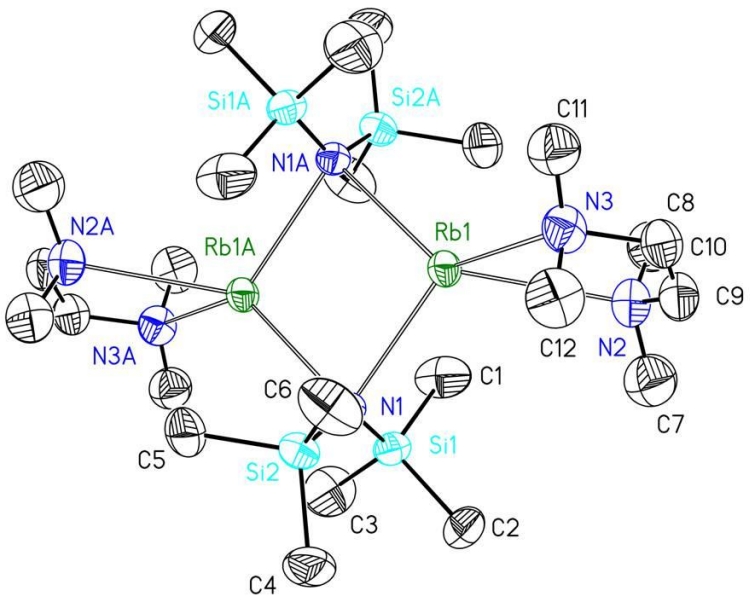

Figure S7. Molecular structure and numbering scheme of $[(tmeda)RbN(SiMe_3)_2]_2$ (**4a**). The ellipsoids represent a probability of 30 %, H atoms are omitted for clarity reasons. Symmetry-related atoms (-x+0.5, -y+1.5, -z+1) are marked with the letter "A". Selected bond lengths (pm): Rb1-N1 293.1(6), Rb1-N1A 303.1(6), Rb1-N2 316.1(7), Rb1-N3 308.1(7), N1-Si1 166.4(7), N1-Si2 166.7(6), Rb1⋯Rb1A 406.06(13), Rb⋯Si1 376.7(2), Rb⋯Si2 389.8(2), Rb1⋯Si1A 378.5(2), Rb1⋯Si2A 388.3(2); angles (deg.): N1-Rb1-N1A 94.16(15), Rb1-N1-Si1 106.9(3), Rb1-N1-Si2 113.1(3), Si1-N1-Si2 130.0(4), N2-Rb1-N3 58.8(2).

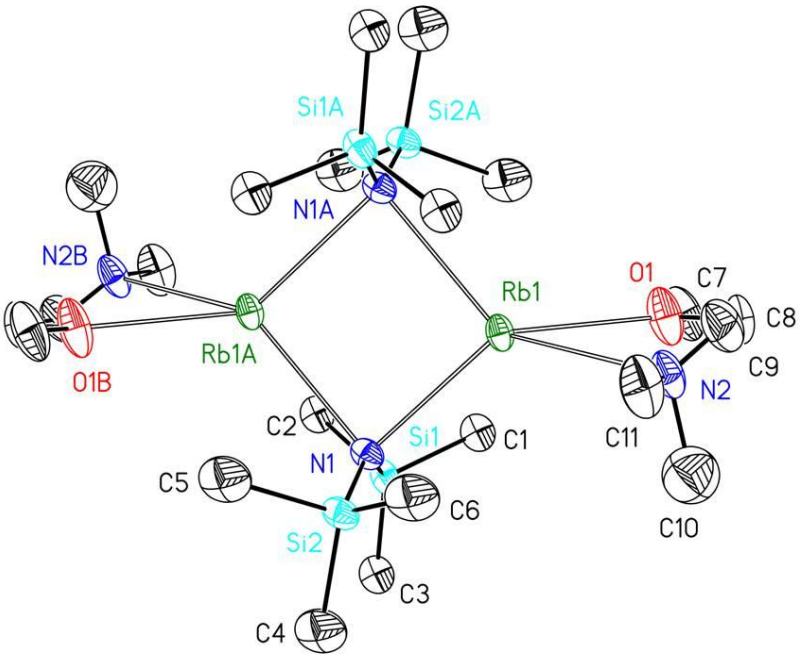

Figure S8. Molecular structure and numbering scheme of $[(dmmea)RbN(SiMe_3)_2]_2$ (**4b**). The ellipsoids represent a probability of 30 %, H atoms are omitted for clarity reasons. The second half of the molecule is generated by (-x+1, -y+1, -z+1). Selected bond lengths (pm): Rb1-N1 294.5(3), Rb1-N1A 296.7(4), N1-Si1 166.6(3), Rb1-O1 281.9(6), Rb1-N2 299.6(10); angles (deg.): N1-Rb1-N1A 92.96(9), Rb1-N1-Si1 107.34(15), Rb1-N1-Si2 105.14(15), Si1-N1-Si2 132.8(2), O1-Rb1-N2 59.6(2).

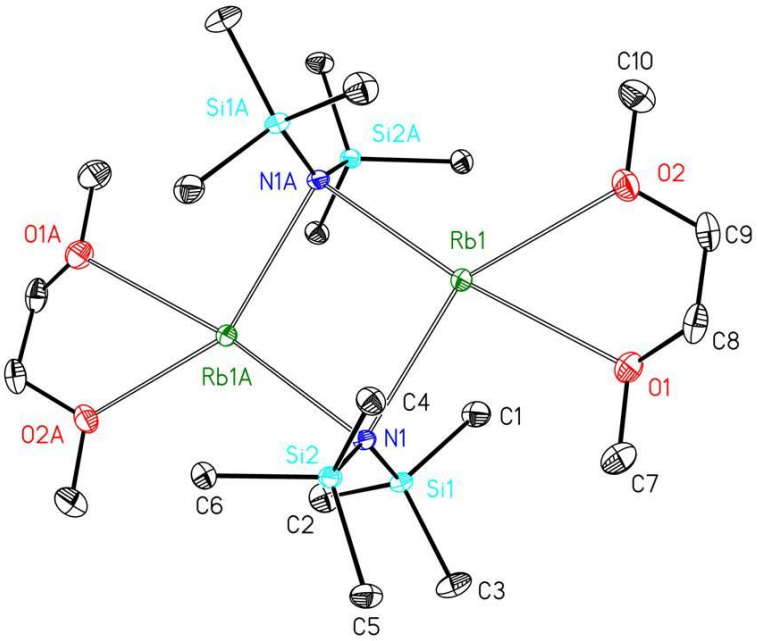

Figure S9. Molecular structure and numbering scheme of $[(dme)RbN(SiMe_3)_2]_2$ (**4c**). The ellipsoids represent a probability of 30 %, H atoms are omitted for clarity reasons. Symmetry-related atoms (-x+1, -y+1, -z+1) are marked with the letter "A". Selected bond lengths (pm): Rb1-N1 297.09(15), Rb1-N1A 299.52(15), Rb1-O1 292.91(15), Rb1-O2 296.27(15), N1-Si1 166.98(16), N1-Si2 166.67(16), Rb1⋯Rb1A 415.04(4), Rb1⋯Si1 385.19(5), Rb1⋯Si2 377.87(5), Rb1⋯Si1A 376.22(5), Rb1⋯Si2A 376.74(5); angles (deg.): N1-Rb1-N1A 91.84(4), Rb1-N1-Si1 46.84(5), Rb1-N1-Si2 47.753(11), Si1-N1-Si2 135.62(9), O1-Rb1-O2 56.19(5).

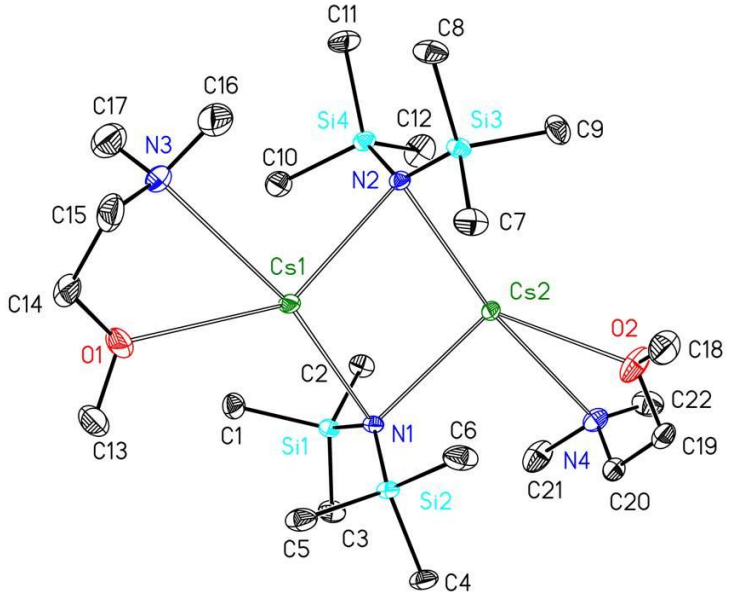

Figure S10. Molecular structure and numbering scheme of $[(dmmea)CsN(SiMe_3)_2]_2$ (**5b**). The ellipsoids represent a probability of 30 %, H atoms are omitted for clarity reasons. Selected bond lengths (pm): Cs1-N1 326.56(19), Cs1-N2 306.98(19), Cs1-O1 311.5(2), Cs1-N3 323.9(2), Cs2-N1 307.74(18), Cs2-N2 324.48(19), Cs2-O2 307.0(2), Cs2-N4 320.2(2), N1-Si1 167.0(2), N1-Si2 166.9(2), N2-Si3 166.6(2), N2-Si4 166.5(2), Cs1⋯Cs2 430.58(2), Cs1⋯Si1 411.76(7), Cs1⋯Si2 382.11(7), Cs1⋯Si3 404.33(7), Cs1⋯Si4 392.34(7), Cs2⋯Si1 397.01(7), Cs2⋯Si2 407.28(7), Cs2⋯Si3 394.28(7), Cs2⋯Si4 396.99(7); angles (deg.): N1-Cs1-N2 93.36(5), N1-Cs2-N2 93.63(5), Cs1-N1-Cs2 85.45(4), Cs1-N2-Cs2 85.93(5), O1-Cs1-N3 53.72(6), O2-Cs2-N4 55.10(6), Si1-N1-Si2 129.97(12), Si3-N2-Si4 131.88(12).

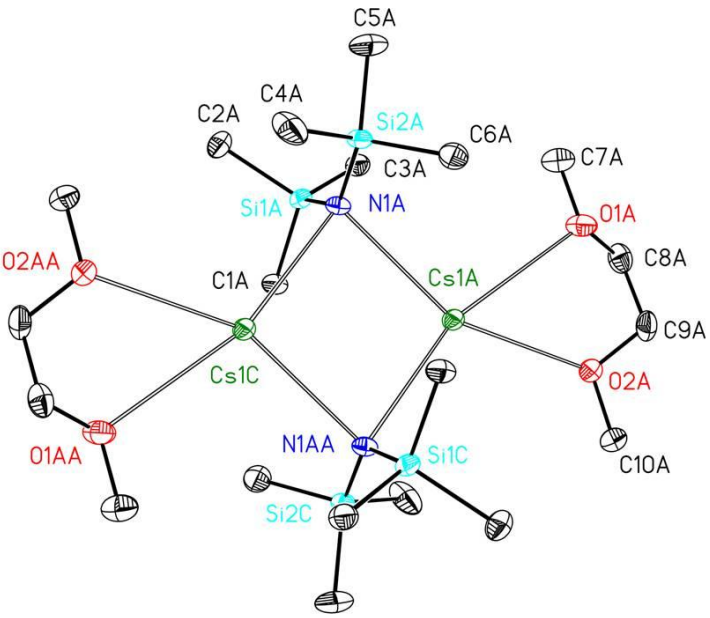

Figure S11. Molecular structure and numbering scheme of $[(dme)CsN(SiMe_3)_2]_2$ (**5c**). The ellipsoids represent a probability of 30 %, H atoms are omitted for clarity reasons. The asymmetric unit contains two half molecules A and B which are completed by inversion centers generating the second halves C and D. Selected bond lengths for A [B] (pm): Cs1-N1 306.3(7) [308.1(7)], Cs1-N1' 316.2(7) [317.1(7)], Cs1-O1 318.0(7) [321.0(6)], Cs1-O2 308.9(6) [305.7(6)], N1-Si1 166.0(7) [167.0(7)], N1-Si2 167.7(6) [166.1(6)], Cs1⋯Cs1' 421.47(9) [434.43(8)], Cs1⋯Si1 390.7(2) [396.5(2)], Cs1⋯Si2 401.4(2) [401.8(2)]; angles (deg.): N1-Cs1-N1' 94.78(17) [91.97(18)], O1-Cs1-O2 53.73(19) [53.26(16)], Si1-N1-Si2 129.3(4) [129.7(4)].

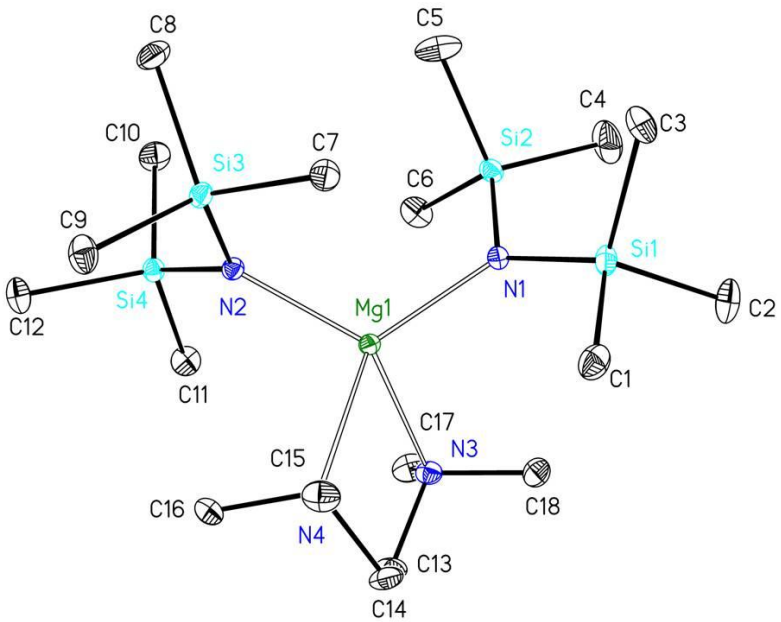

Figure S12. Molecular structure and numbering scheme of $[(tmeda)Mg\{N(SiMe_3)_2\}_2]$ (**6a**). The ellipsoids represent a probability of 30 %, H atoms are omitted for clarity reasons. Selected bond lengths (pm): Mg1-N1 204.47(12), Mg1-N2 205.48(12), Mg1-N3 236.85(13), Mg1-N4 229.66(13), N1-Si1 170.85(13), N1-Si2 171.08(13), N2-Si3 171.67(12), N2-Si4 170.85(12), Mg1⋯Si2 315.37(6), Mg1⋯Si3 320.06(6); angles (deg.): N1-Mg1-N2 117.07(5), N3-Mg1-N4 77.50(5), Mg1-N1-Si1 126.53(7), Mg1-N1-Si2 113.93(6), Si1-N1-Si2 119.18(7), Mg1-N2-Si3 115.83(6), Mg1-N2-Si4 125.08(6), Si3-N2-Si4 119.09(7).

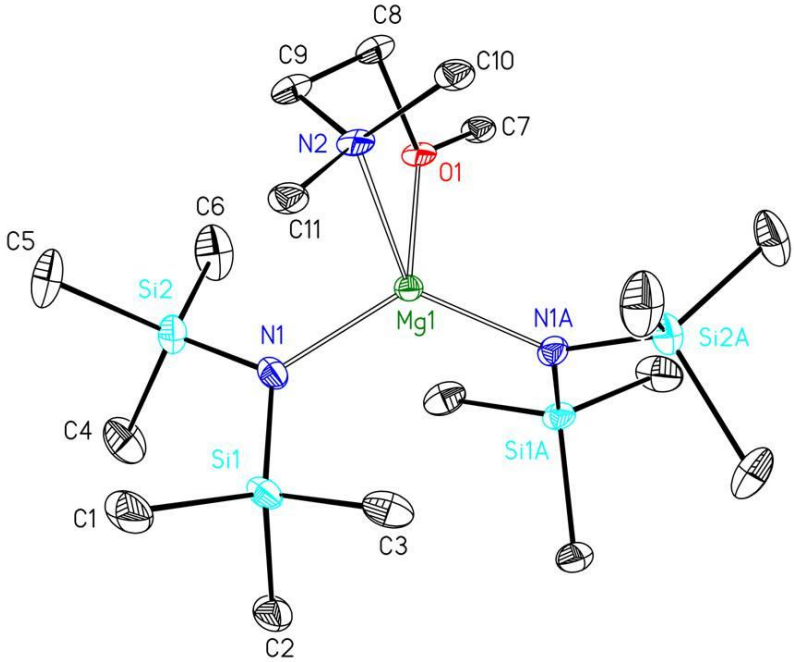

Figure S13. Molecular structure and numbering scheme of [(dmmea)Mg{N(SiMe$_3$)$_2$}$_2$] (**6b**). The ellipsoids represent a probability of 30 %, H atoms are omitted for clarity reasons. Symmetry-related atoms (-x+1, y, -z+3/2) are marked with the letter "A". The disordering of the dmmea ligand is not shown. Selected bond lengths (pm): Mg1-N1 201.58(14), Mg1-O1 208(2), Mg1-N2 239.2(18), N1-Si1 171.36(16), N1-Si2 170.76(16); angles (deg.): N1-Mg1-N1A 123.67(9), O1-Mg1-N2 77.2(4), Mg1-N1-Si1 115.59(8), Mg1-N1-Si2 123.37(8), Si1-N1-Si2 121.01(9).

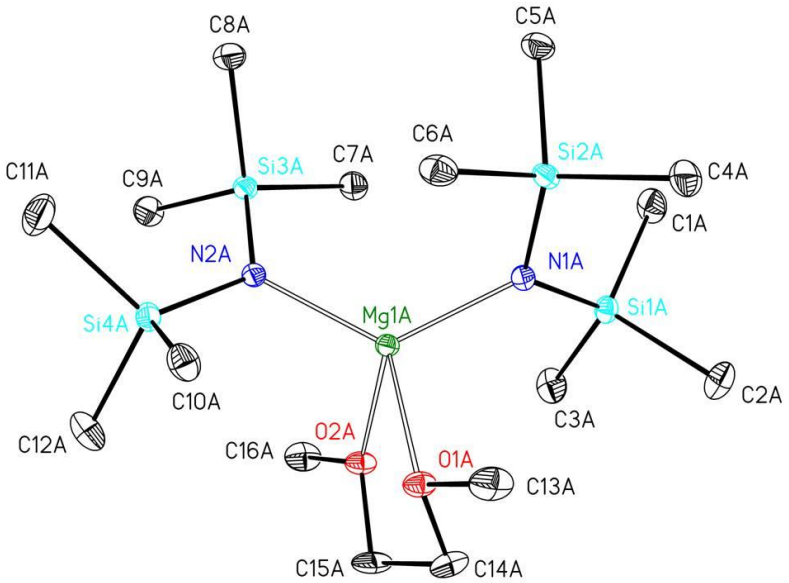

Figure S14. Molecular structure and numbering scheme of [(dme)Mg{N(SiMe$_3$)$_2$}$_2$] (**6c**). The ellipsoids represent a probability of 30 %, H atoms are omitted for clarity reasons. The asymmetric unit contains two molecules A and B. Selected bond lengths of A [B] (pm): Mg1-N1 200.53(17) [200.77(16)], Mg1-N2 200.40(16) [200.28(17)], Mg1-O1 216.52(15) [213.52(16)], Mg1-O2 209.27(15) [211.10(15)], N1-Si1 171.23(16) [171.24(17)], N1-Si2 171.52(17) [171.16(18)], N2-Si3 170.89(17) [170.97(17)], N2-Si4 171.18(16) [170.96(16)], Mg1⋯Si1 325.41(8) [324.05(8)], Mg1⋯Si2 316.04(8) [317.79(8)], Mg1⋯Si3 318.73(8) [316.47(8)], Mg1⋯Si4 320.09(8) [322.09(8)]; angles (deg.): N1-Mg1-N2 125.92(7) [124.59(7)], O1-Mg1-O2 75.15(6) [75.24(6)], Mg1-N1-Si1 121.97(9) [120.96(9)], Mg1-N1-Si2 116.08(8) [117.17(9)], Si1-N1-Si2 121.88(9) [121.77(9)], Mg1-N2-Si3 118.07(9) [116.73(8)], Mg1-N2-Si4 118.74(9) [120.15(9)], Si3-N2-Si4 123.02(9) [123.09(10)].

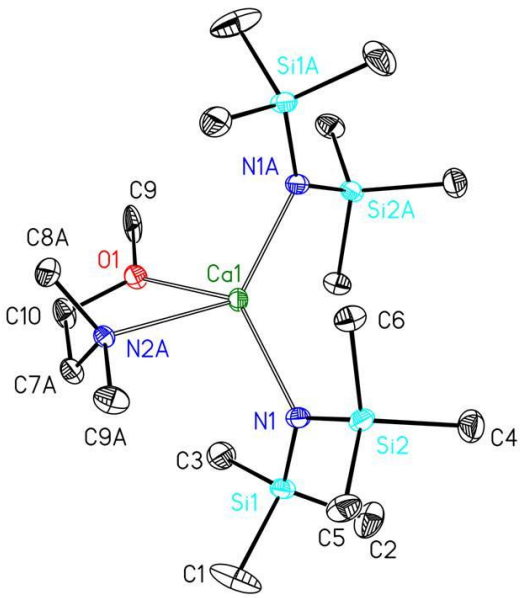

Figure S15. Molecular structure and numbering scheme of [(dmmea)Ca{N(SiMe$_3$)$_2$}$_2$] (**7b**). The ellipsoids represent a probability of 30 %, H atoms are omitted for clarity reasons. Symmetry-related atoms (-x+1, y, -z+1/2) are marked with the letter "A". The dmmea ligand shows a two-site disordering. Selected bond lengths (pm): Ca-N1 229.13(15), Ca1-O1 228.2(7), Ca1-N2A 263.4(8), N1-Si1 169.11(15), N1-Si2 169.40(16), Ca1⋯Si1 349.82(5), Ca1⋯Si2 330.66(6); angles (deg.): N1-Ca1-N1A 126.51(8), O1-Ca1-N2A 68.60(9), Ca1-N1-Si1 122.18(8), Ca1-N1-Si2 111.25(7), Si1-N1-Si2 126.56(9).

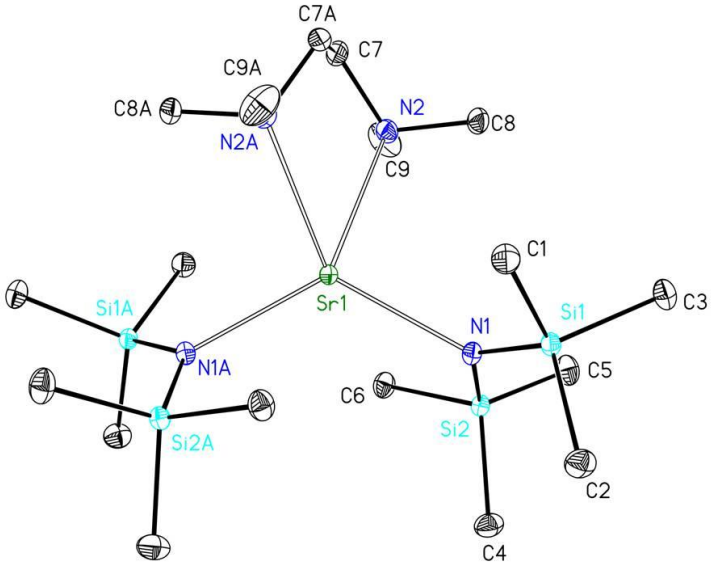

Figure S16. Molecular structure and numbering scheme of [(tmeda)Sr{N(SiMe$_3$)$_2$}$_2$] (**8a**). The ellipsoids represent a probability of 30 %, H atoms are omitted for clarity reasons. Symmetry-related atoms (-x+1, y, -z+0.5) are marked with the letter "A". Selected bond lengths (pm): Sr1-N1 245.61(12), Sr1-N2 272.64(13), N1-Si1 168.65(13), N1-Si2 168.35(13)Sr1⋯Si1 359.11(4), Sr1⋯Si2 345.54(4); angles (deg.): N1-Sr1-N1A 122.47(6), N2-Sr1-N2A 67.54(6), Sr1-N1-Si1 119.02(6), Sr1-N1-Si2 111.82(6), Si1-N1-Si2 129.14(8).

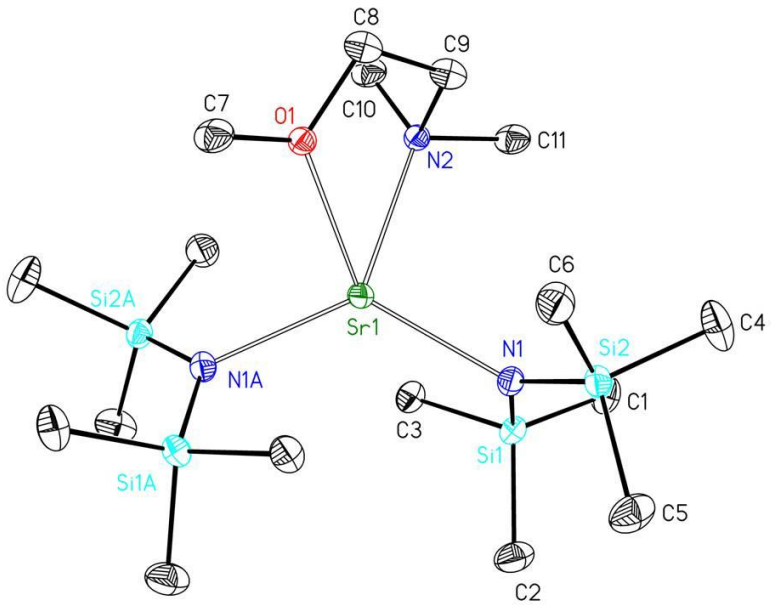

Figure S17. Molecular structure and numbering scheme of [(dmmea)Sr{N(SiMe$_3$)$_2$}$_2$] (**8b**). The ellipsoids represent a probability of 30 %, H atoms are omitted for clarity reasons. Symmetry-related atoms (-x+1, y, -z+0.5) are marked with the letter "A". The disordering of the dmmea ligand is omitted. Selected bond lengths (pm): Sr1-N1 244.44(19), Sr1-O1 253.1(11), Sr1-N2 263.7(13), N1-Si1 168.6(2), N1-Si2 168.4(2); angles (deg.): N1-Sr1-N1A 125.72(9), O1-Sr1-N2 64.3(4), Sr1-N1-Si1 111.43(9), Sr1-N1-Si2 119.39(10), Si1-N1-Si2 129.18(12).

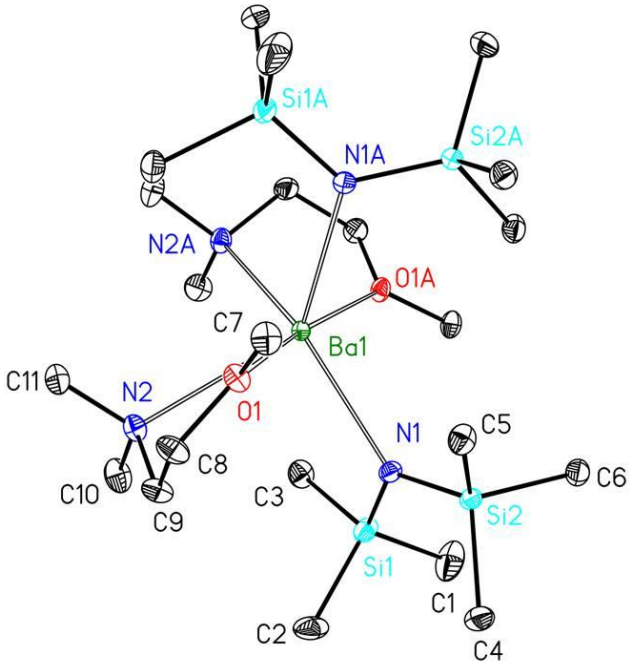

Figure S18. Molecular structure and numbering scheme of [(dmmea)Ba{N(SiMe$_3$)$_2$}$_2$] (**9b**). The ellipsoids represent a probability of 30 %, H atoms are omitted for clarity reasons. Symmetry-related atoms (-x+1, y, -z+0.5) are marked with the letter "A". Selected bond lengths (pm): Ba1-N1 271.12(11), Ba1-O1 278.44(9), Ba1-N2 306.04(11), N1-Si1 169.16(11), N1-Si2 169.34(11), Ba1⋯Si2 381.70(4); angles (deg.): N1-Ba1-N1A 128.97(5), O1-Ba1-N2 58.07(3), Ba1-N1-Si1 119.76(5), Ba1-N1-Si2 118.28(5), Si1-N1-Si2 121.91(7).

NMR and IR spectra

[(dmmea)Li(hmds)] **1b**

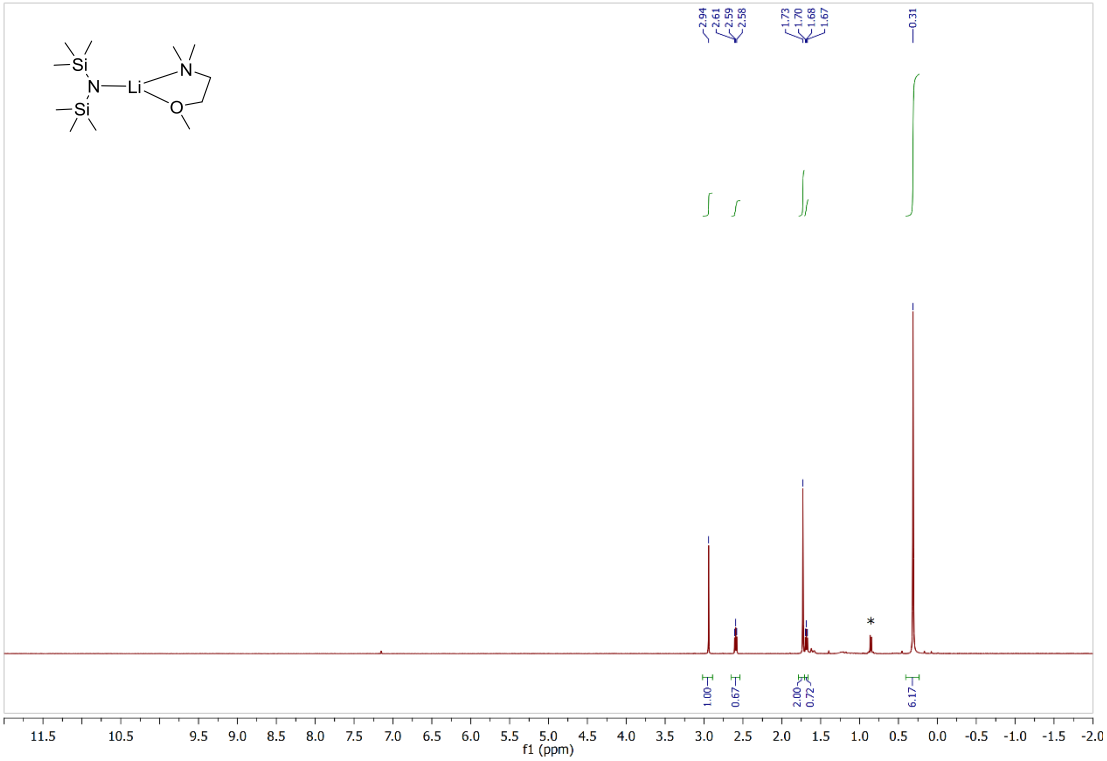

Figure S19: ^{1}H NMR spectrum (400 MHz, C_6D_6, 296 K) of [(dmmea)Li(hmds)] **1b** (* - n-pentane, n-hexane).

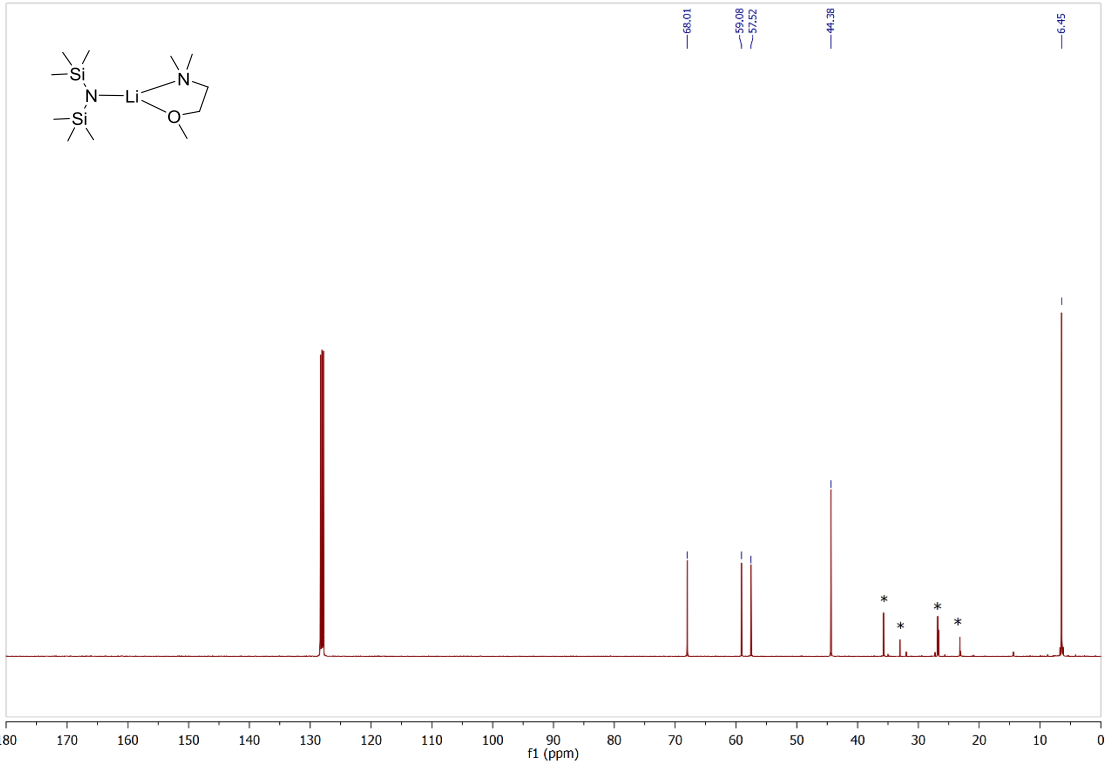

Figure S20: ^{13}C{^{1}H} NMR spectrum (101 MHz, C_6D_6, 296 K) of [(dmmea)Li(hmds)] **1b** (* - n-pentane, n-hexane).

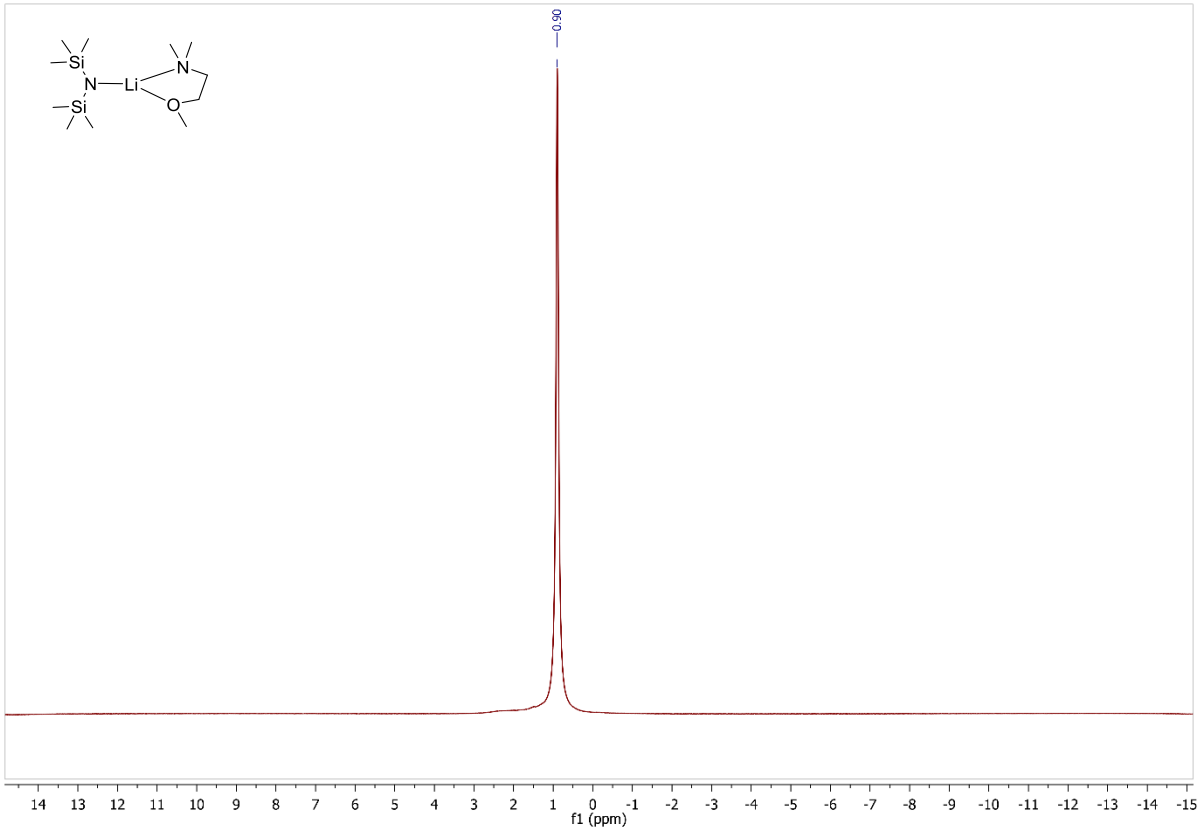

Figure S21: ^{7}Li NMR spectrum (155.5 MHz, C_6D_6, 296 K) of [(dmmea)Li(hmds)] **1b**.

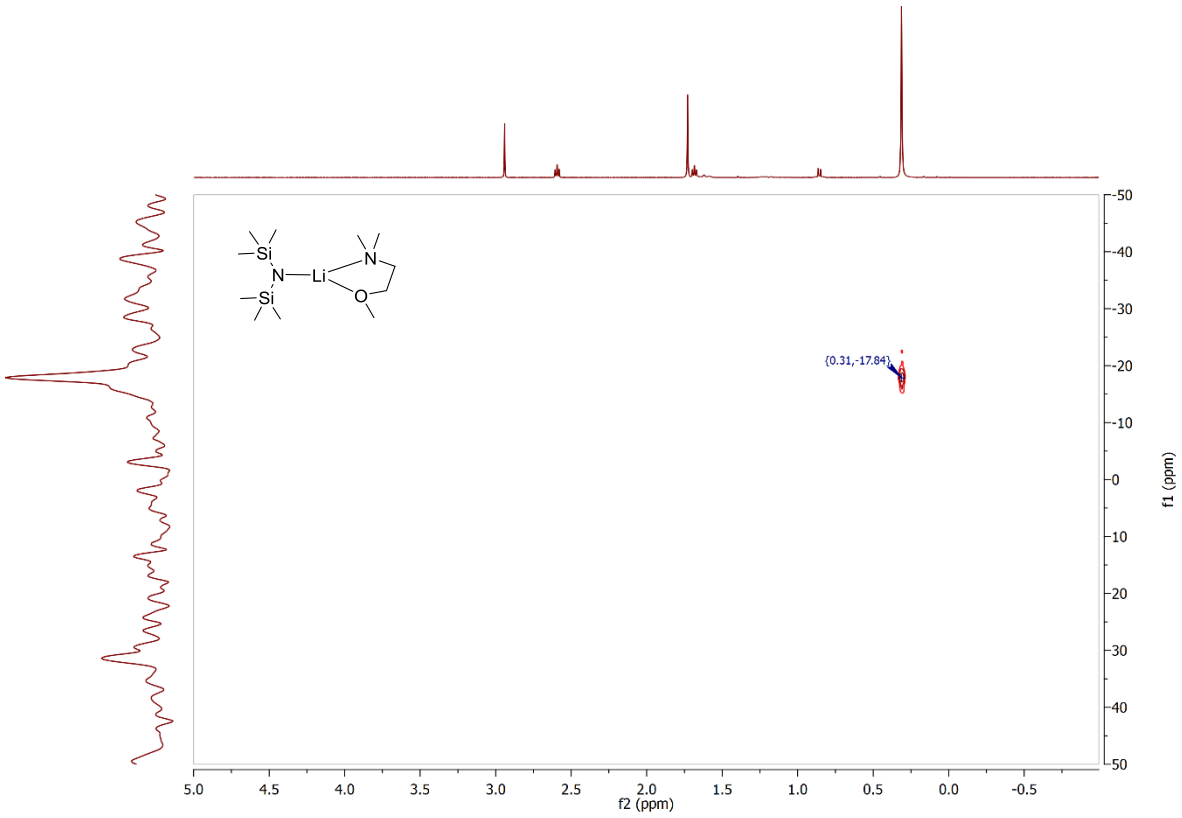

Figure S22: ^{29}Si-^{1}H-HMBC NMR spectrum (79.5 MHz, C_6D_6, 296 K) of [(dmmea)Li(hmds)] **1b**.

[(tmeda)Na(hmds)] **2a**

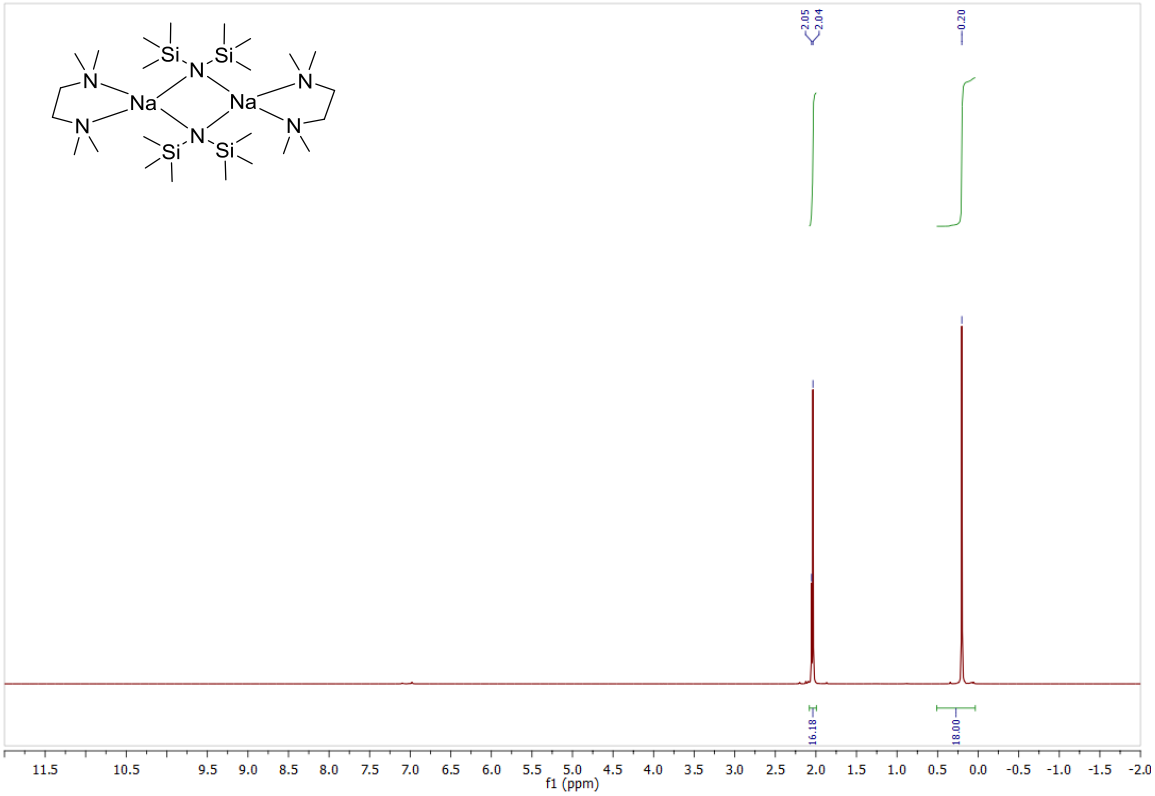

Figure S23: ^{1}H NMR spectrom (400 MHz, Tol-d$_8$, 296 K) of [(tmeda)Na(hmds)]$_2$ **2a$_2$**.

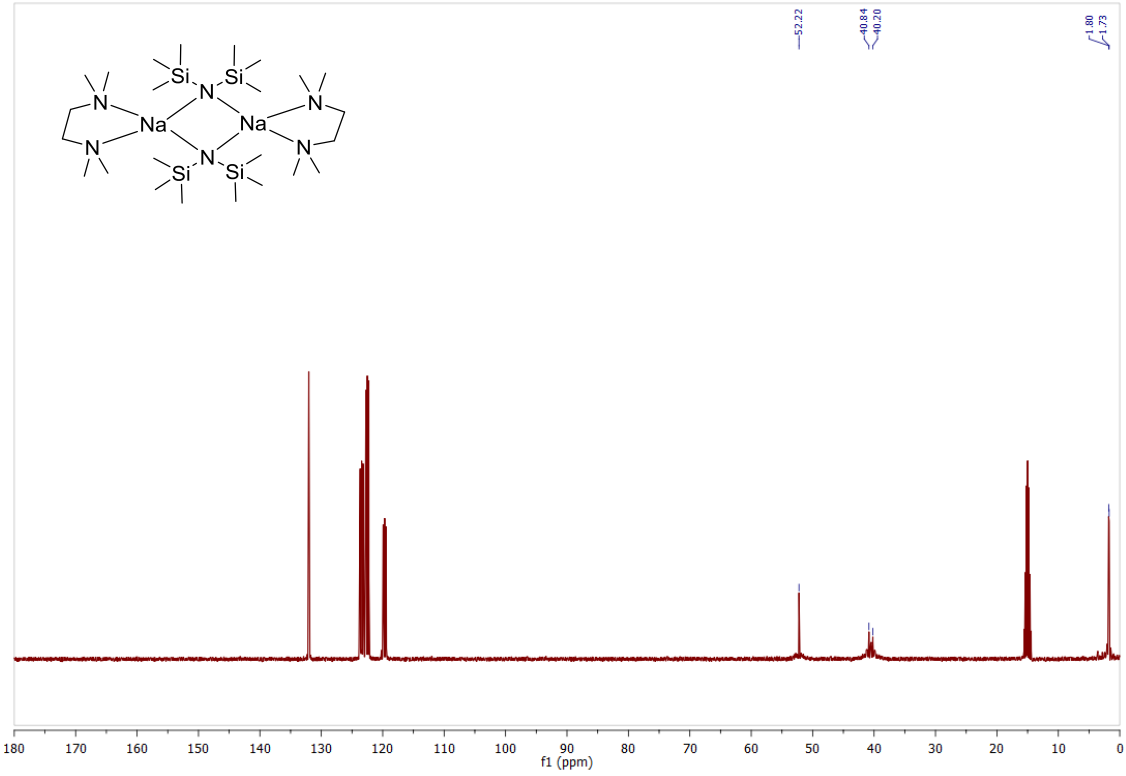

Figure S24: ^{13}C{^{1}H} NMR spectrum (101 MHz, Tol-d$_8$, 296 K) of [(tmeda)Na(hmds)]$_2$ **2a$_2$**.

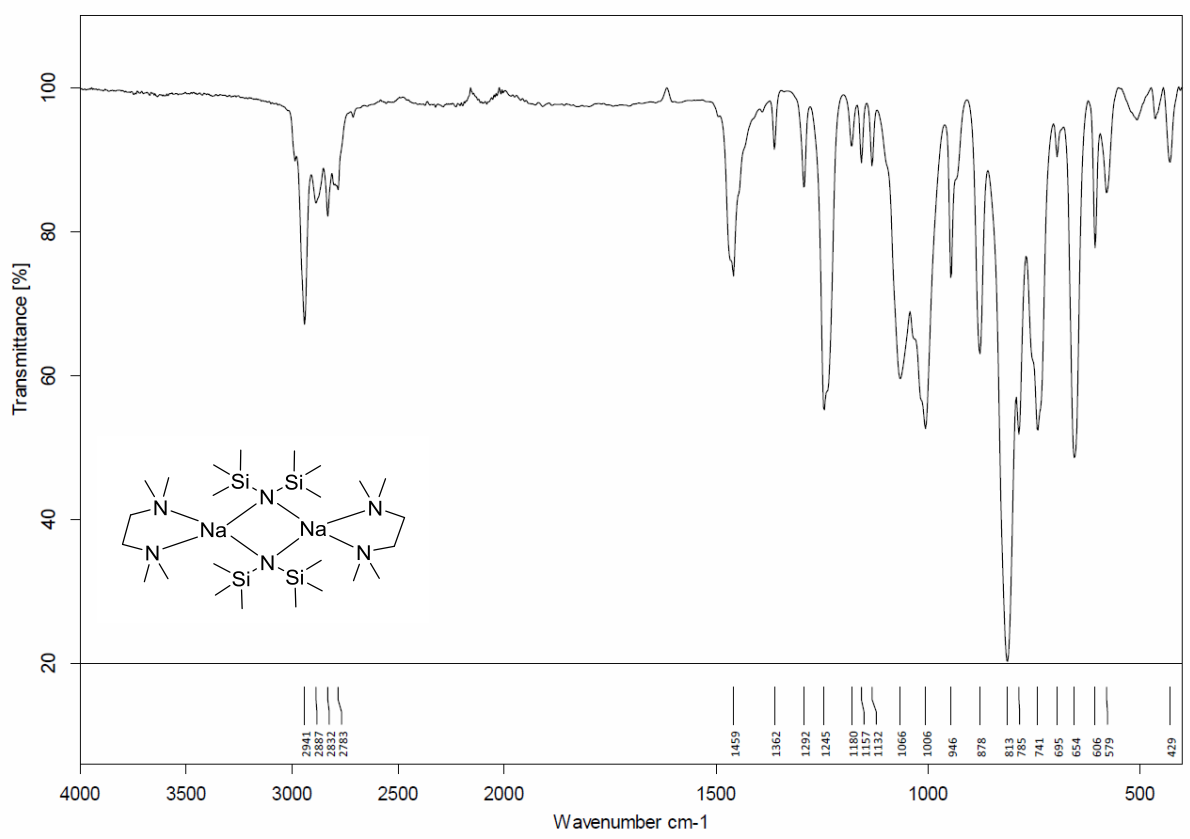

Figure S25: IR spectrum (neat, ATR) of crystalline [(tmeda)Na(hmds)]$_2$ **2a$_2$**.

[(dmmea)$_2$Na(hmds)] **2b**

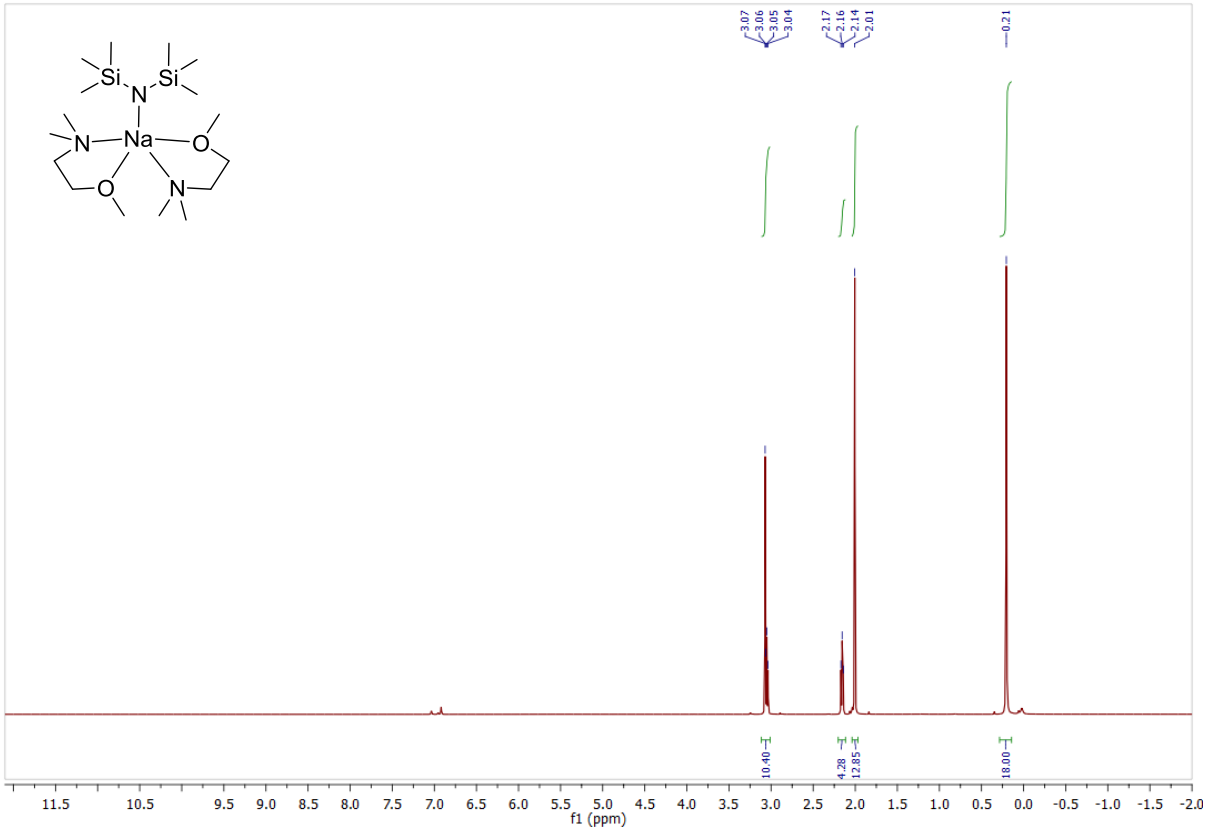

Figure S26: ^{1}H NMR spectrum (400 MHz, Tol-d$_8$, 296 K) of [(dmmea)$_2$Na(hmds)] **2b**.

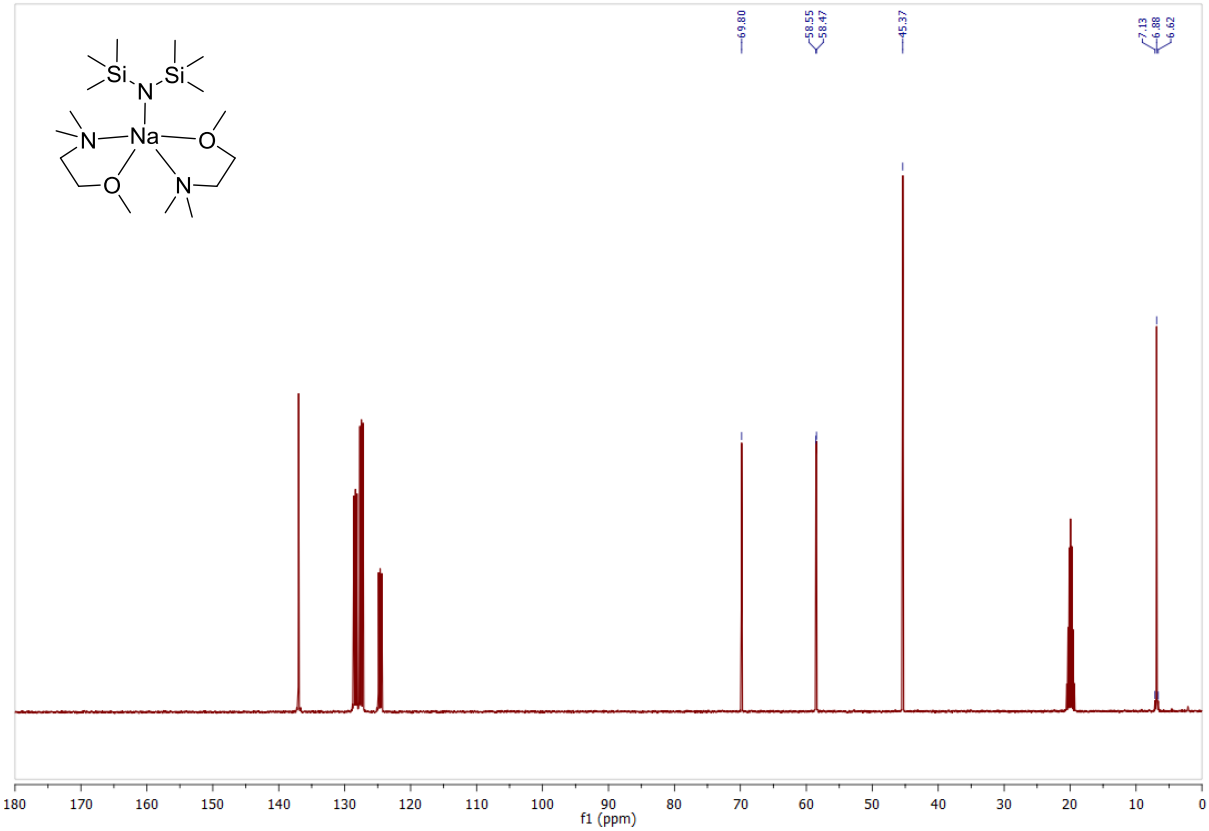

Figure S27: ^{13}C{^{1}H} NMR spectrum (100 MHz, Tol-d$_8$, 296 K) of [(dmmea)$_2$Na(hmds)] **2b**.

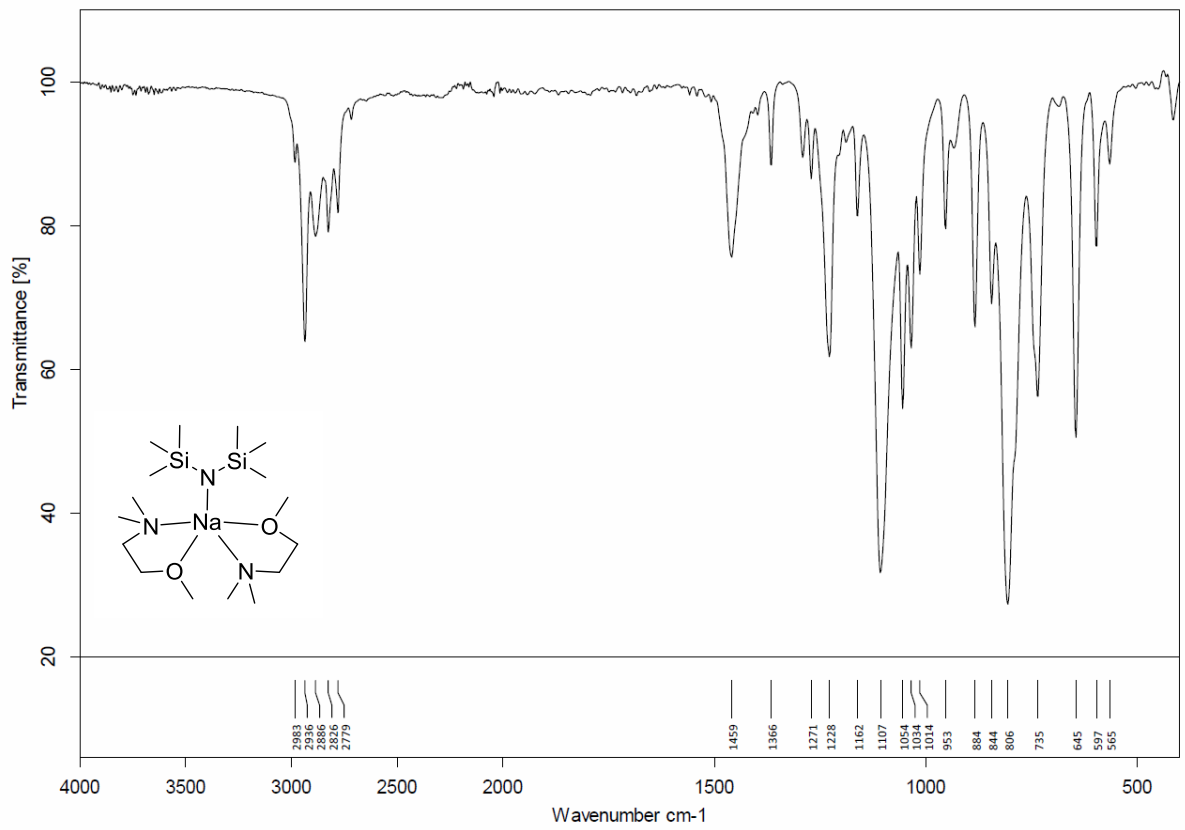

Figure S28: IR spectrum (neat, ATR) of isolated crystals of [(dmmea)$_2$Na(hmds)] **2b**.

[(dme)$_2$Na(hmds)] **2c**

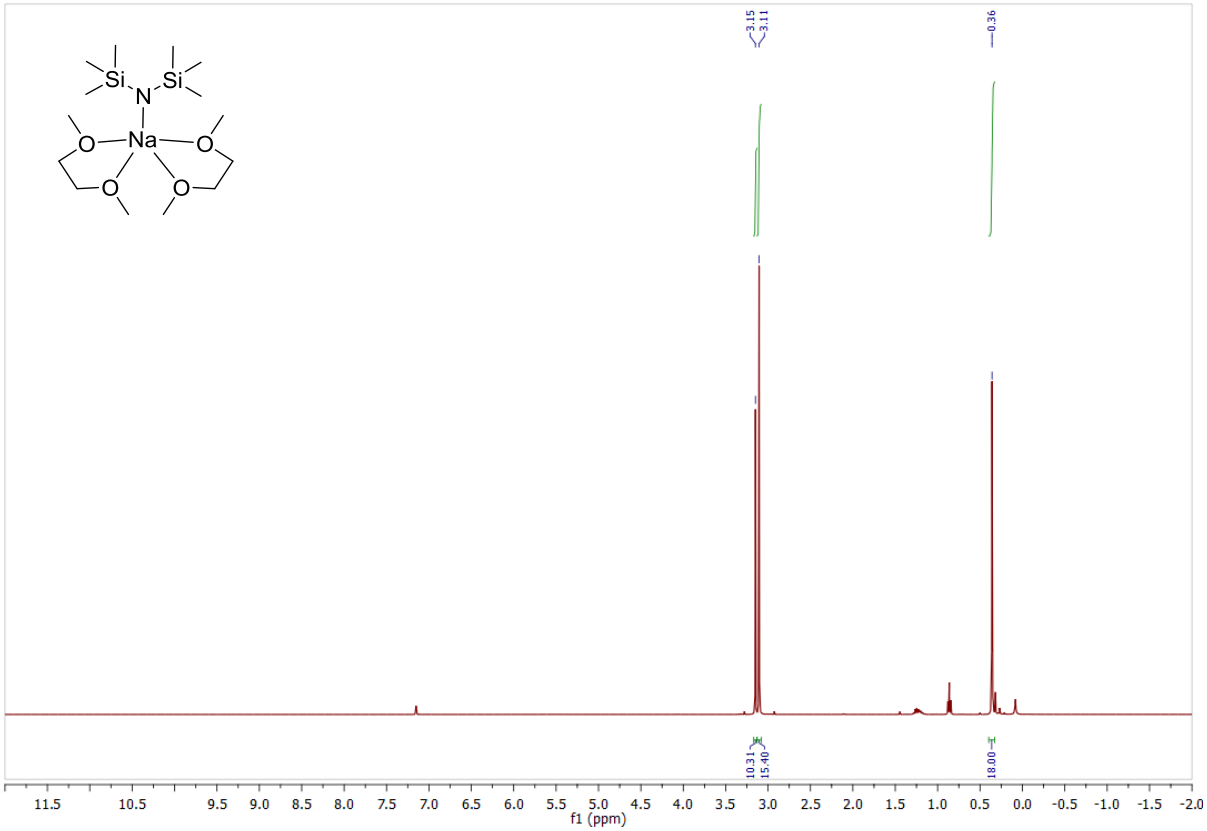

Figure S29: ^{1}H NMR spectrum (400 MHz, C_6D_6, 296 K) of [(dme)$_2$Na(hmds)] **2c**.

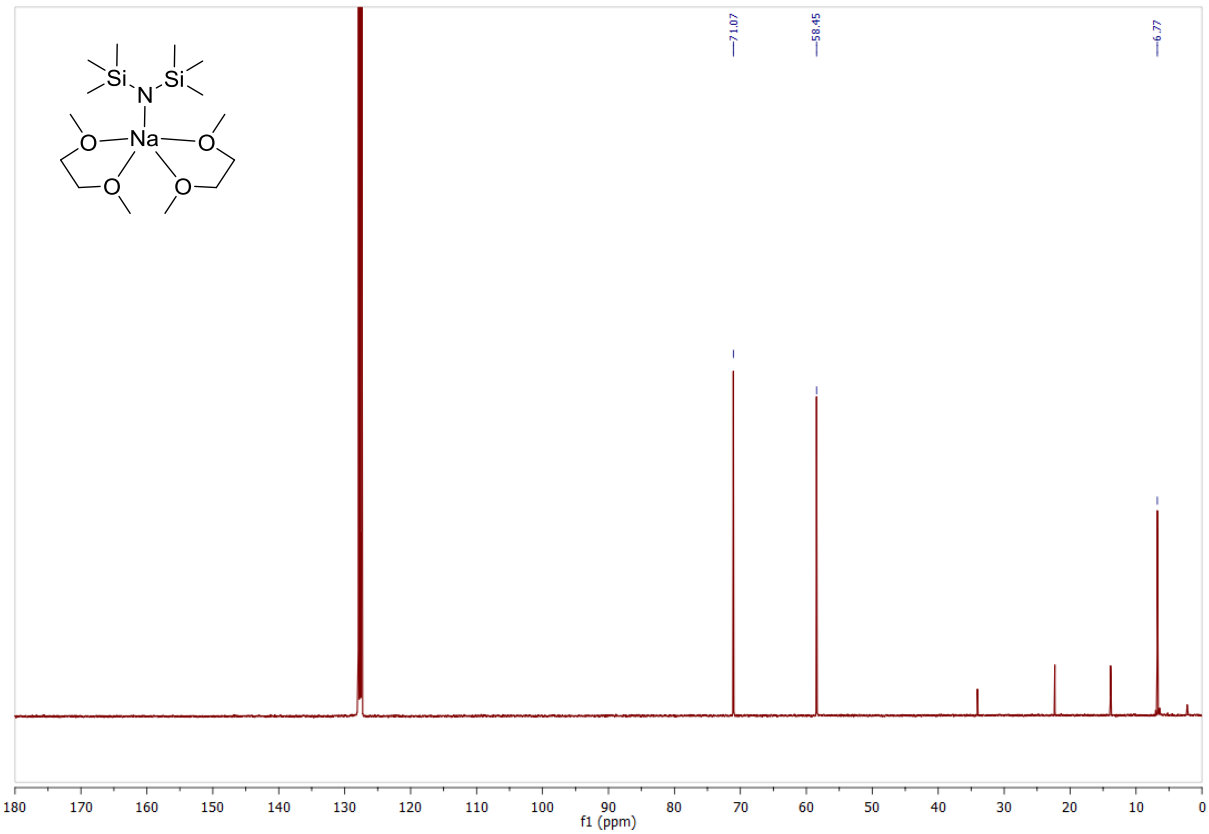

Figure S30: ^{13}C{^{1}H} NMR spectrum (101 MHz, C_6D_6, 296 K) of [(dme)$_2$Na(hmds)] **2c**.

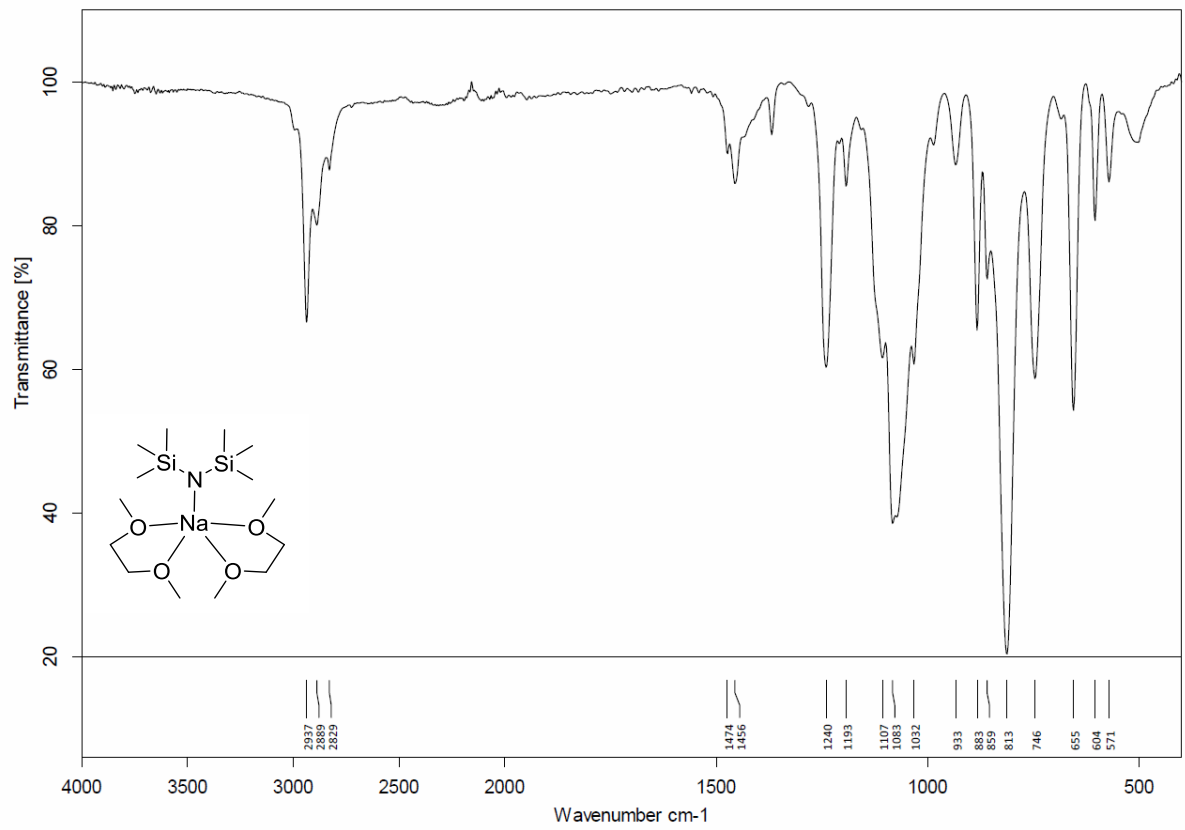

Figure S31: IR spectrum (ATR) of crystalline [(dme)$_2$Na(hmds)] **2c**.

[(dme)K(hmds)]$_2$ **3c**

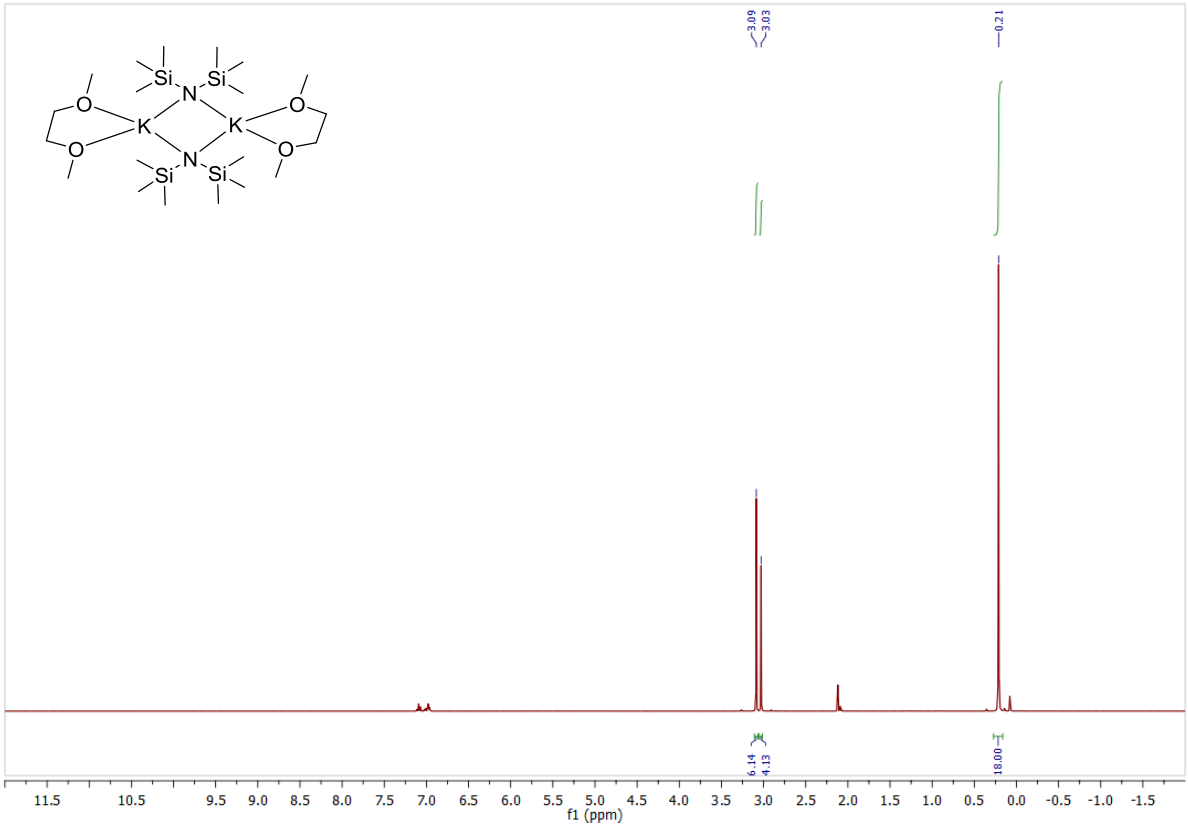

Figure S32: ^{1}H NMR spectrum (400 MHz, Tol-d$_8$, 296 K) of [(dme)K(hmds)]$_2$ **3c**.

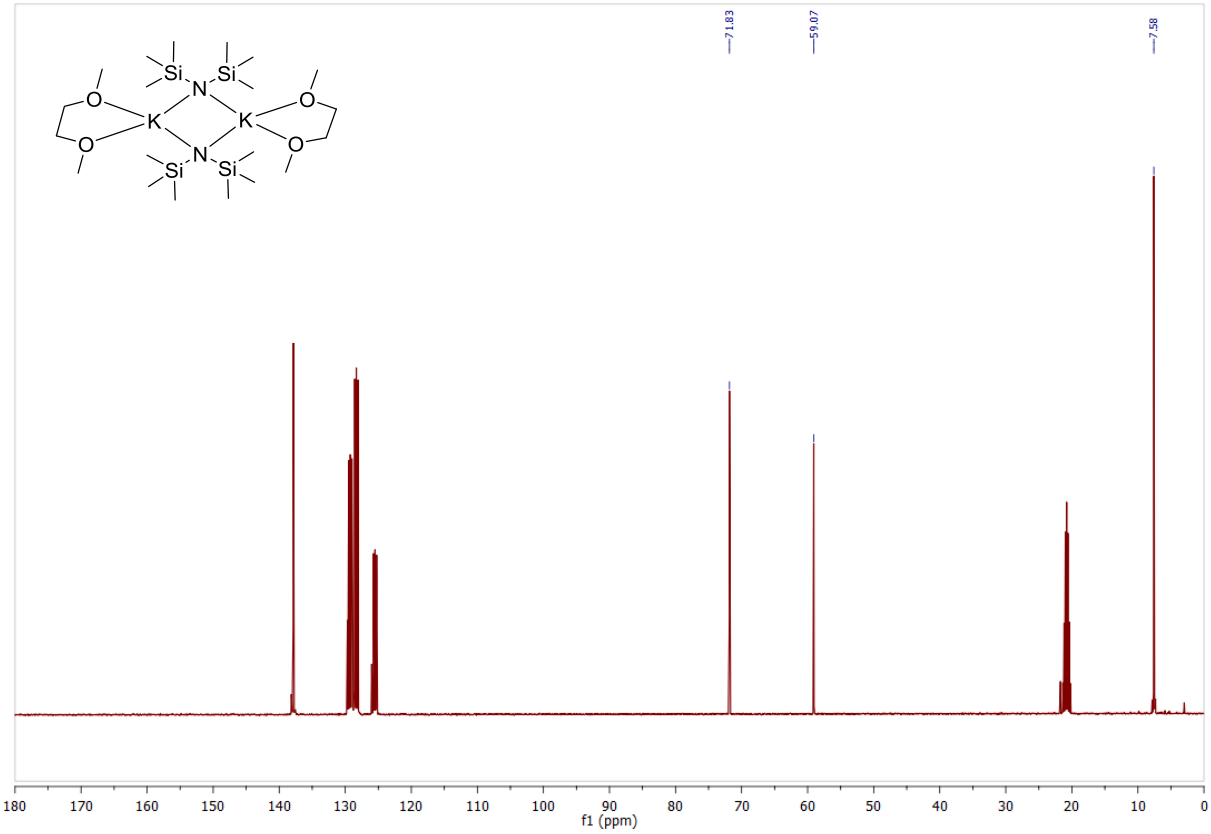

Figure S33: ^{13}C{^{1}H} NMR spectrum (101 MHz, Tol-d$_8$, 296 K) of [(dme)K(hmds)]$_2$ **3c**.

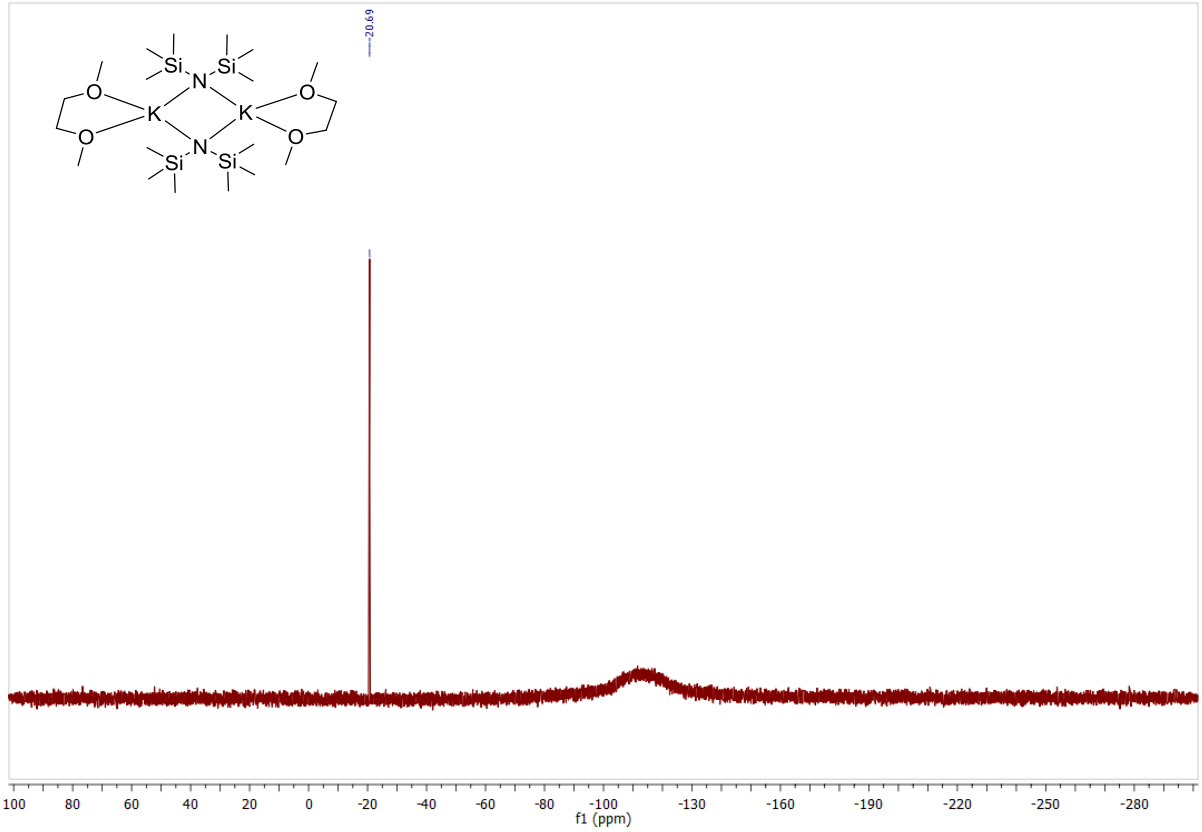

Figure S34: $^{29}Si\{^{1}H\}$ NMR spectrum (79 MHz, Tol-d_8, 296 K) of $[(dme)K(hmds)]_2$ **3c**.

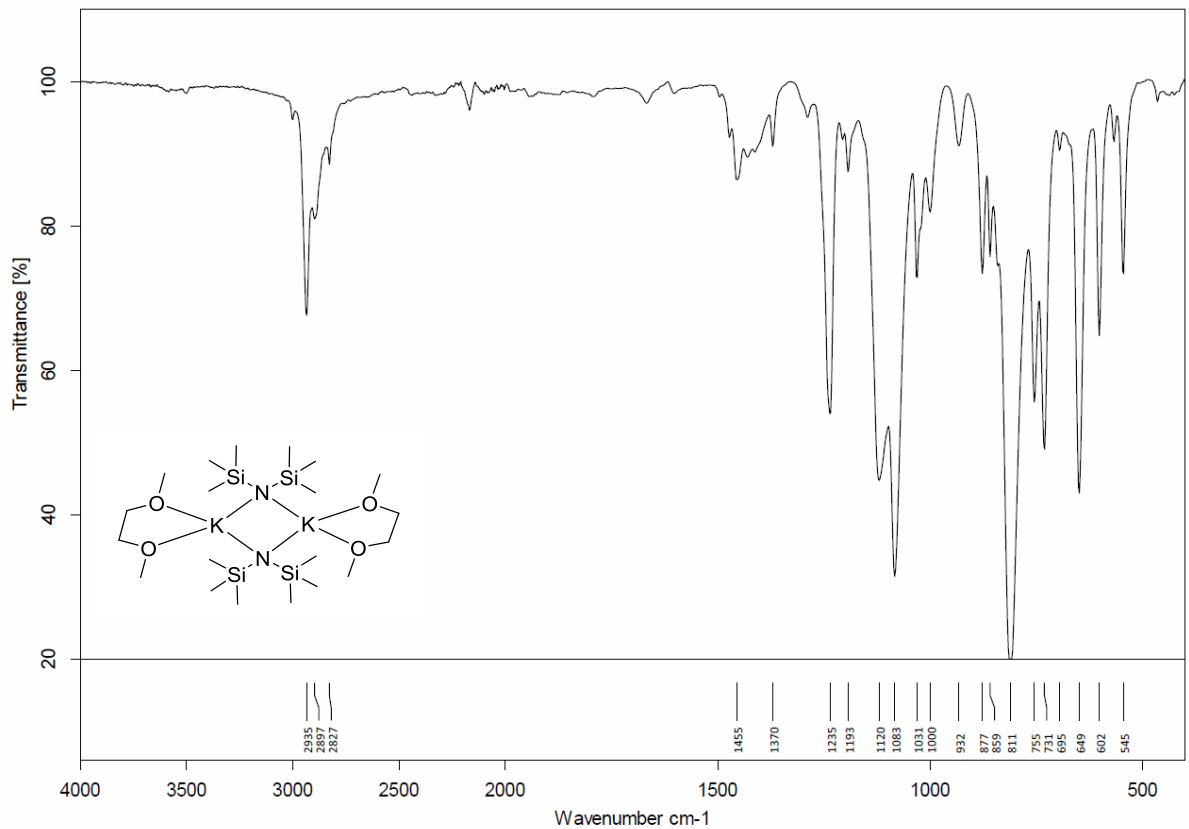

Figure S35: IR spectrum (ATR) of isolated crystals of $[(dme)K(hmds)]_2$ **3c**.

[(dmmea)K(hmds)]$_2$ **3b**

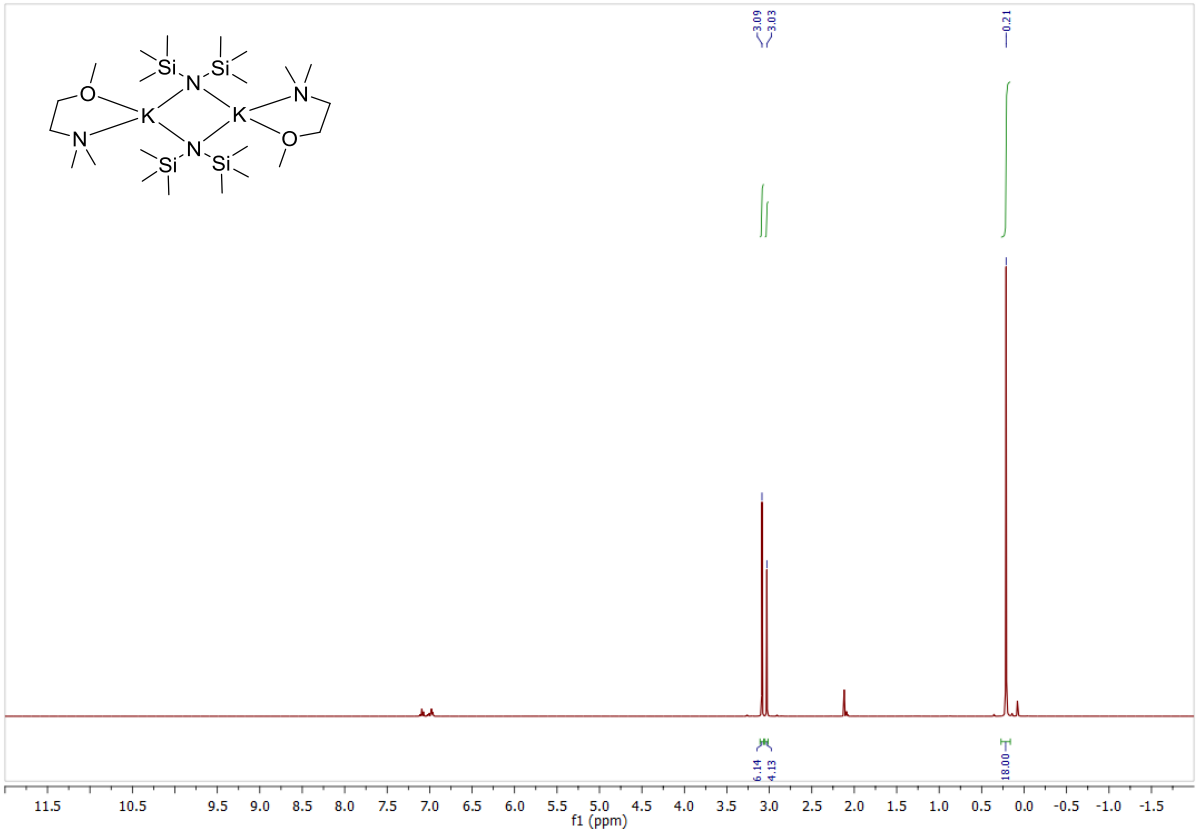

Figure S36: ^{1}H NMR spectrum (400 MHz, Tol-d$_8$, 296 K) of [(dmmea)K(hmds)]$_2$ **3b**.

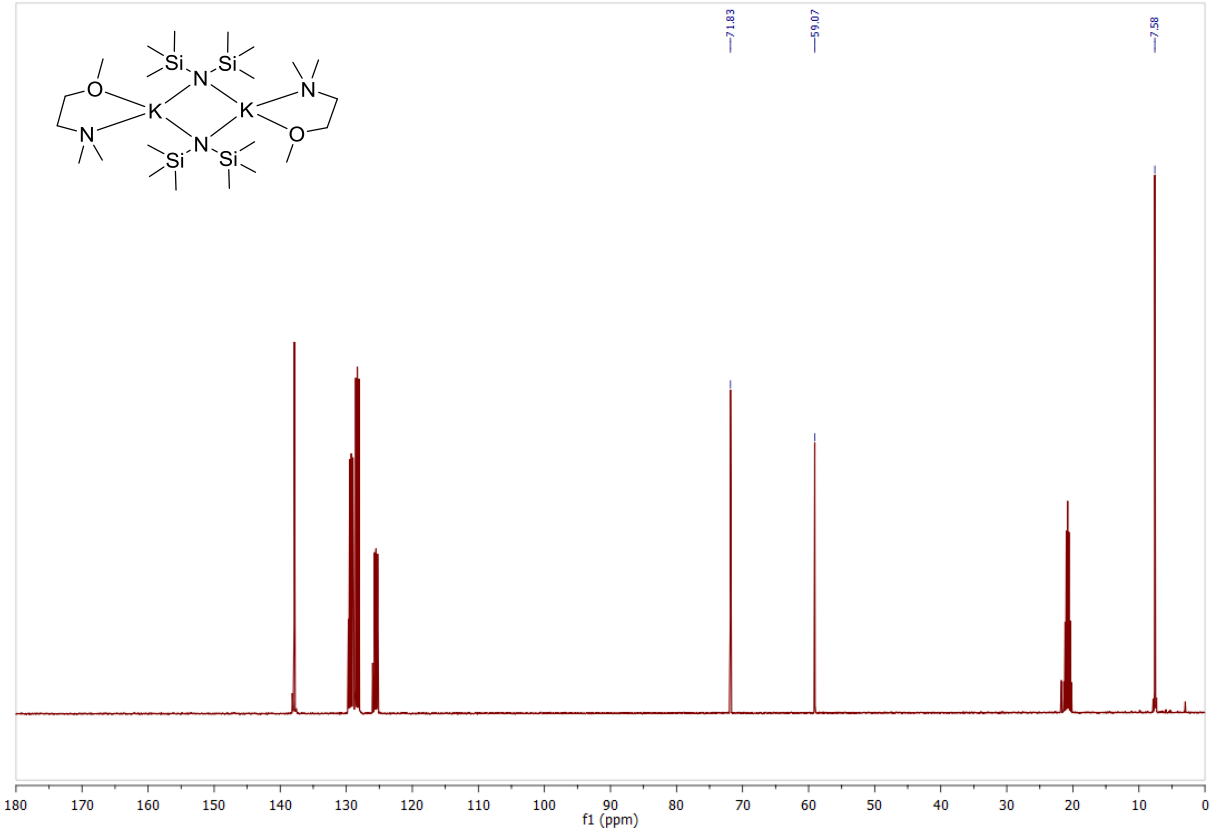

Figure S37: ^{13}C{^{1}H} NMR spectrum (101 MHz, Tol-d$_8$, 296 K) of [(dmmea)K(hmds)]$_2$ **3b**.

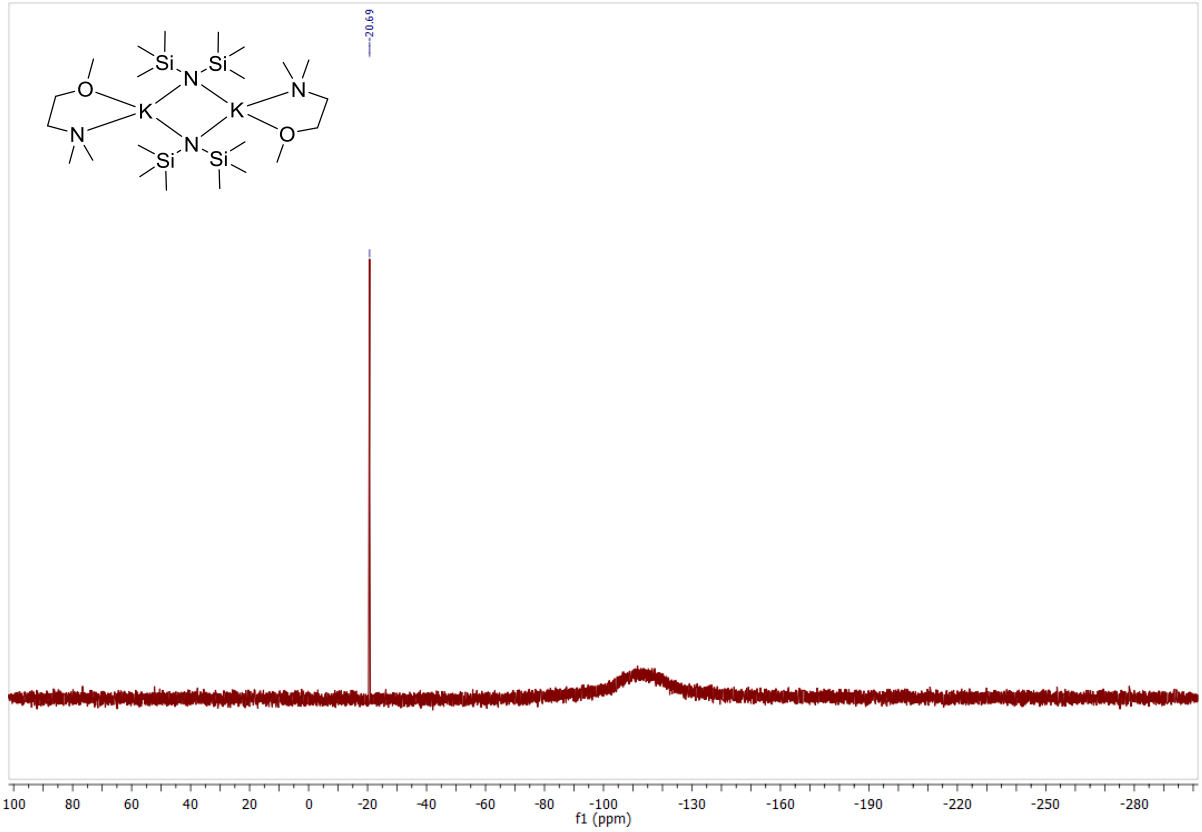

Figure S38: $^{29}Si\{^{1}H\}$ NMR spectrum (79 MHz, Tol-d_8, 296 K) of $[(dmmea)K(hmds)]_2$ **3b**.

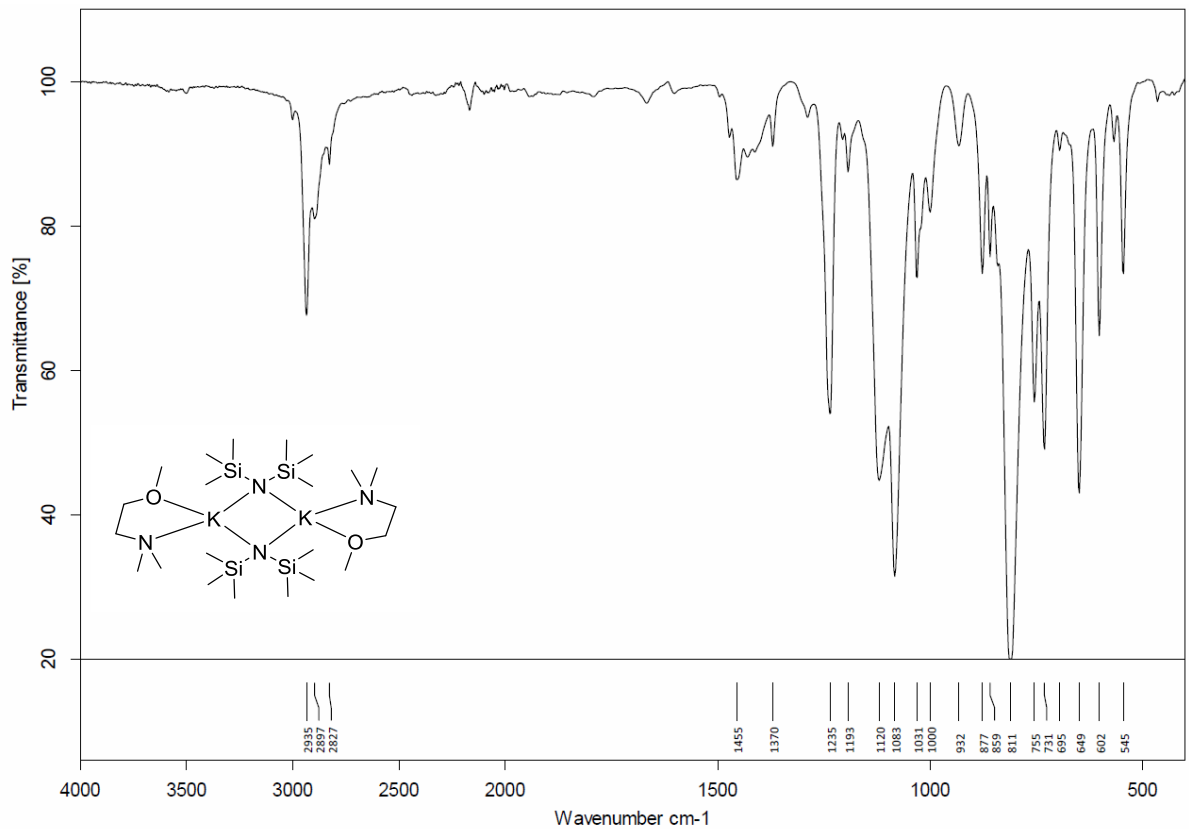

Figure S39: IR spectrum (ATR) of isolated crystals of $[(dmmea)K(hmds)]_2$ **3b**.

[(dme)Rb(hmds)]$_2$ **4c**

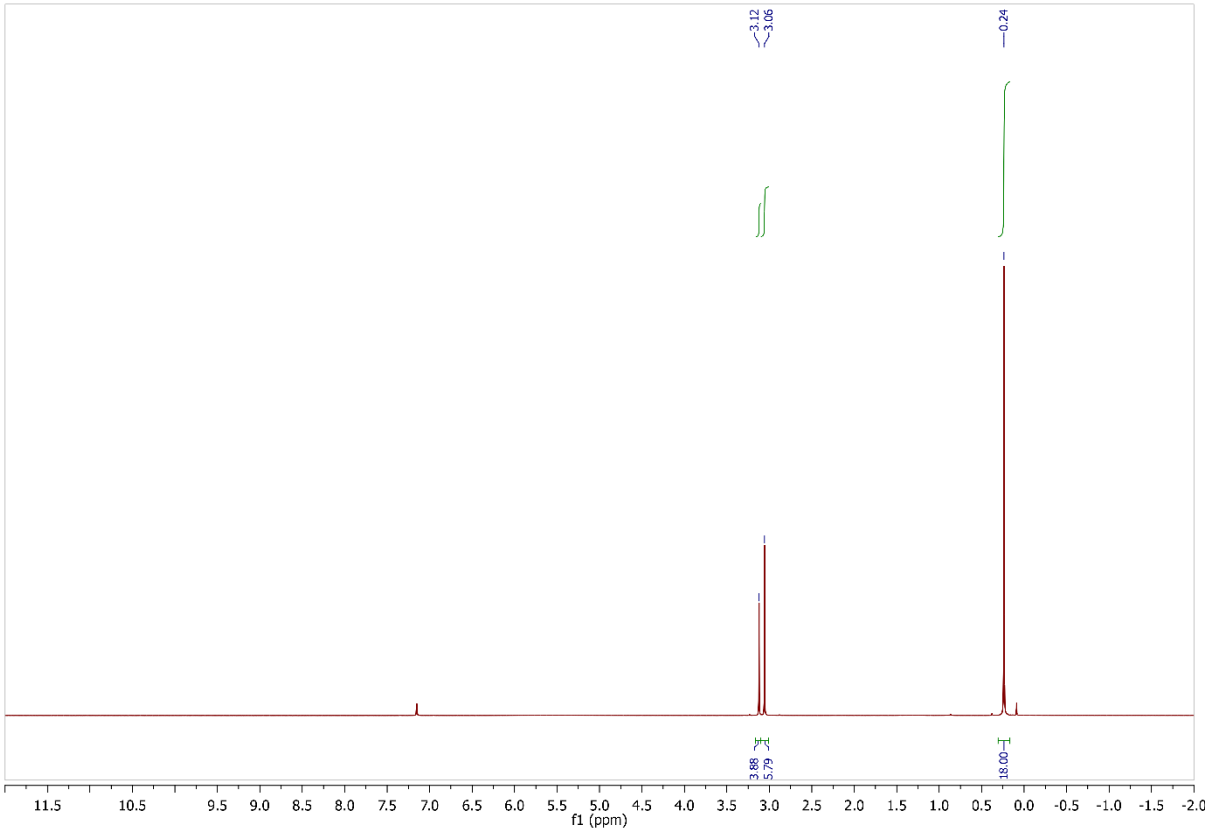

Figure S40: ^{1}H NMR spectrum (400 MHz, C_6D_6, 296 K) of [(dme)Rb(hmds)]$_2$ **4c**.

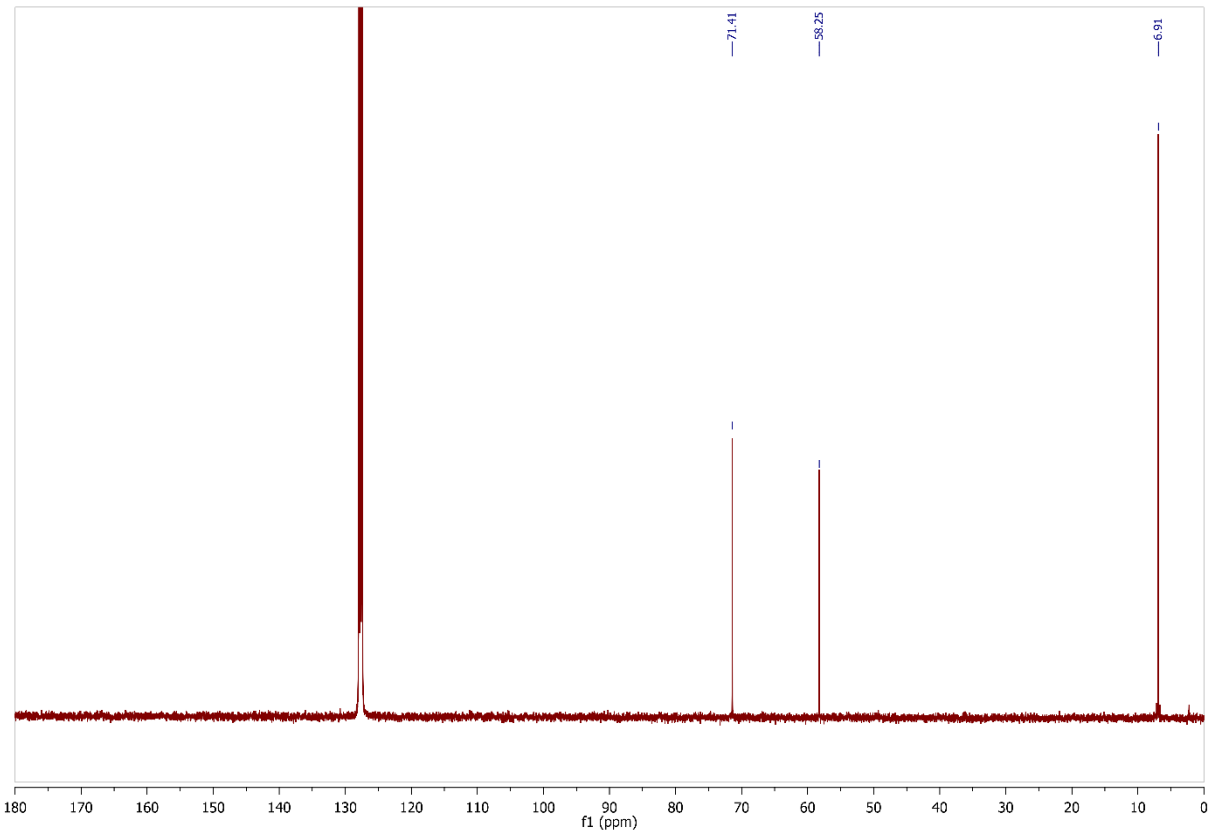

Figure S41: ^{13}C{^{1}H} NMR spectrum (101 MHz, C_6D_6, 296 K) of [(dme)Rb(hmds)]$_2$ **4c**.

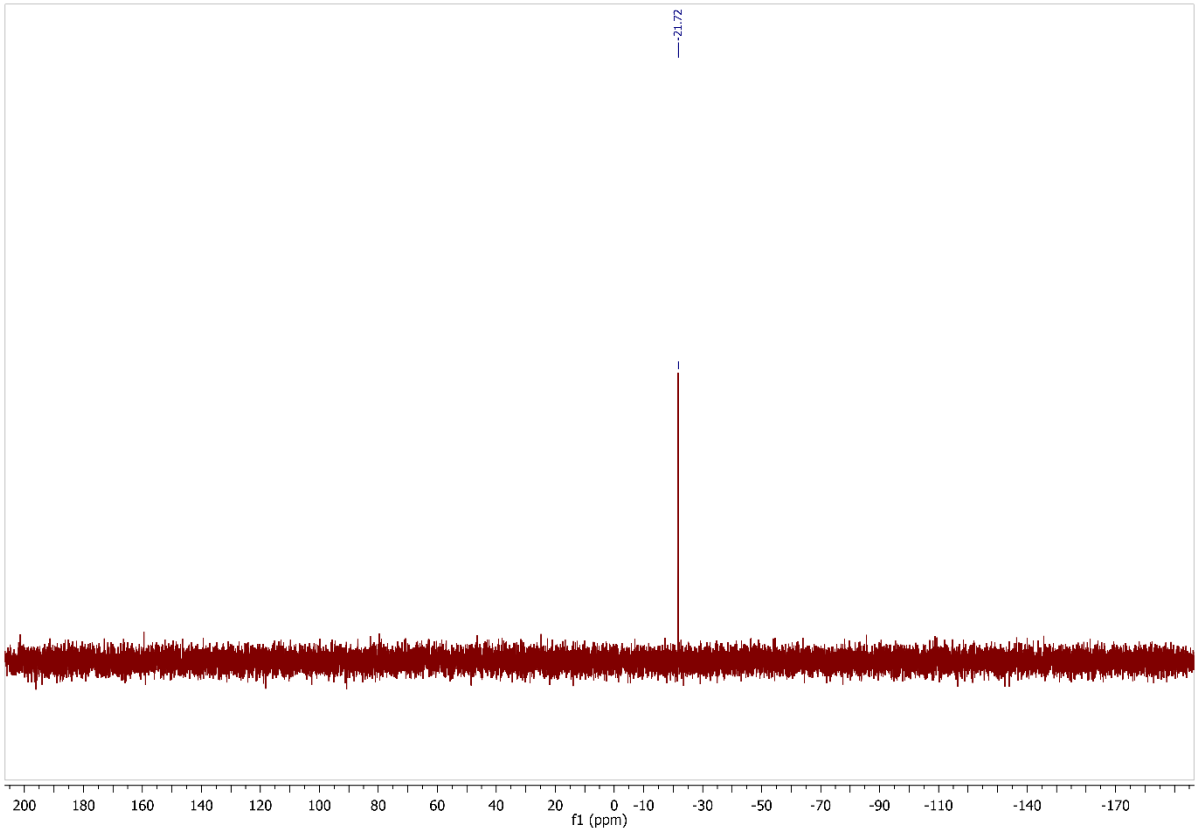

Figure S42: ^{29}Si-^{1}H-DEPT-NMR (79.49 MHz, C_6D_6, 296 K) of [(dme)Rb(hmds)]$_2$ **4c**.

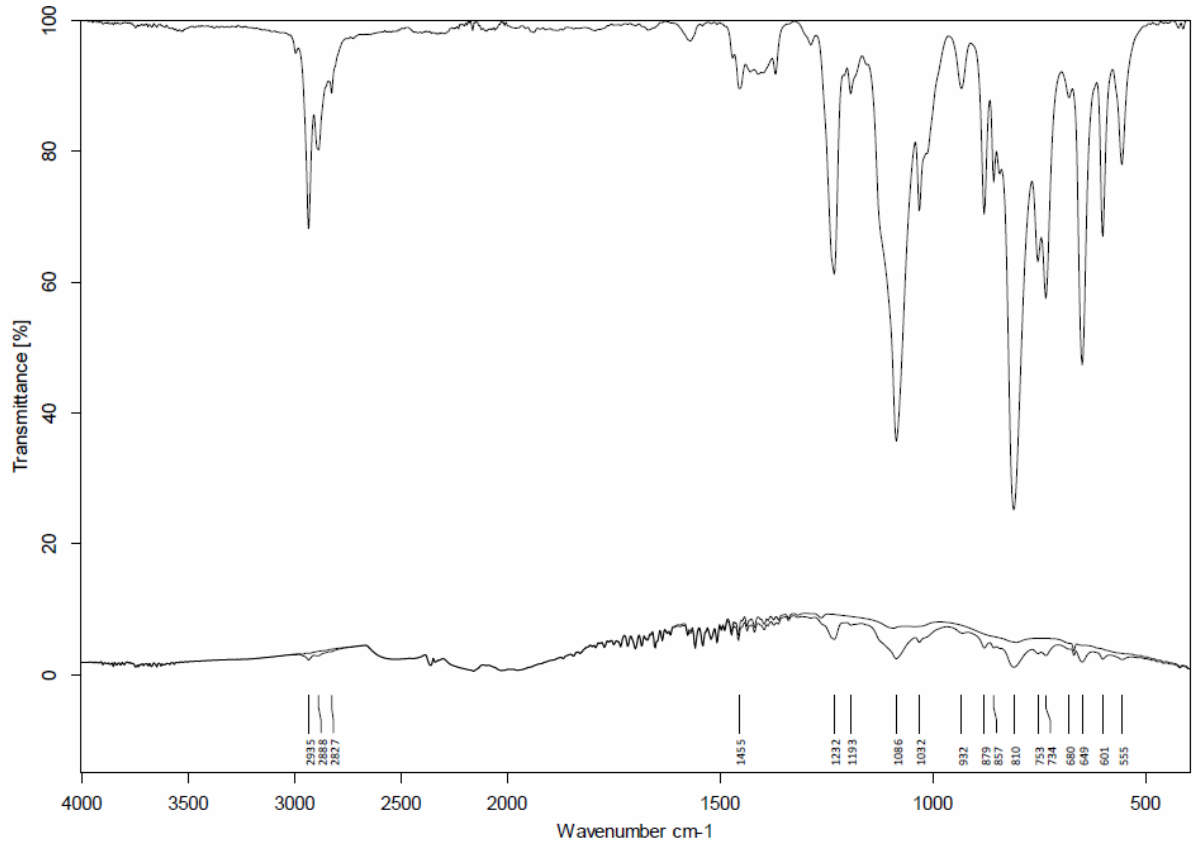

Figure S43: IR spectrum (ATR) of isolated crystals of [(dme)Rb(hmds)]$_2$ **4c**.

[(dmmea)Rb(hmds)]$_2$ **4b**

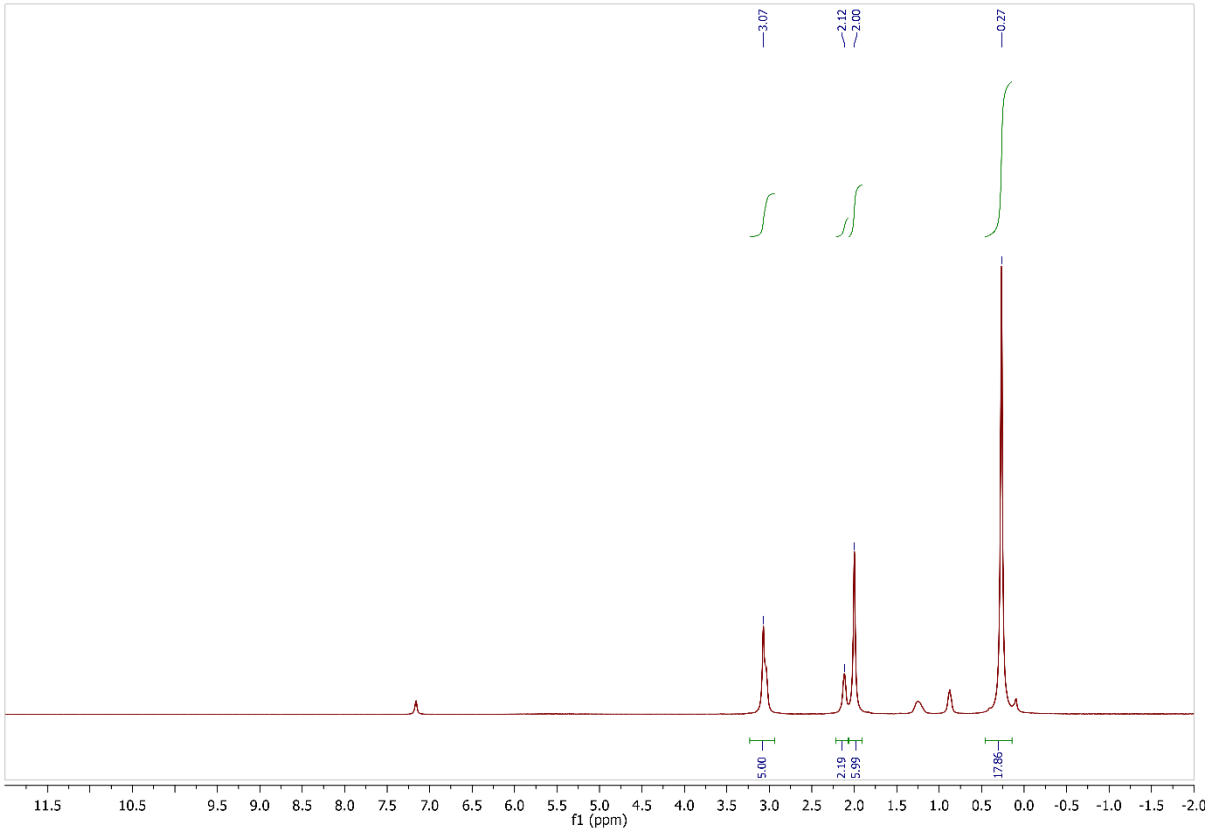

Figure S44: ^{1}H-NMR (400 MHz, C_6D_6, 296 K) of [(dmmea)Rb(hmds)]$_2$ **4b**.

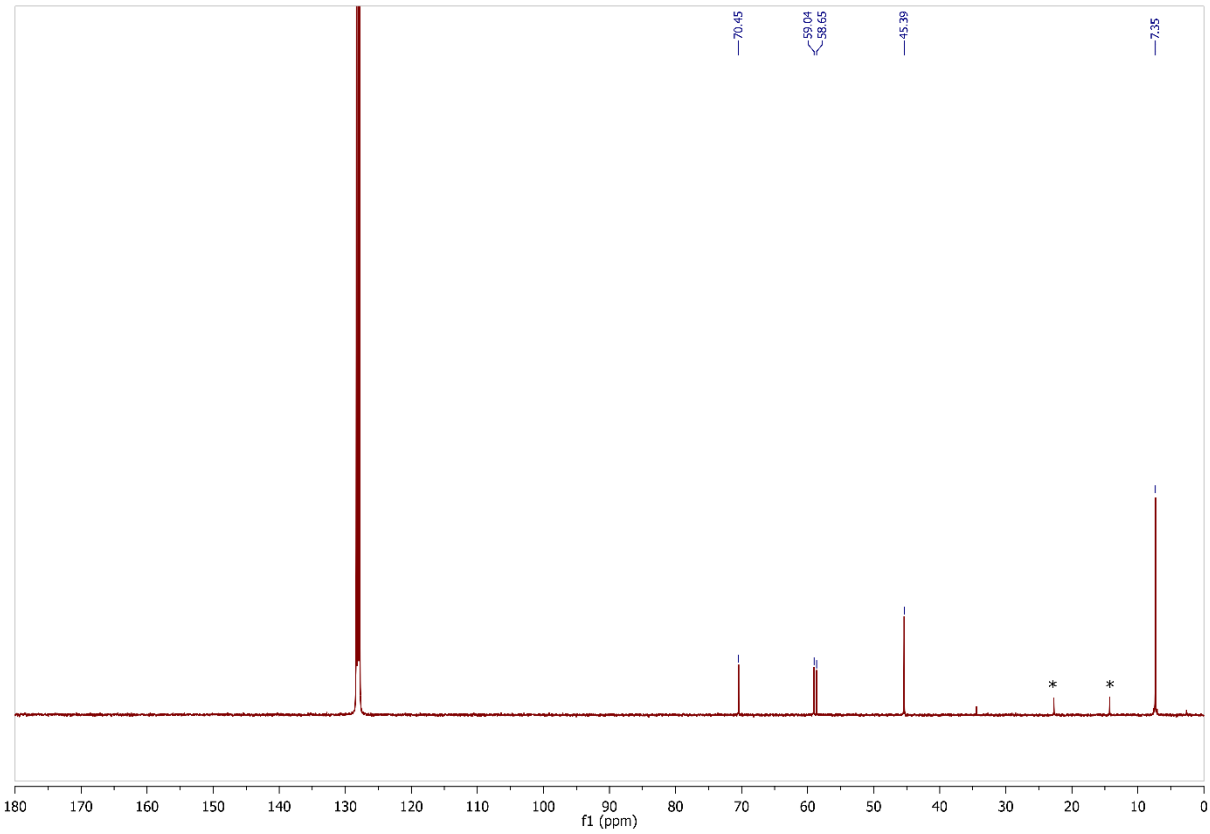

Figure S45: ^{13}C{^{1}H} NMR spectrum (101 MHz, C_6D_6, 296 K) of [(dmmea)Rb(hmds)]$_2$ **4b**.

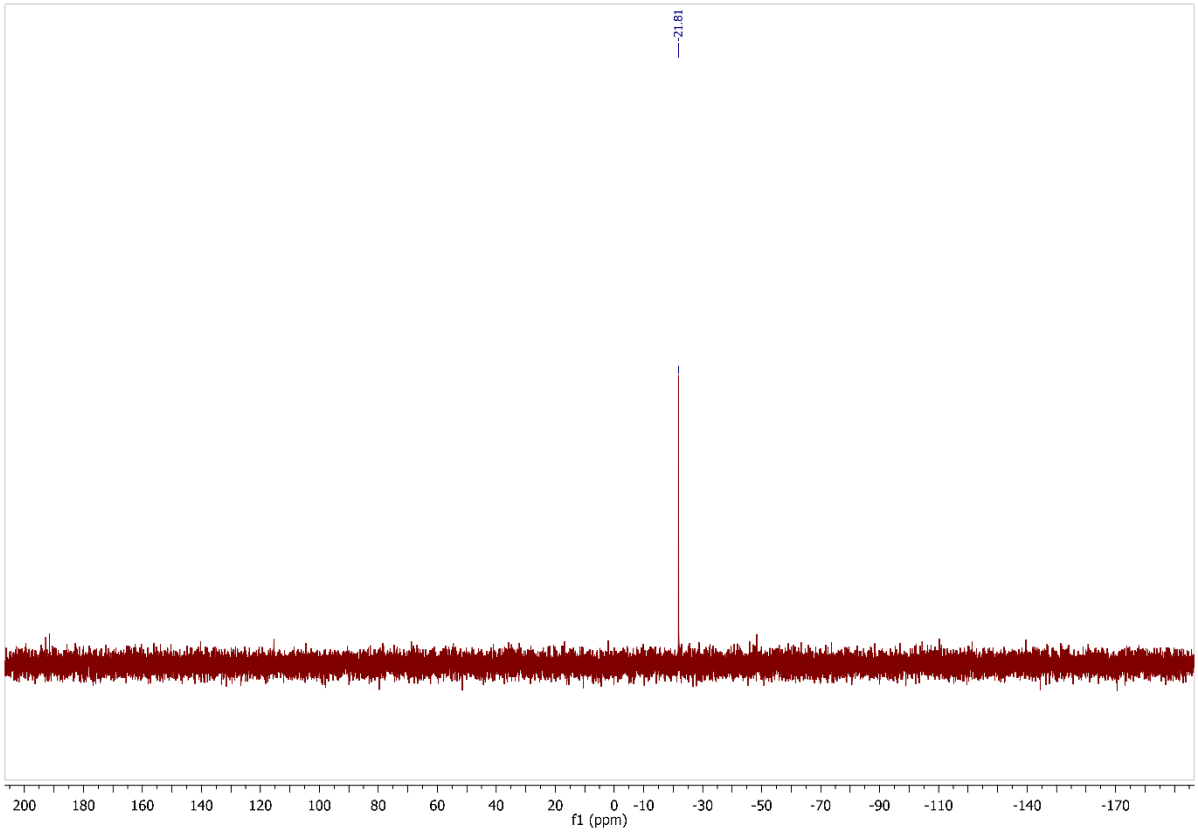

Figure S46: ^{29}Si-^{1}H-DEPT NMR spectrum (79.49 MHz, C_6D_6, 296 K) of $[(dmmea)Rb(hmds)]_2$ **4b**.

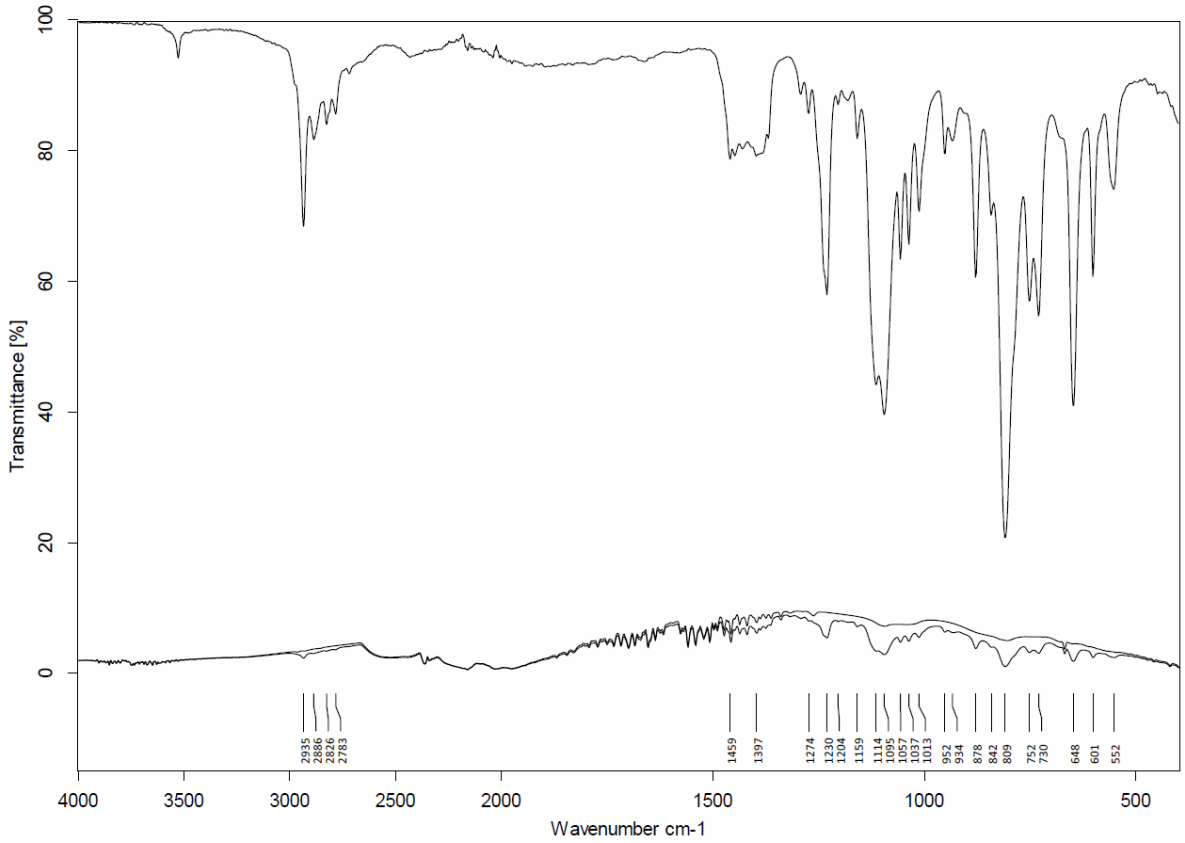

Figure S47: IR spectrum (ATR) of isolated crystals of $[(dmmea)Rb(hmds)]_2$ **4b**.

[(tmeda)Rb(hmds)]$_2$ **4a**

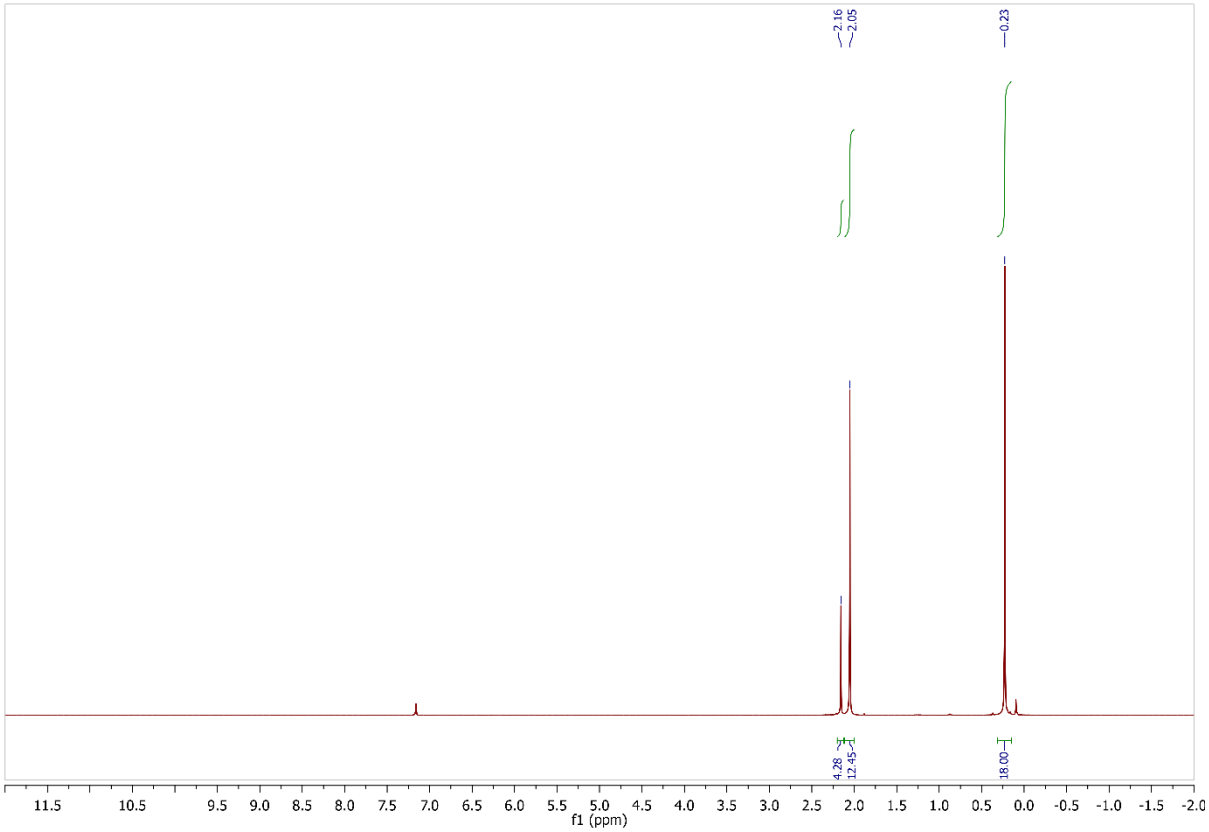

Figure S48: ^{1}H NMR spectrum (400 MHz, C_6D_6, 296 K) of [(tmeda)Rb(hmds)]$_2$ **4a**.

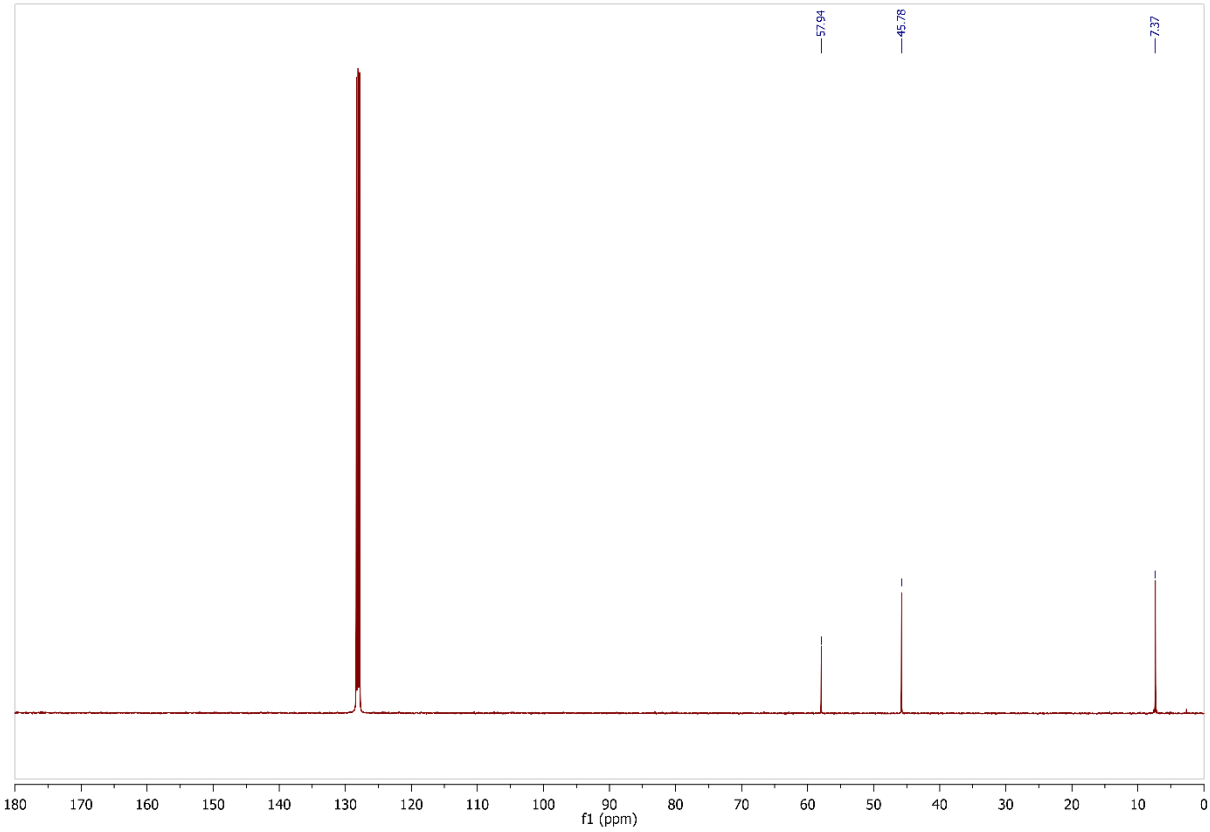

Figure S49: ^{13}C{^{1}H}-NMR (101 MHz, C_6D_6, 296 K) of [(tmeda)Rb(hmds)]$_2$ **4a**.

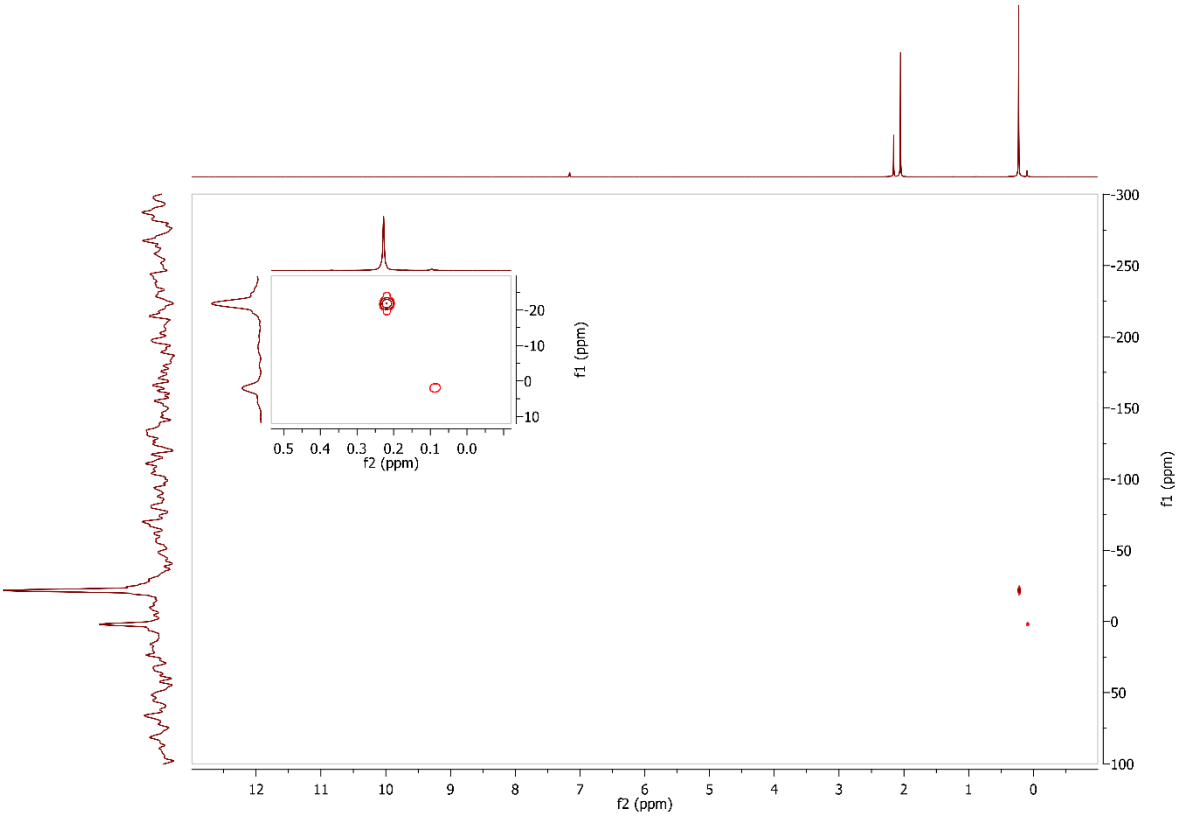

Figure S50: ^{29}Si-^{1}H-HMBC NMR spectrum (79.49 MHz, C_6D_6, 296 K) of $[(tmeda)Rb(hmds)]_2$ **4a**.

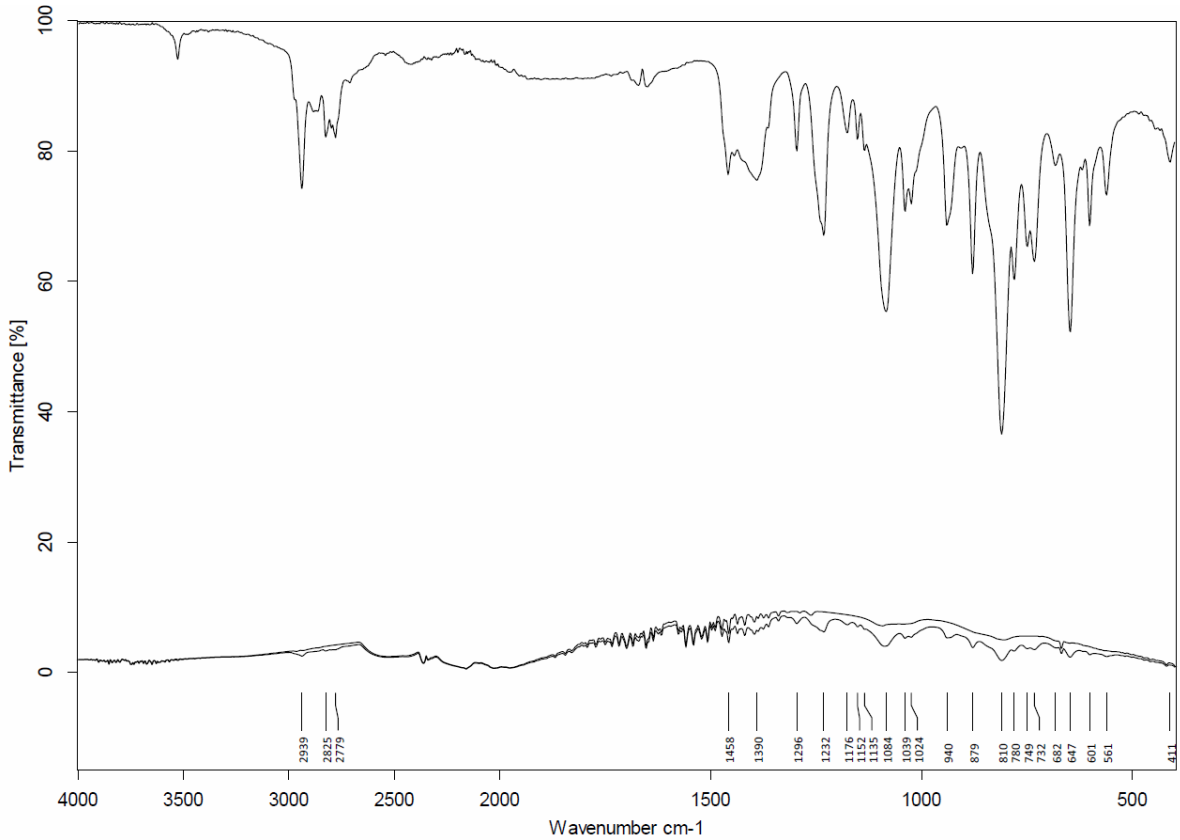

Figure S51: IR spectrum (ATR) of isolated crystals of $[(tmeda)Rb(hmds)]_2$ **4a**.

[(dmmea)Cs(hmds)]$_2$ **5b**

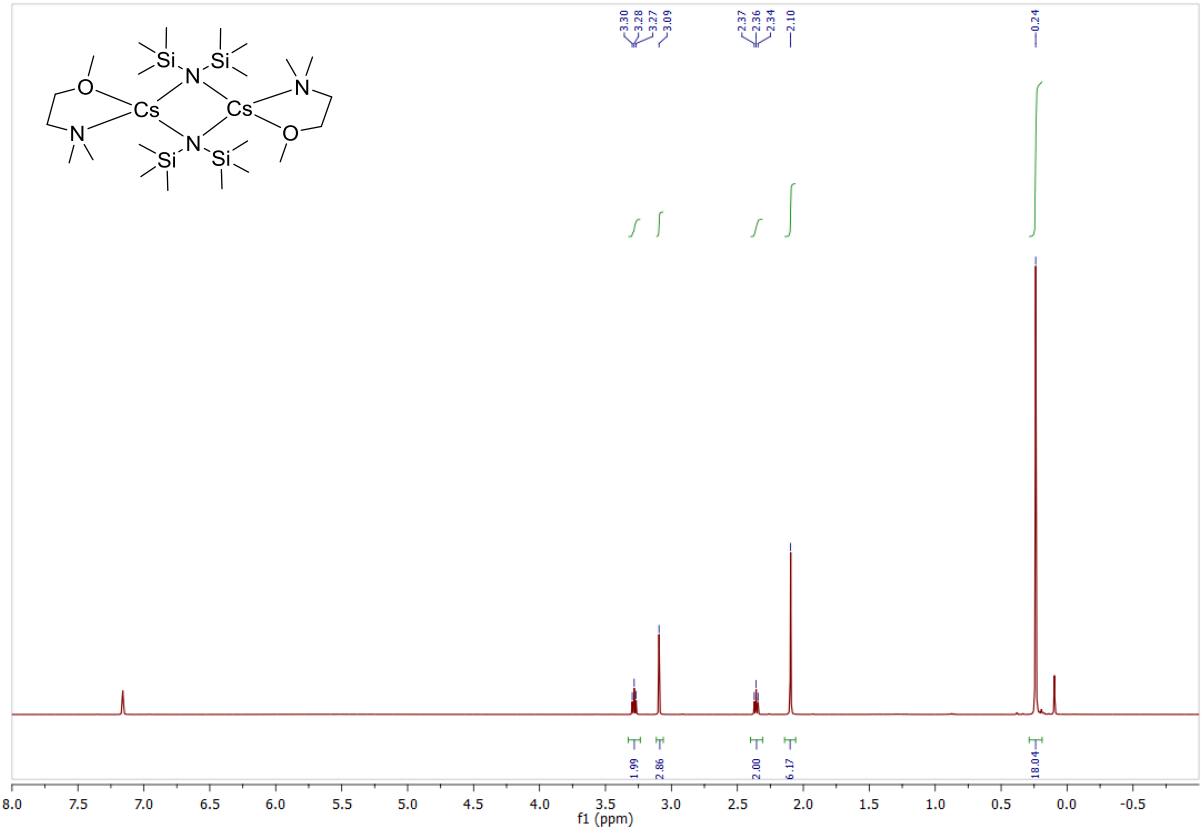

Figure S52: ^{1}H NMR spectrum (400 MHz, C_6D_6, 296 K) of [(dmmea)Cs(hmds)]$_2$ **5b**.

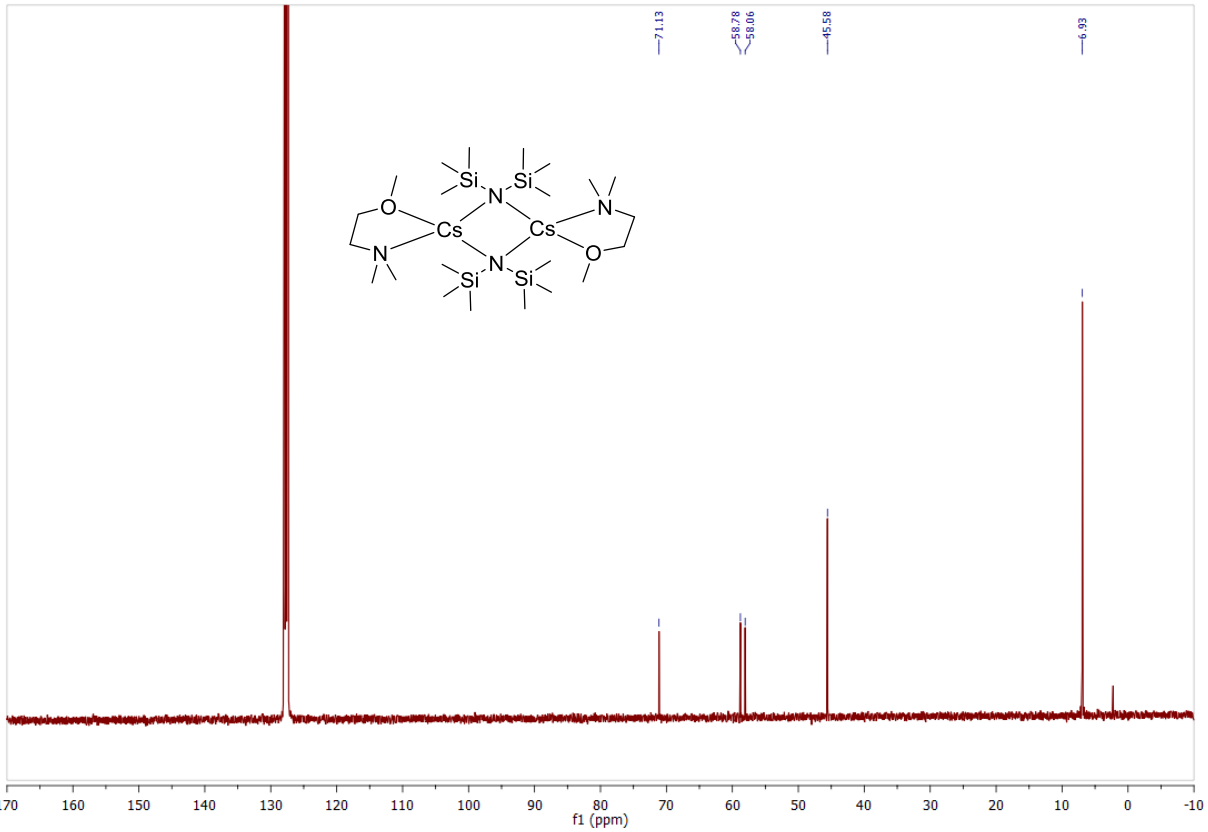

Figure S53: ^{13}C{^{1}H} NMR spectrum (101 MHz, C_6D_6, 296 K) of [(dmmea)Cs(hmds)]$_2$ **5b**.

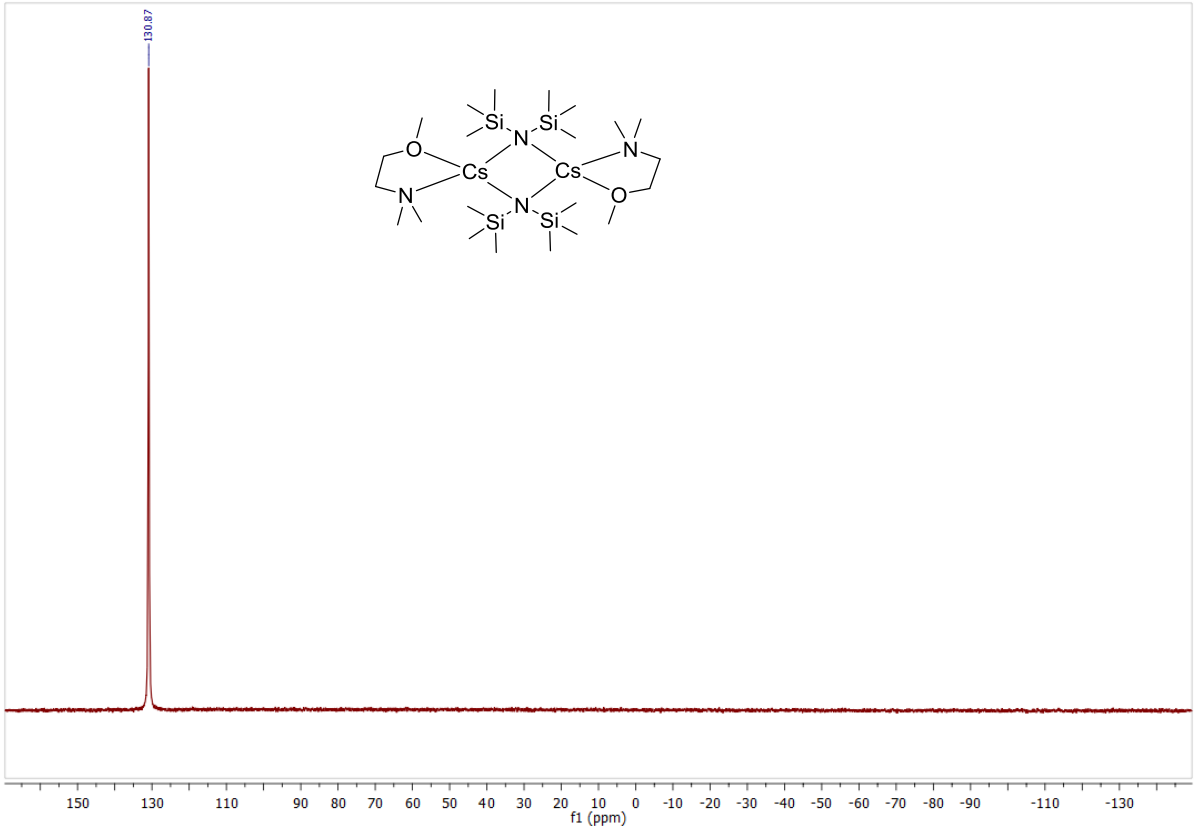

Figure S54: ^{133}Cs NMR spectrum (52.5 MHz, C_6D_6, 296 K) of $[(dmmea)Cs(hmds)]_2$ **5b**.

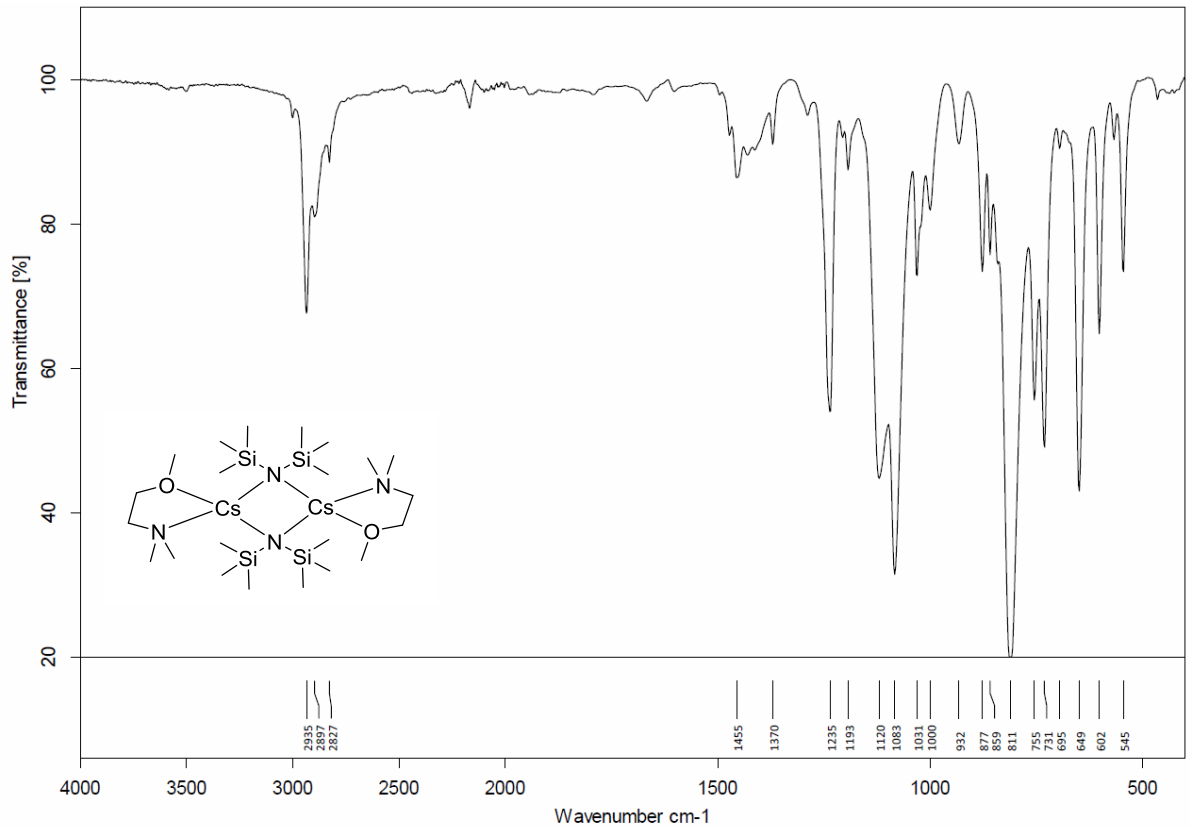

Figure S55: IR spectrum (ATR) of isolated crystals of $[(dmmea)Cs(hmds)]_2$ **5b**.

[(dme)Cs(hmds)]$_2$ **5c**

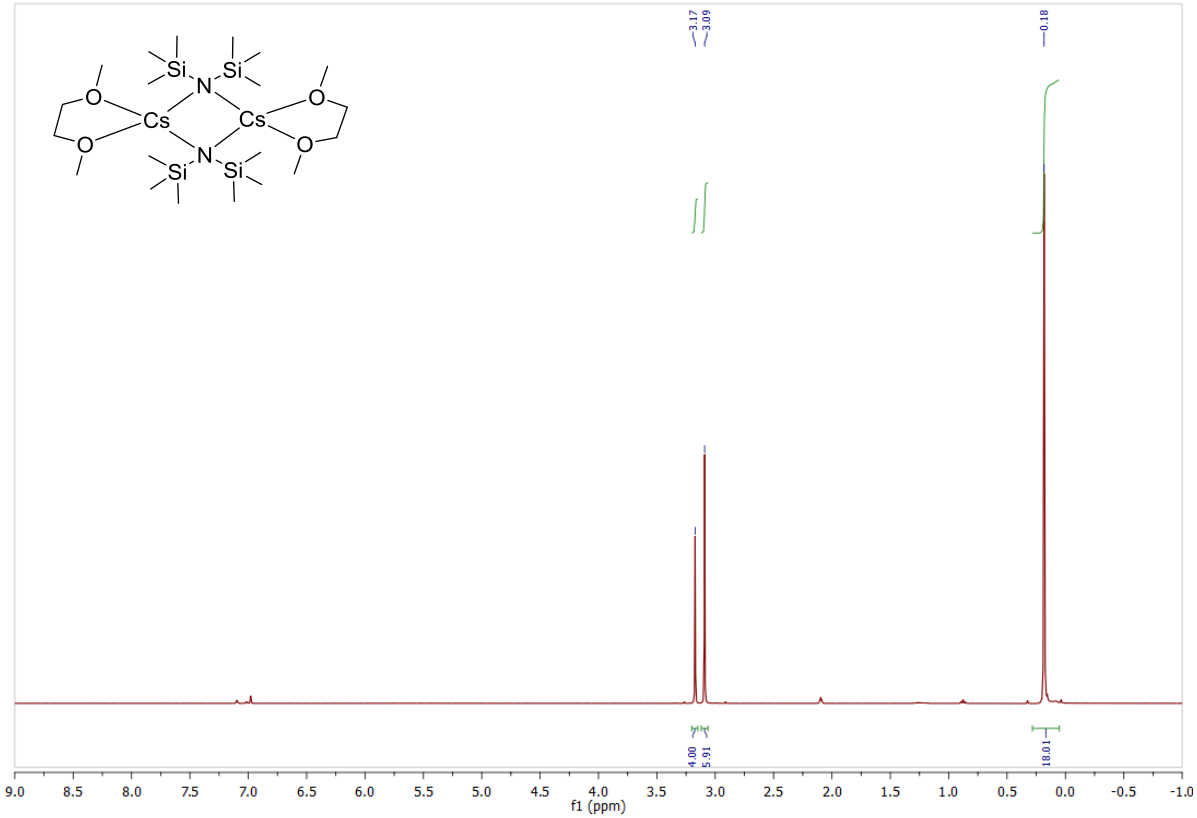

Figure S56: ^{1}H NMR spectrum(400 MHz, Tol-d$_8$, 296 K) of [(dme)Cs(hmds)]$_2$ **5c**.

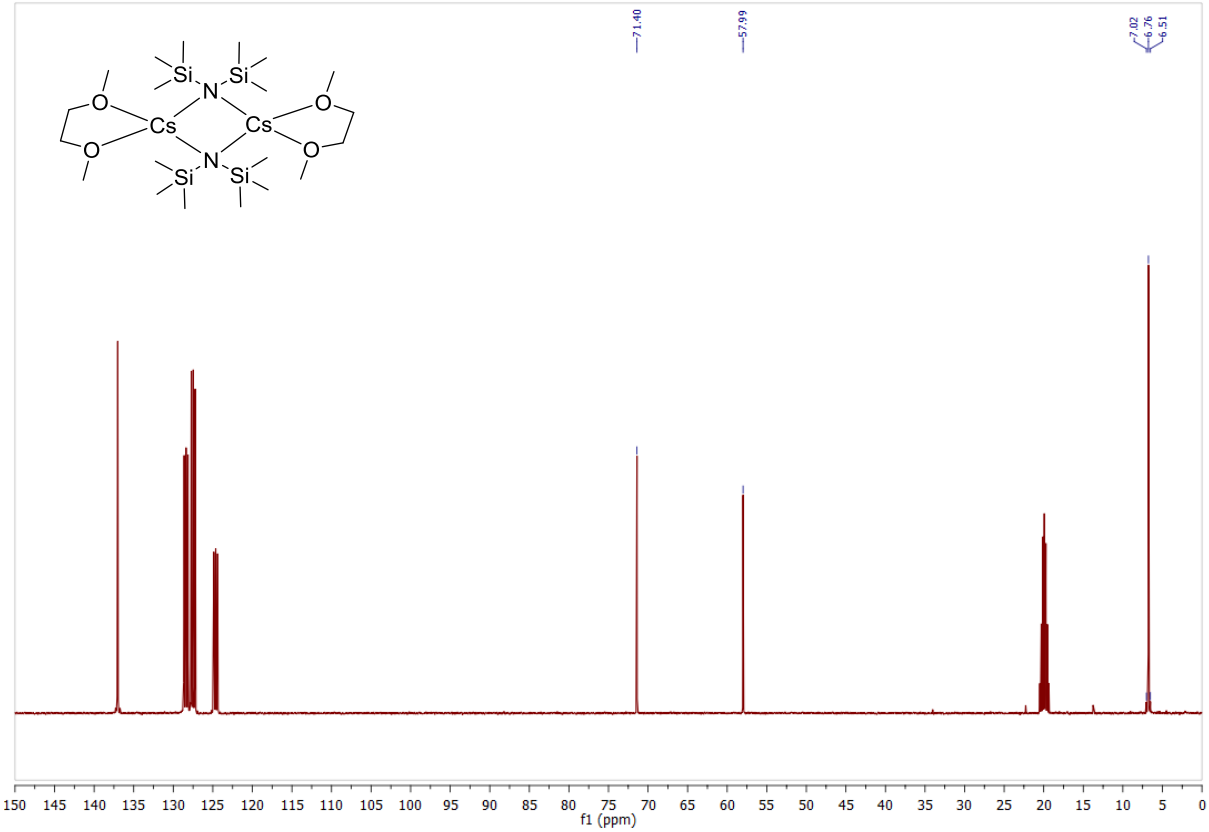

Figure S57: ^{13}C{^{1}H} NMR spectrum (101 MHz, Tol-d$_8$, 296 K) of [(dme)Cs(hmds)]$_2$ **5c**.

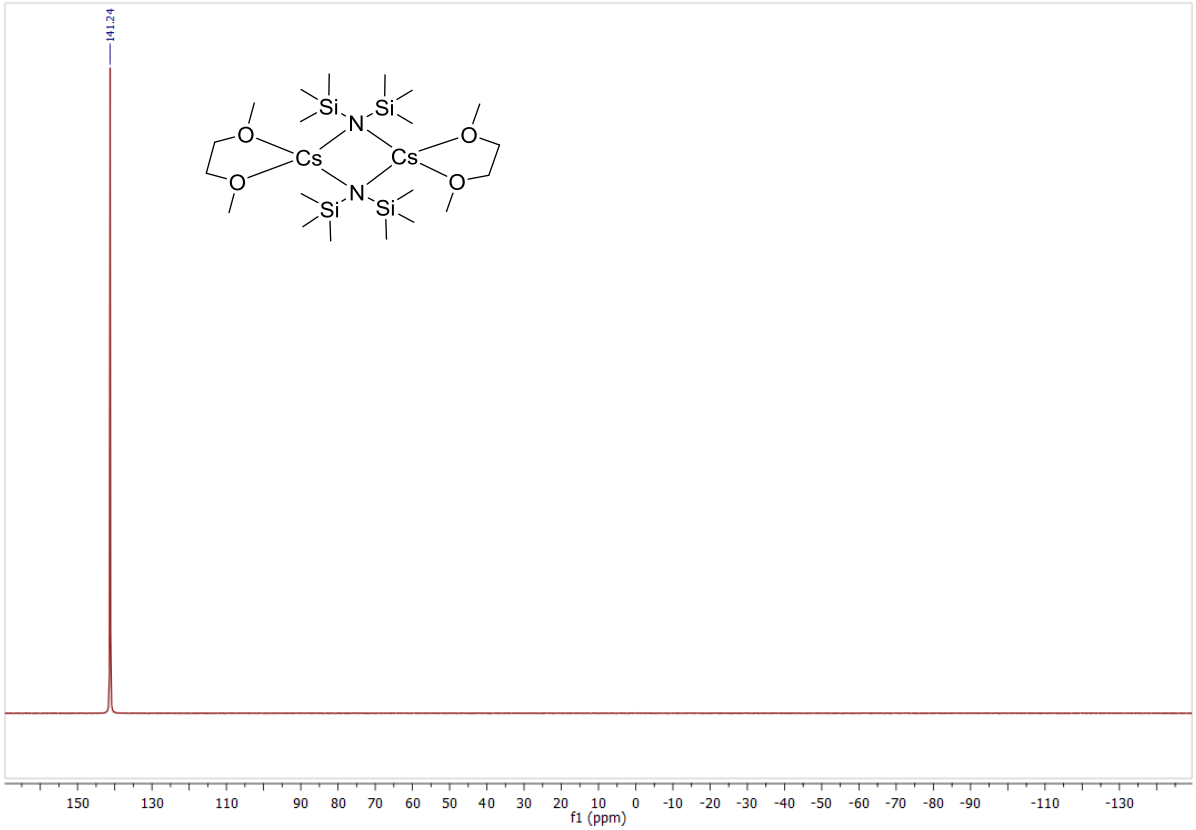

Figure S58: ^{133}Cs NMR spectrum (52.5 MHz, Tol-d_8, 296 K) of $[(dme)Cs(hmds)]_2$ **5c**.

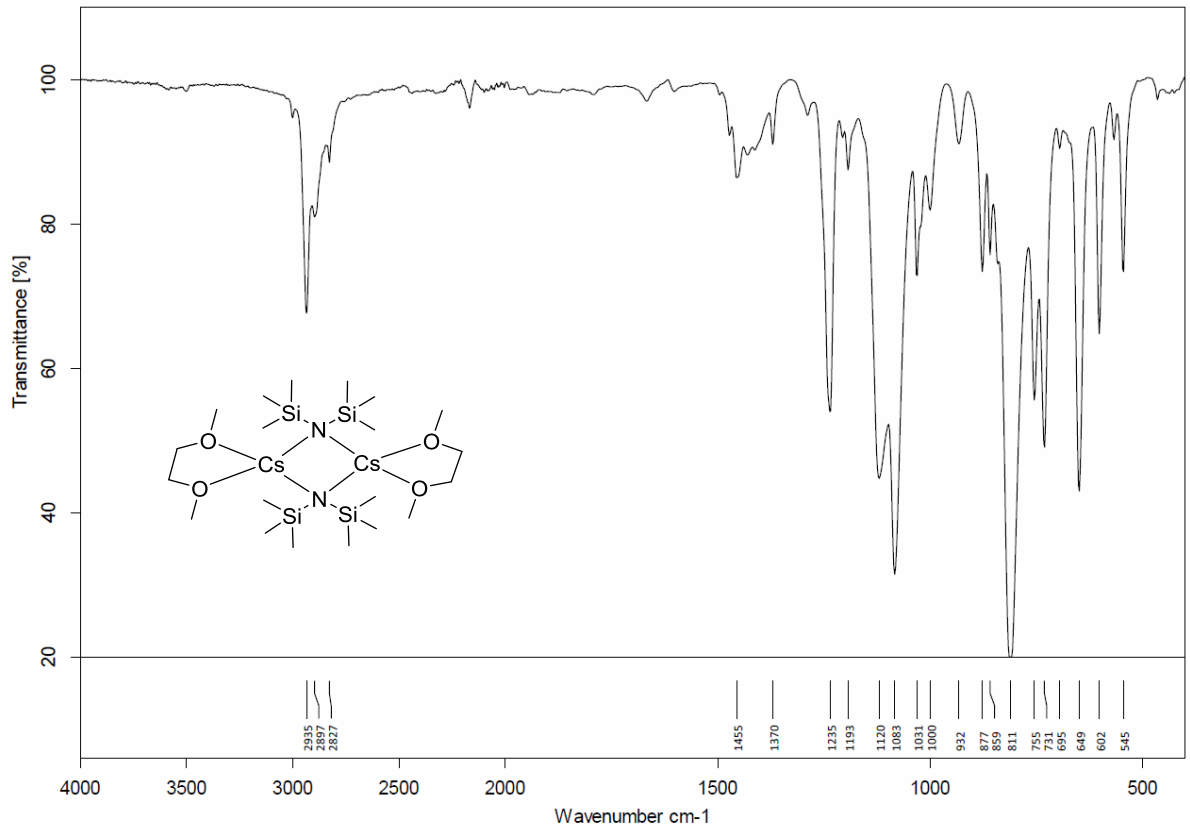

Figure S59: IR spectrum (ATR) of isolated crystals of $[(dme)Cs(hmds)]_2$ **5c**.

[(dme)Mg(hmds)$_2$] **6c**

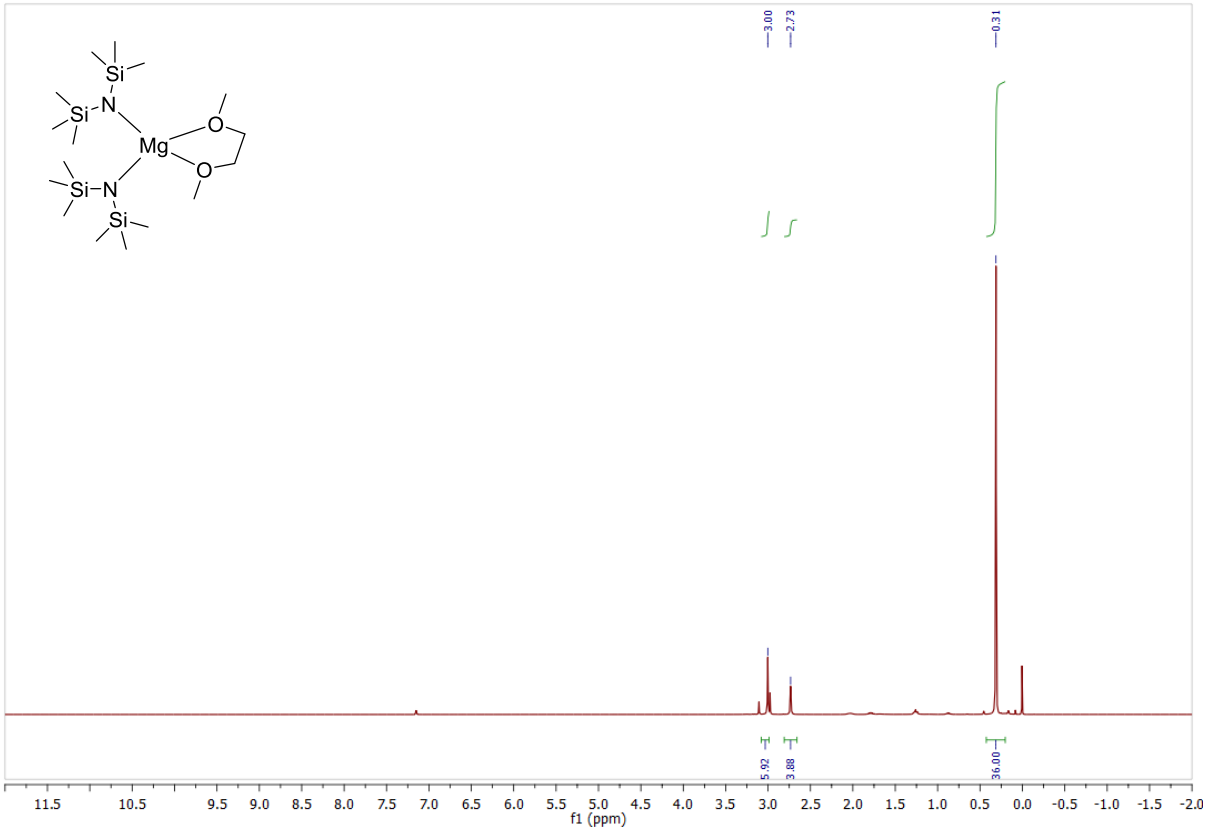

Figure S60: ^{1}H NMR spectrum (400 MHz, C_6D_6, 296 K) of [(dme)Mg(hmds)$_2$] **6c**.

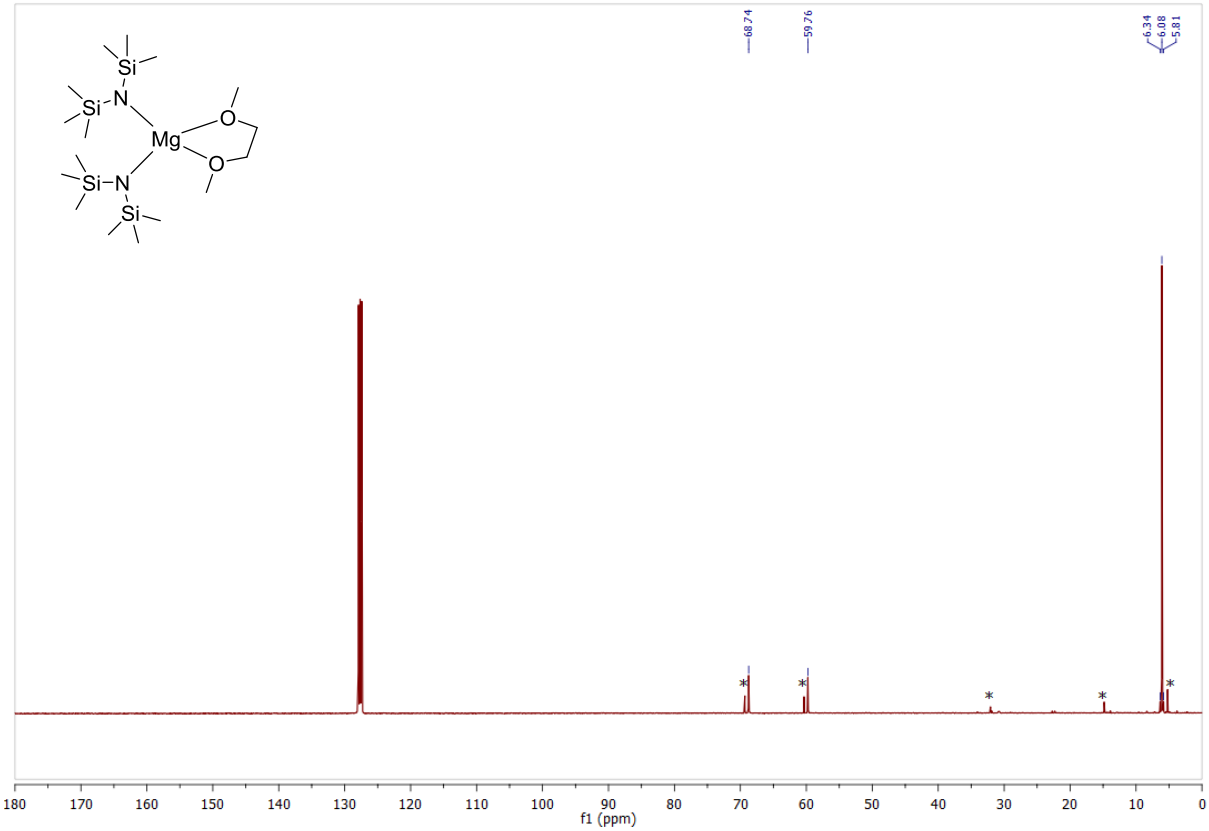

Figure S61: ^{13}C{^{1}H} NMR spectrum (101 MHz, C_6D_6, 296 K) of [(dme)Mg(hmds)$_2$] **6c**.

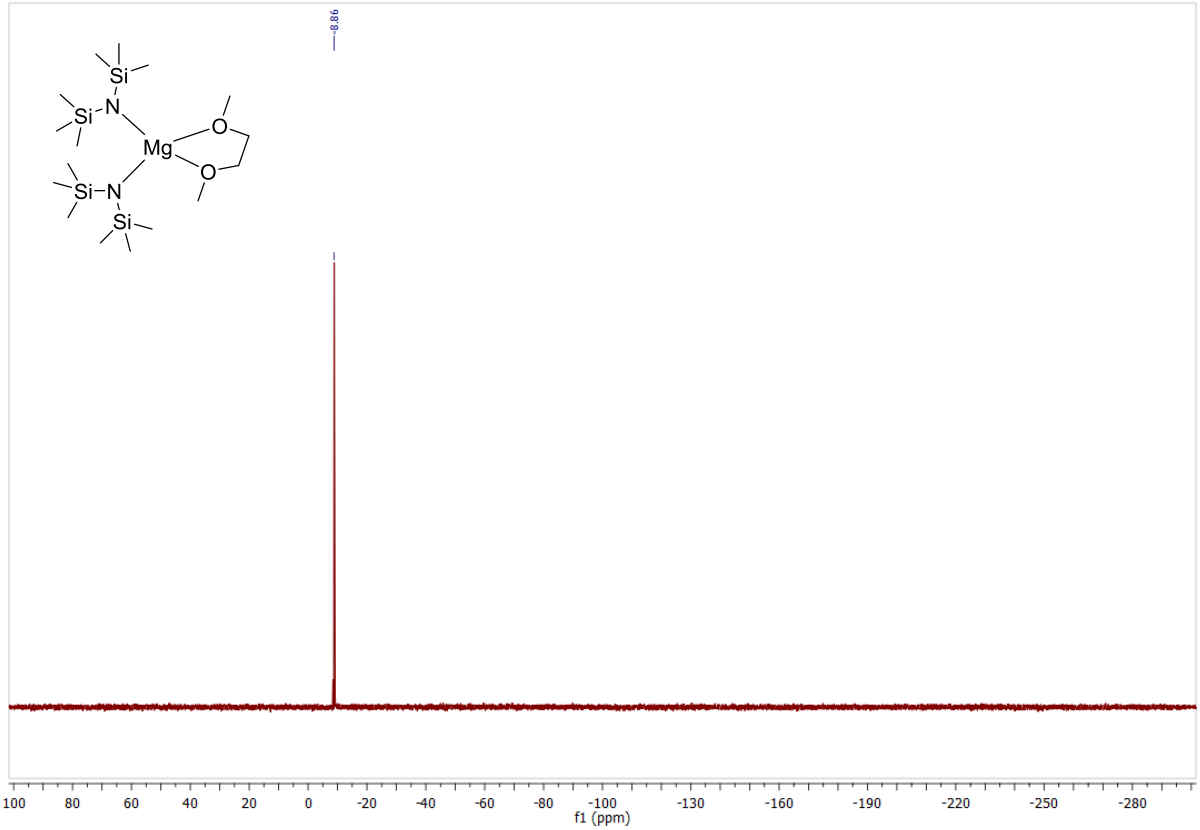

Figure S62: $^{29}Si\{^{1}H\}$ NMR spectrum (79.5 MHz, C_6D_6, 296 K) of [(dme)Mg(hmds)$_2$] **6c**.

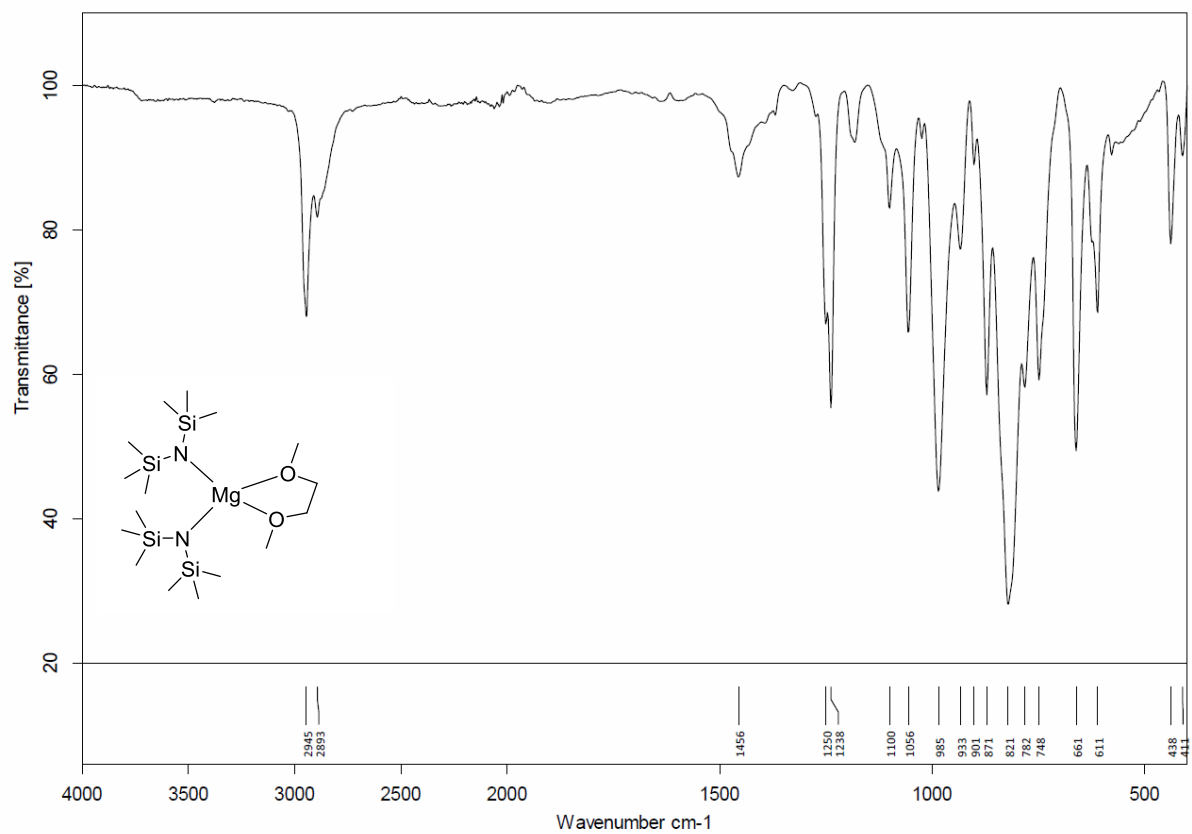

Figure S63: IR spectrum (ATR) of isolated crystals of [(dme)Mg(hmds)$_2$] **6c**.

[(dmmea)Mg(hmds)$_2$] **6b**

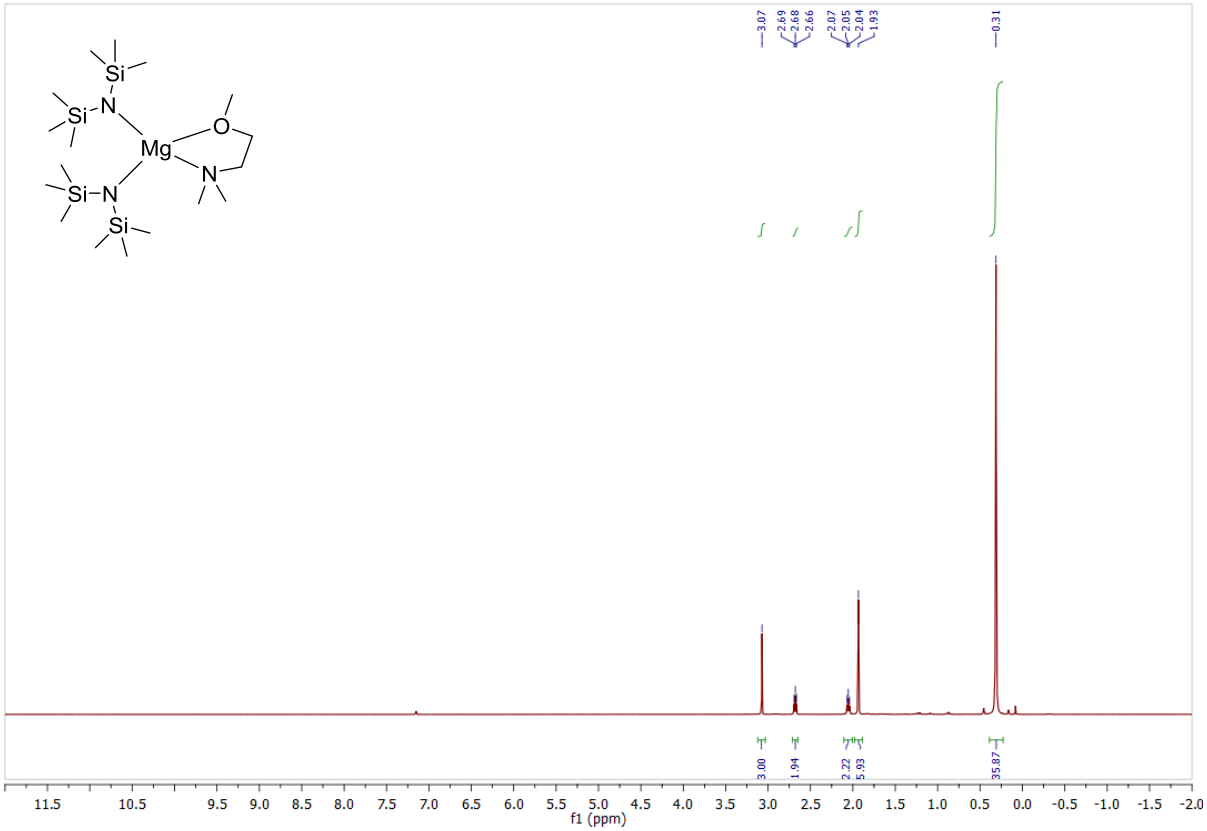

Figure S64: ^{1}H NMR spectrum (400 MHz, C_6D_6, 296 K) of [(dmmea)Mg(hmds)$_2$] **6b**.

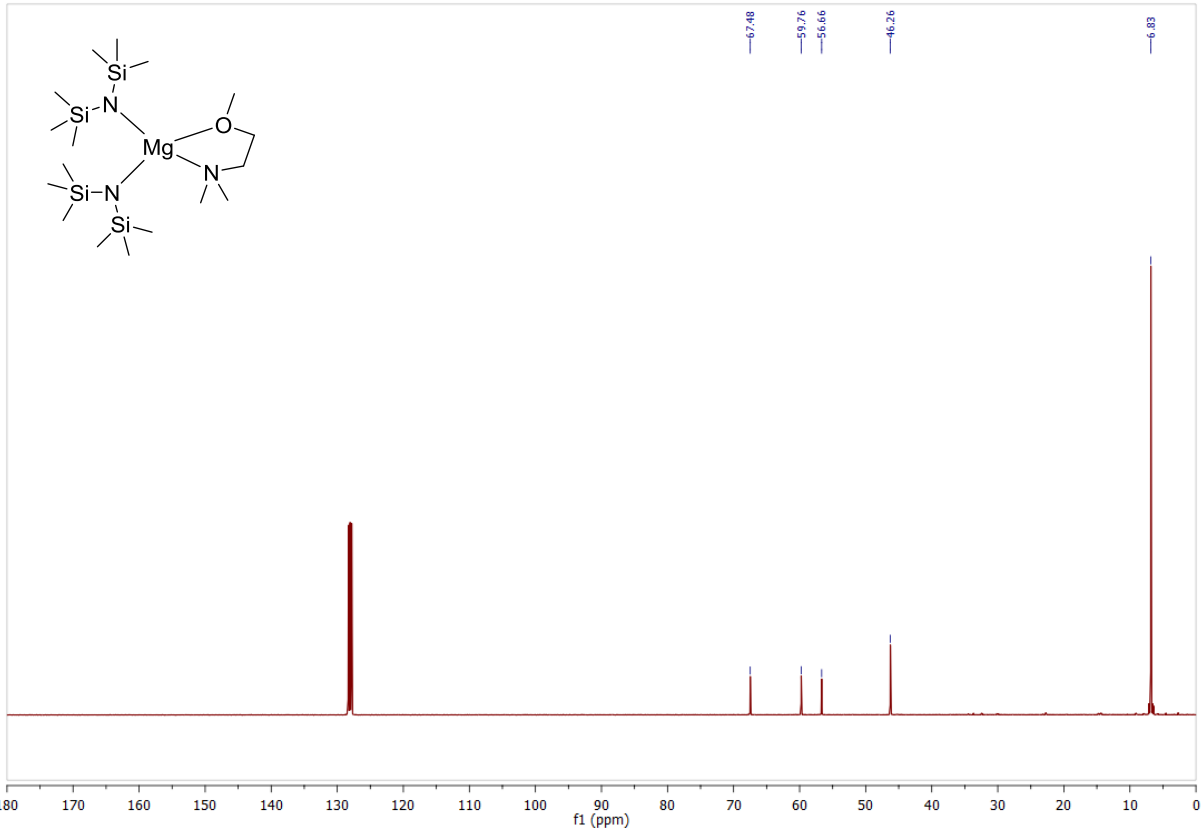

Figure S65: ^{13}C{^{1}H} NMR spectrum (101 MHz, C_6D_6, 296 K) of [(dmmea)Mg(hmds)$_2$] **6b**.

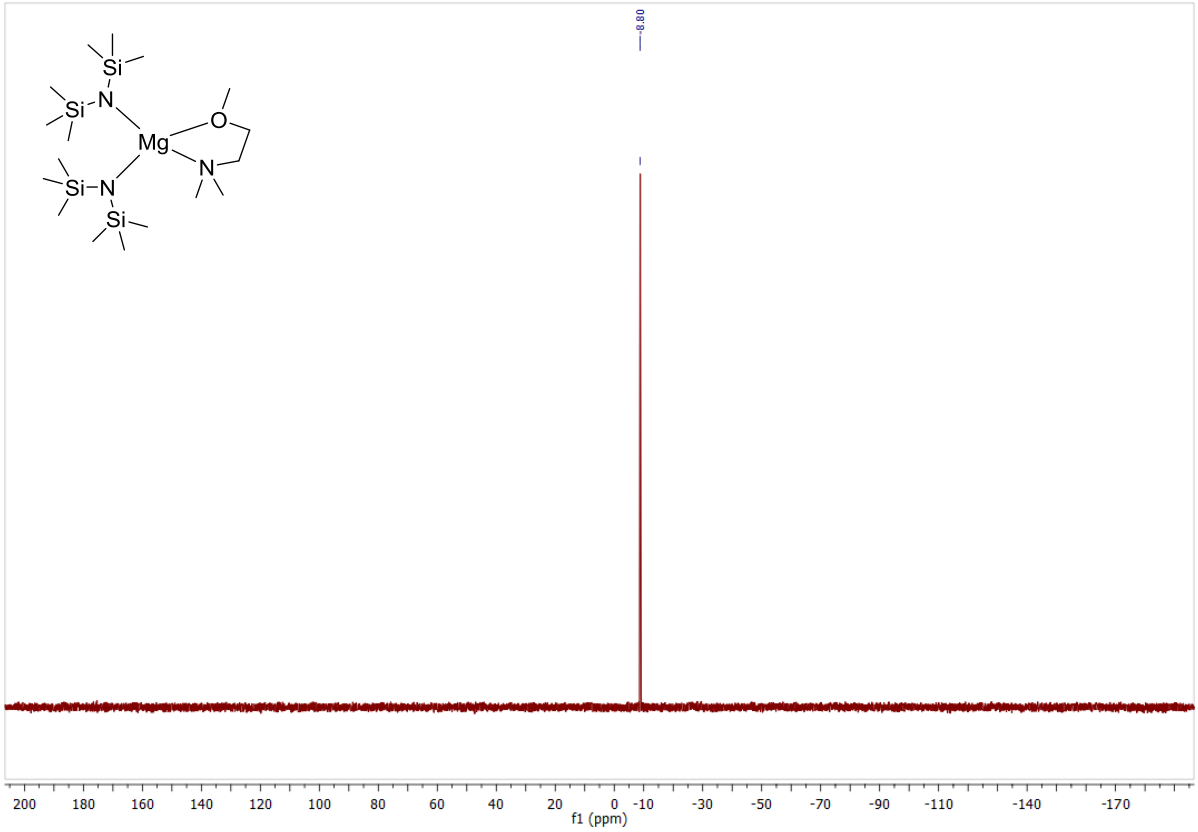

Figure S66: ^{29}Si-^{1}H-DEPT NMR spectrum (79 MHz, C_6D_6, 296 K) of [(dmmea)Mg(hmds)$_2$] **6b**.

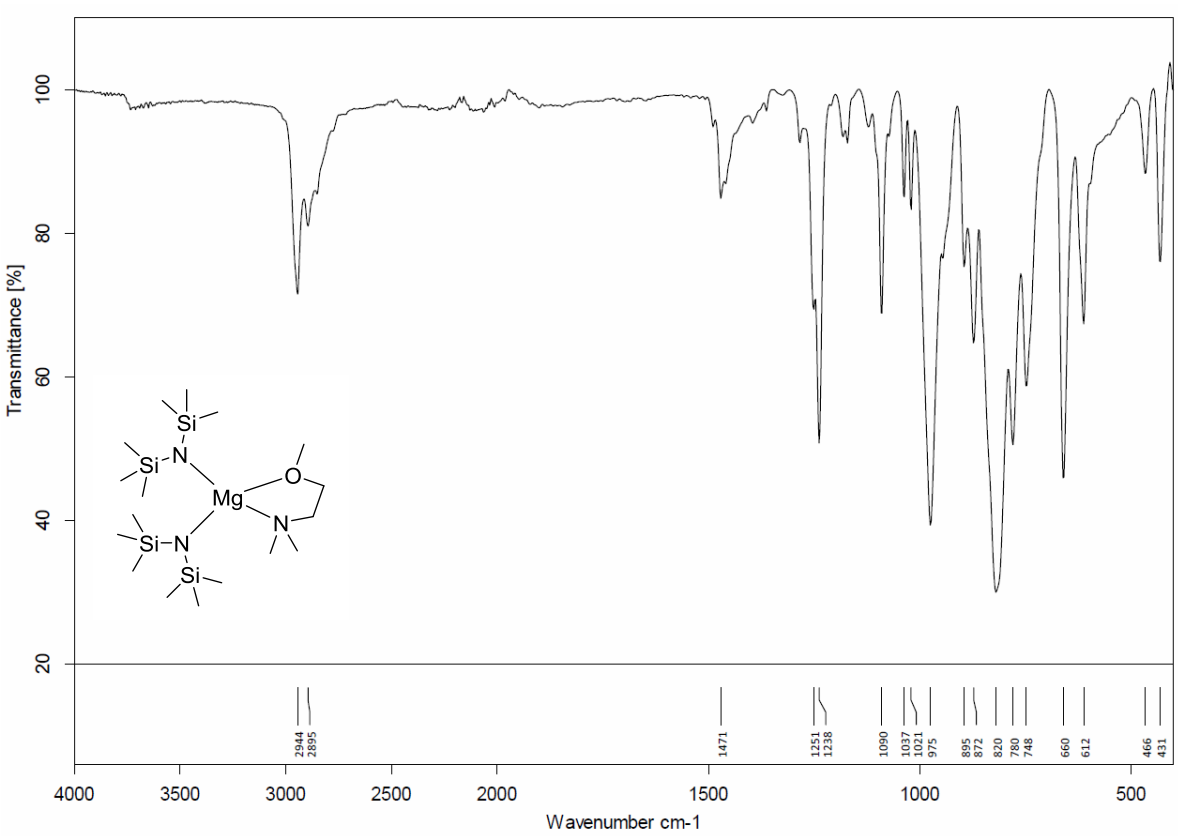

Figure S67: IR spectrum (ATR) of isolated crystals of [(dmmea)Mg(hmds)$_2$] **6b**.

[(tmeda)Mg(hmds)$_2$]
6a

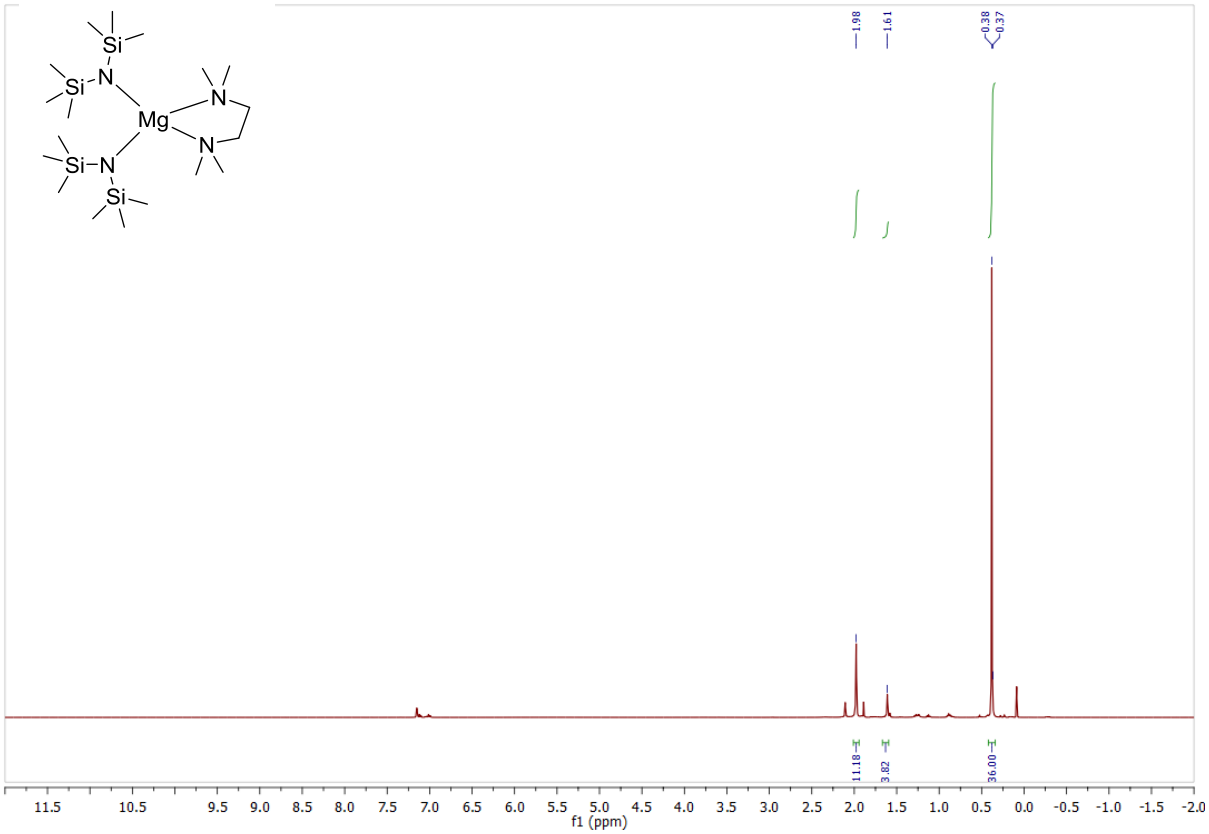

Figure S68: ^{1}H NMR spectrum (400 MHz, C_6D_6, 296 K) of [(tmeda)Mg(hmds)$_2$] **6a**.

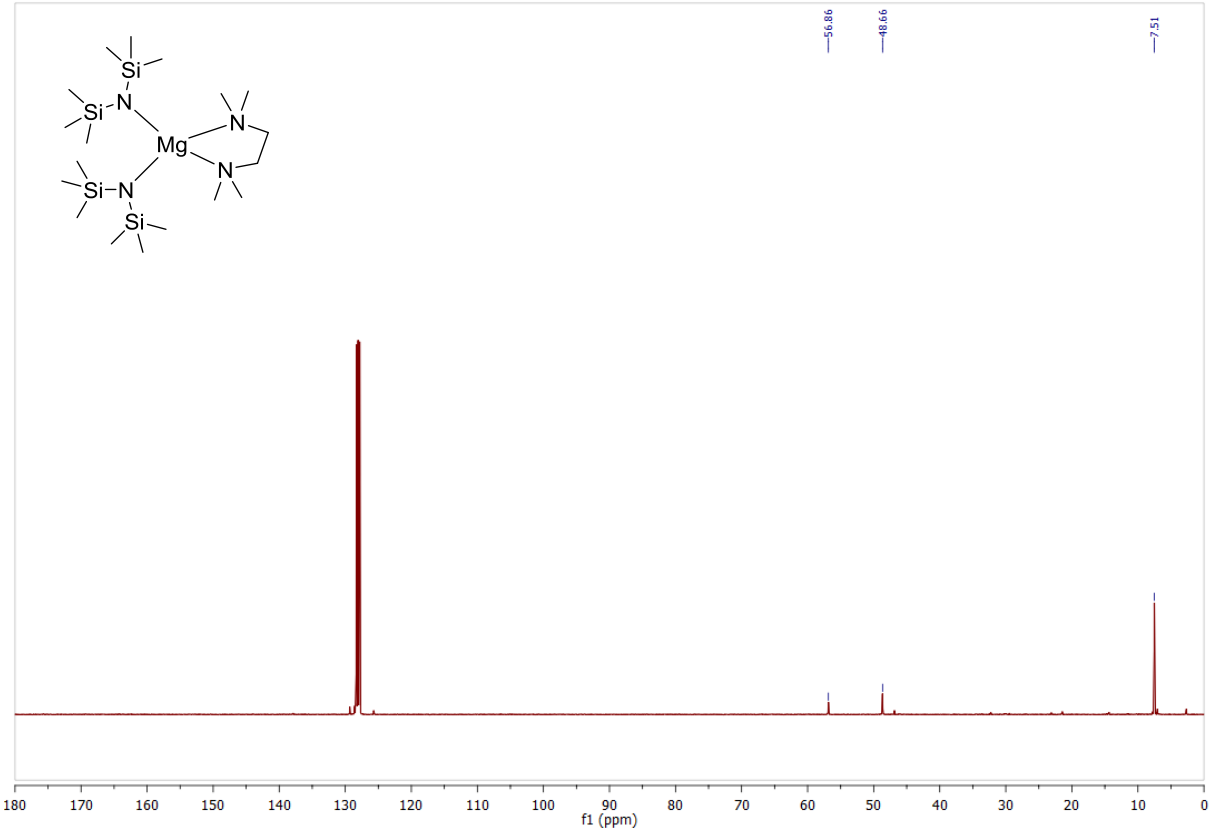

Figure S69: ^{13}C{^{1}H} NMR spectrum (101 MHz, C_6D_6, 296 K) of [(tmeda)Mg(hmds)$_2$] **6a**.

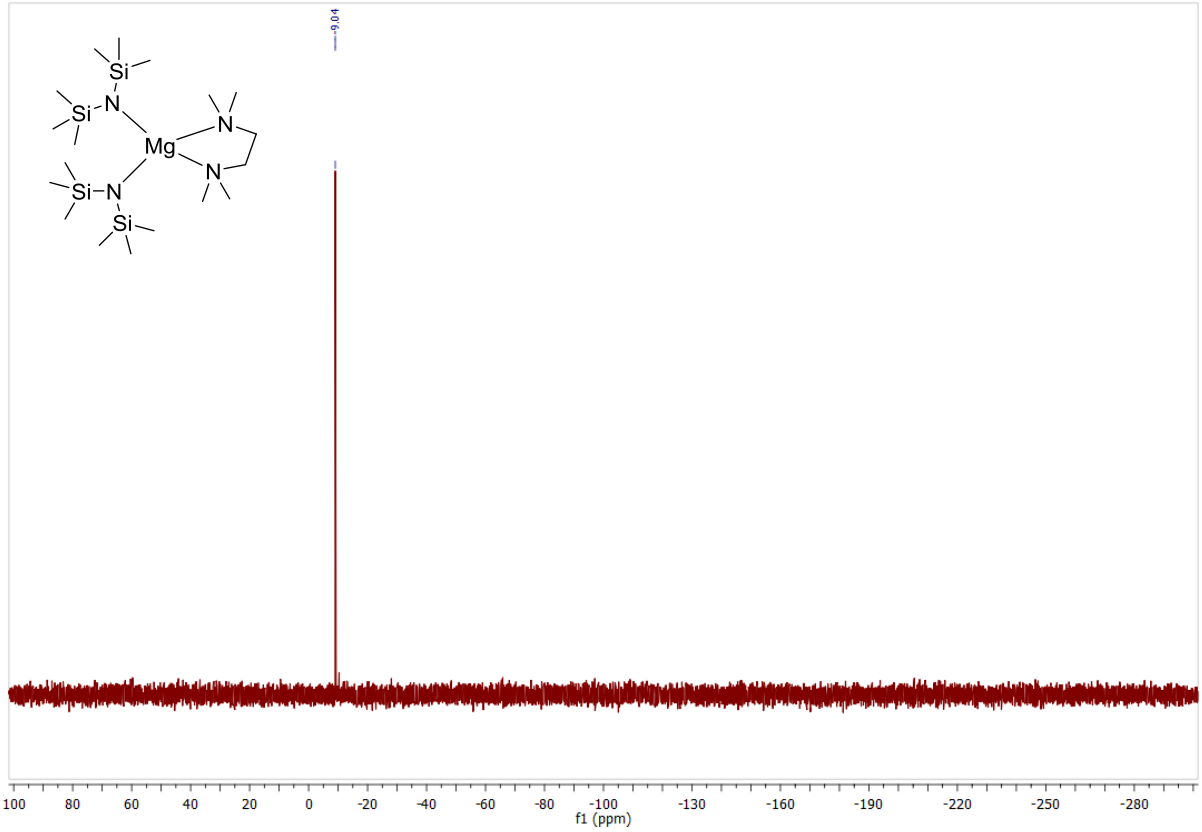

Figure S70: $^{29}Si\{^{1}H\}$ NMR spectrum (79.5 MHz, C_6D_6, 296 K) of [(tmeda)Mg(hmds)$_2$] **6a**.

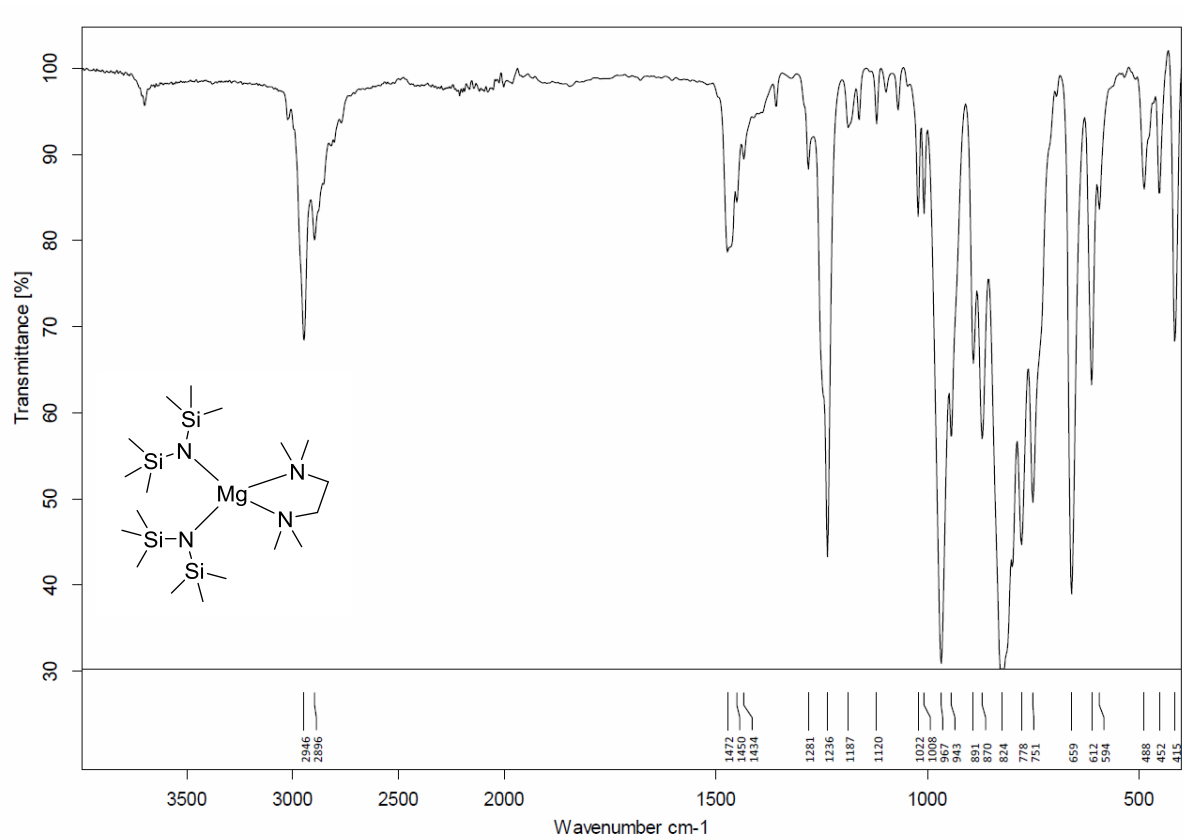

Figure S71: IR spectrum (ATR) of isolated crystals of [(tmeda)Mg(hmds)$_2$] **6a**.

[(dmmea)Ca(hmds)$_2$] **6b**

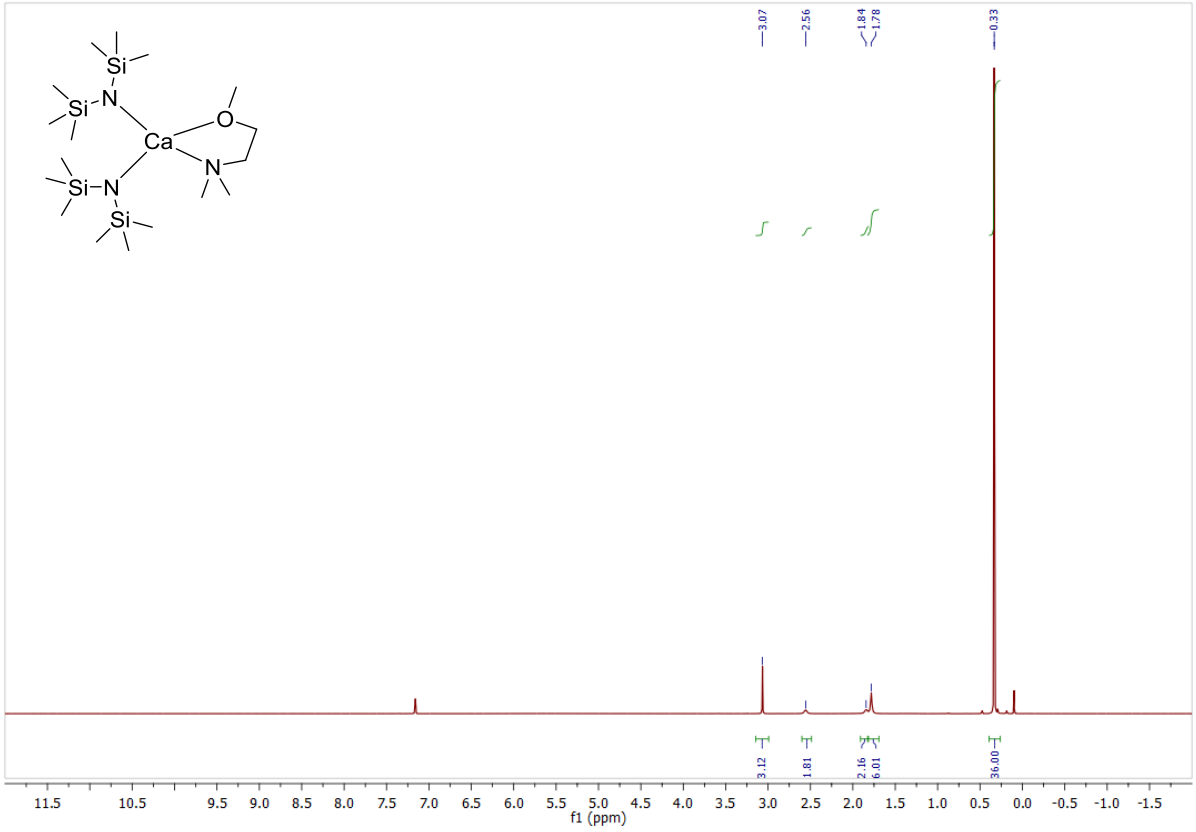

Figure S72: ^{1}H NMR spectrum (400 MHz, C_6D_6, 296 K) of [(dmmea)Ca(hmds)$_2$] **7b**.

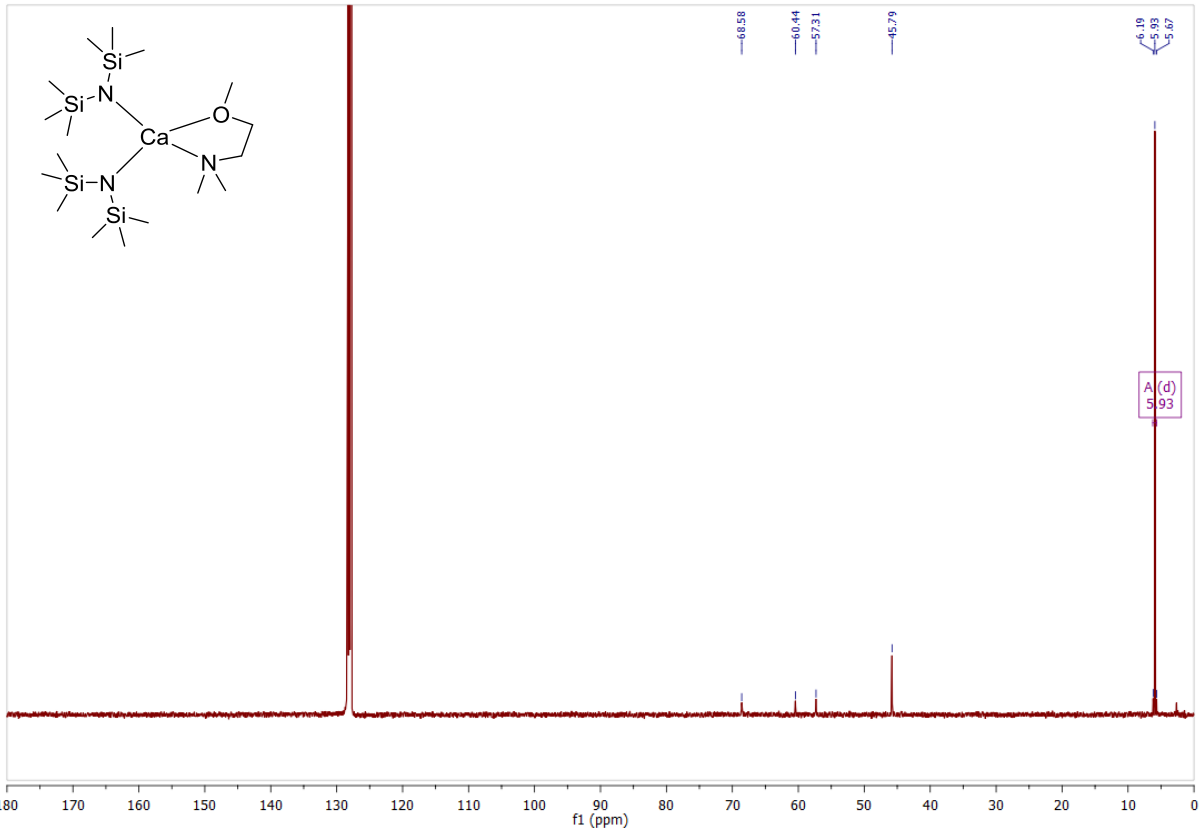

Figure S73: ^{13}C{^{1}H} NMR spectrum (101 MHz, C_6D_6, 296 K) of [(dmmea)Ca(hmds)$_2$] **7b**.

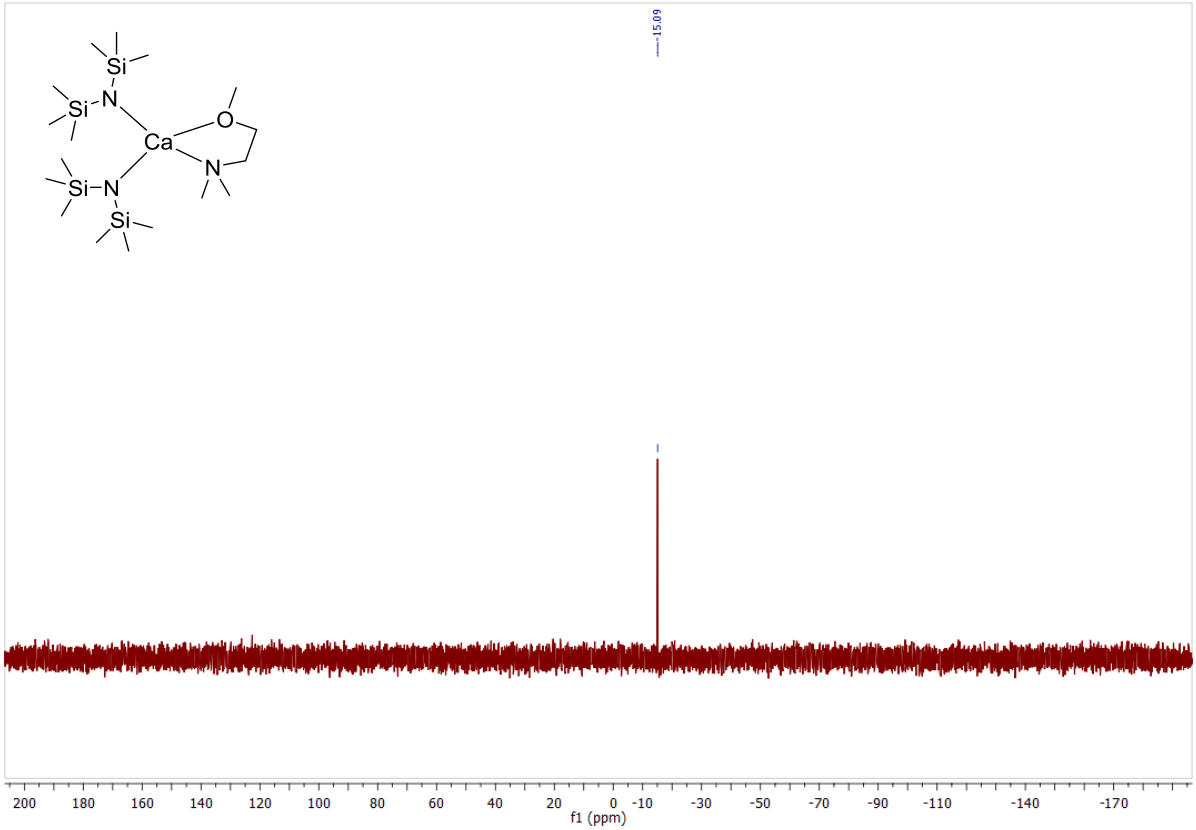

Figure S74: ^{29}Si-^{1}H-DEPT NMR spectrum (79 MHz, C_6D_6, 296 K) of [(dmmea)Ca(hmds)$_2$] **7b**.

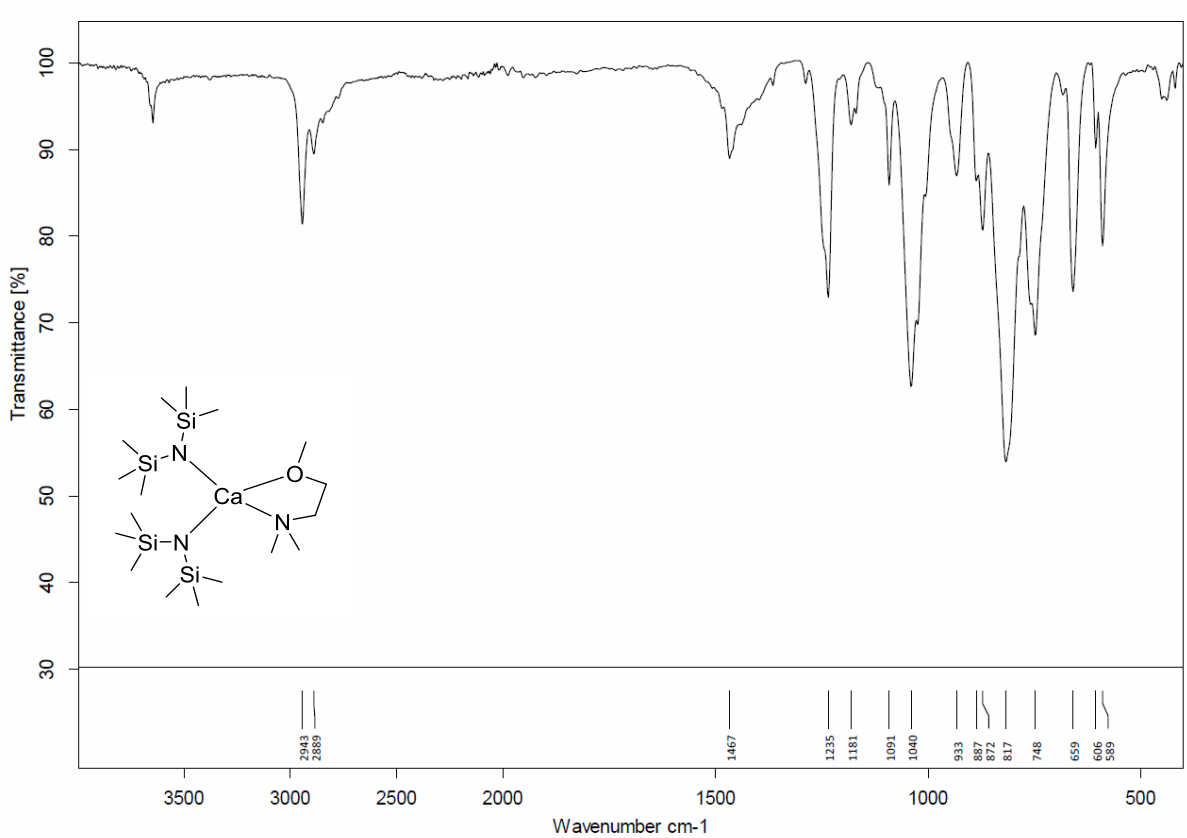

Figure S75: IR spectrum (ATR) of isolated crystals of [(dmmea)Ca(hmds)$_2$] **7b**.

[(tmeda)Sr(hmds)$_2$] **8a**

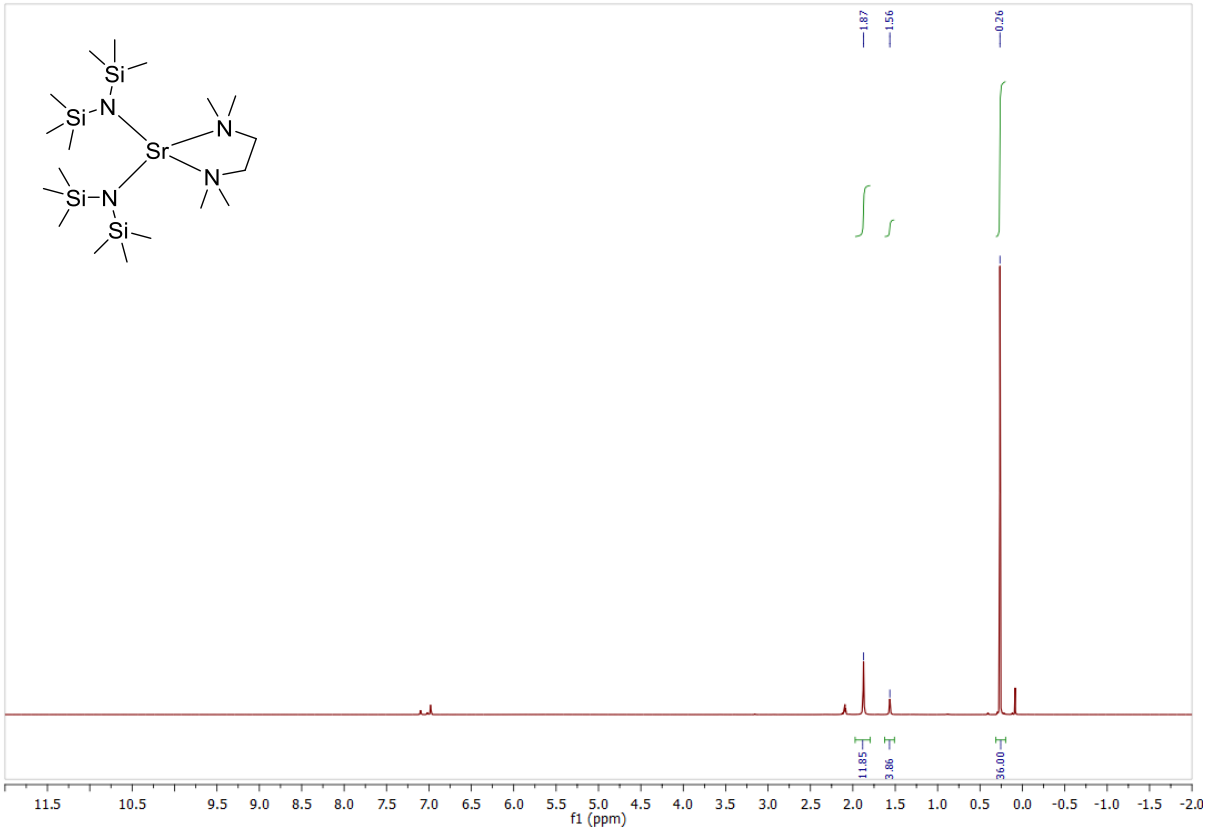

Figure S76: ^{1}H NMR spectrum (400 MHz, Tol-d$_8$, 296 K) of [(tmeda)Sr(hmds)$_2$] **8a**.

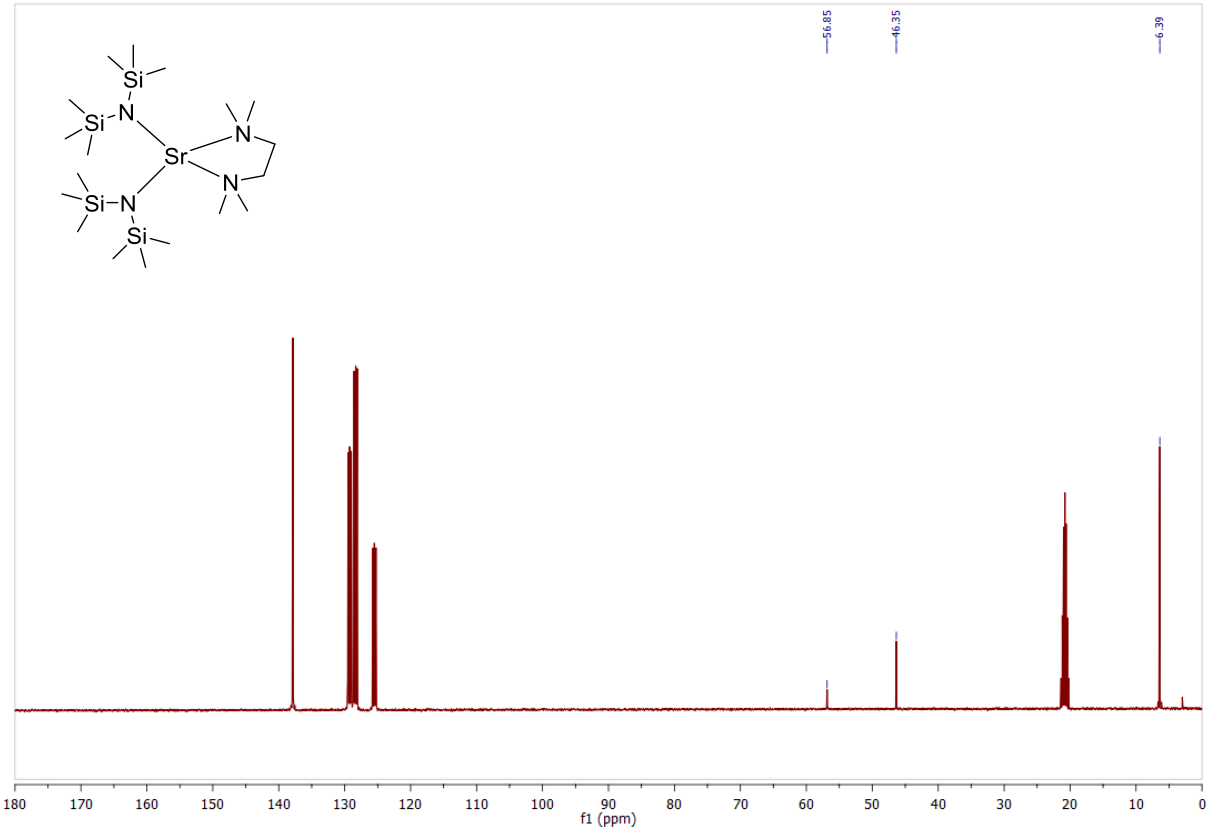

Figure S77: ^{13}C{^{1}H} NMR spectrum (101 MHz, Tol-d$_8$, 296 K) of [(tmeda)Sr(hmds)$_2$] **8a**.

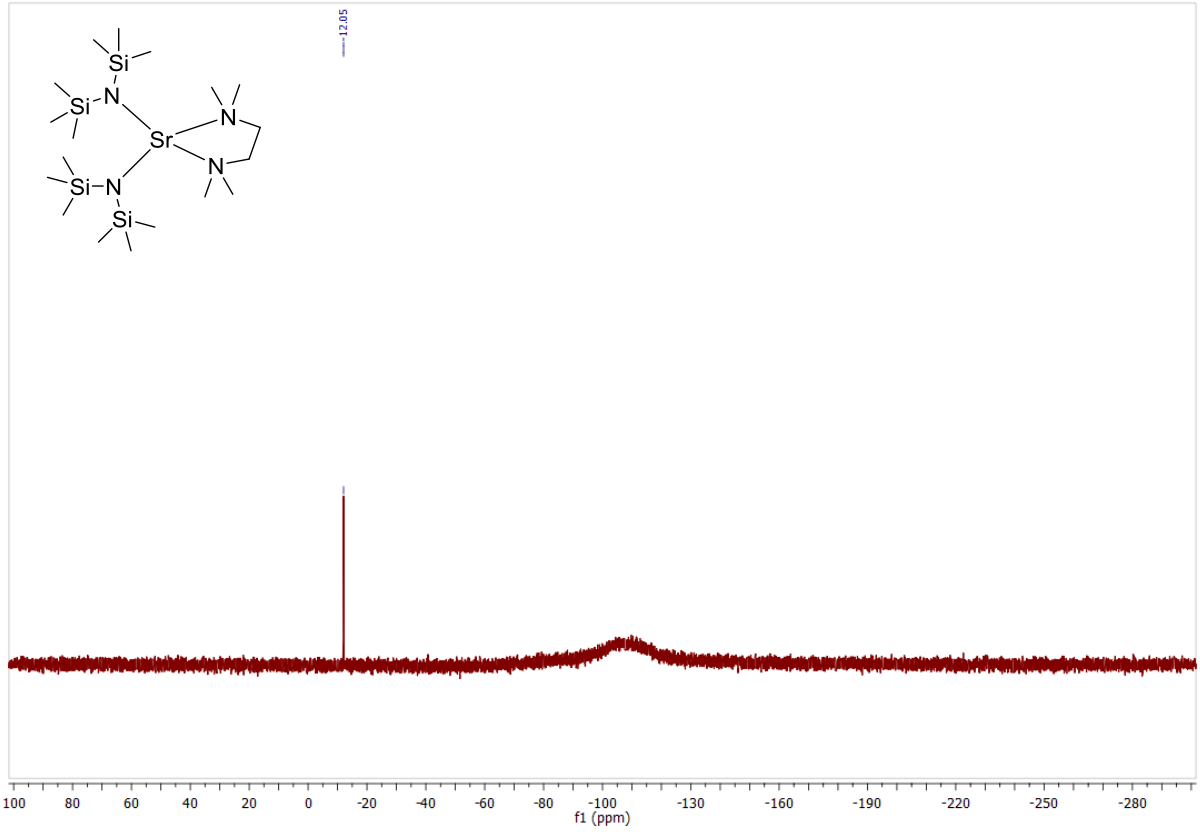

Figure S78: $^{29}Si\{^{1}H\}$ NMR spectrum (79.5 MHz, C_6D_6, 296 K) of [(tmeda)Sr(hmds)$_2$] **8a**.

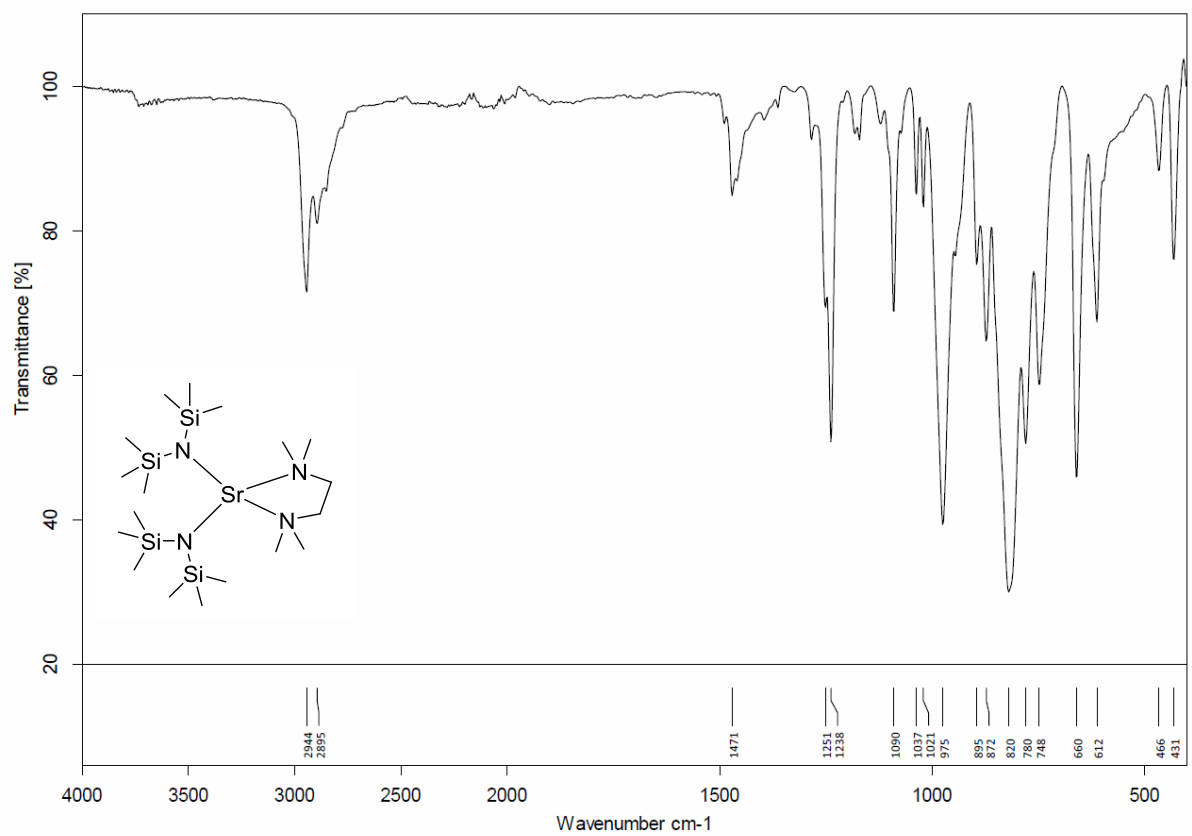

Figure S79: IR spectrum (ATR) of isolated crystals of [(tmeda)Sr(hmds)$_2$] **8a**.

[(dmmea)Sr(hmds)$_2$] **8b**

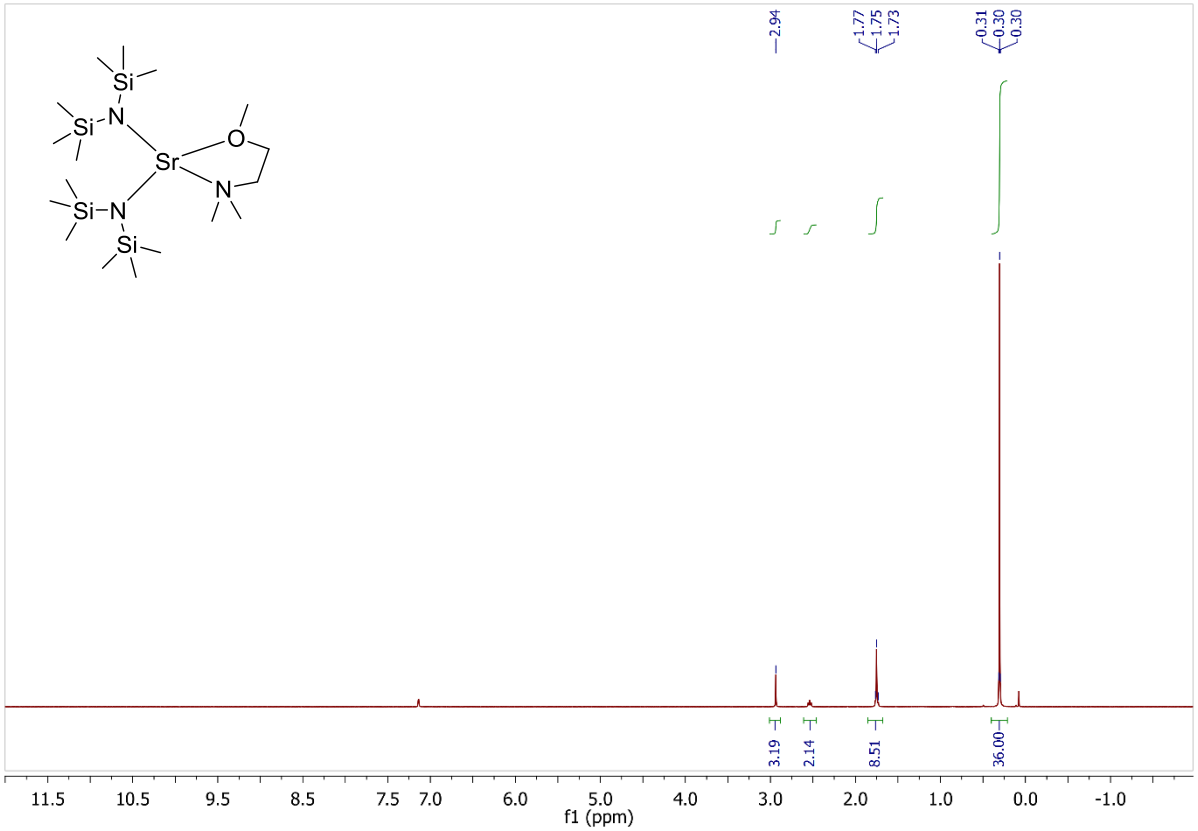

Figure S80: ^{1}H NMR spectrum (300 MHz, C_6D_6, 298 K) of [(dmmea)Sr(hmds)$_2$] **8b**.

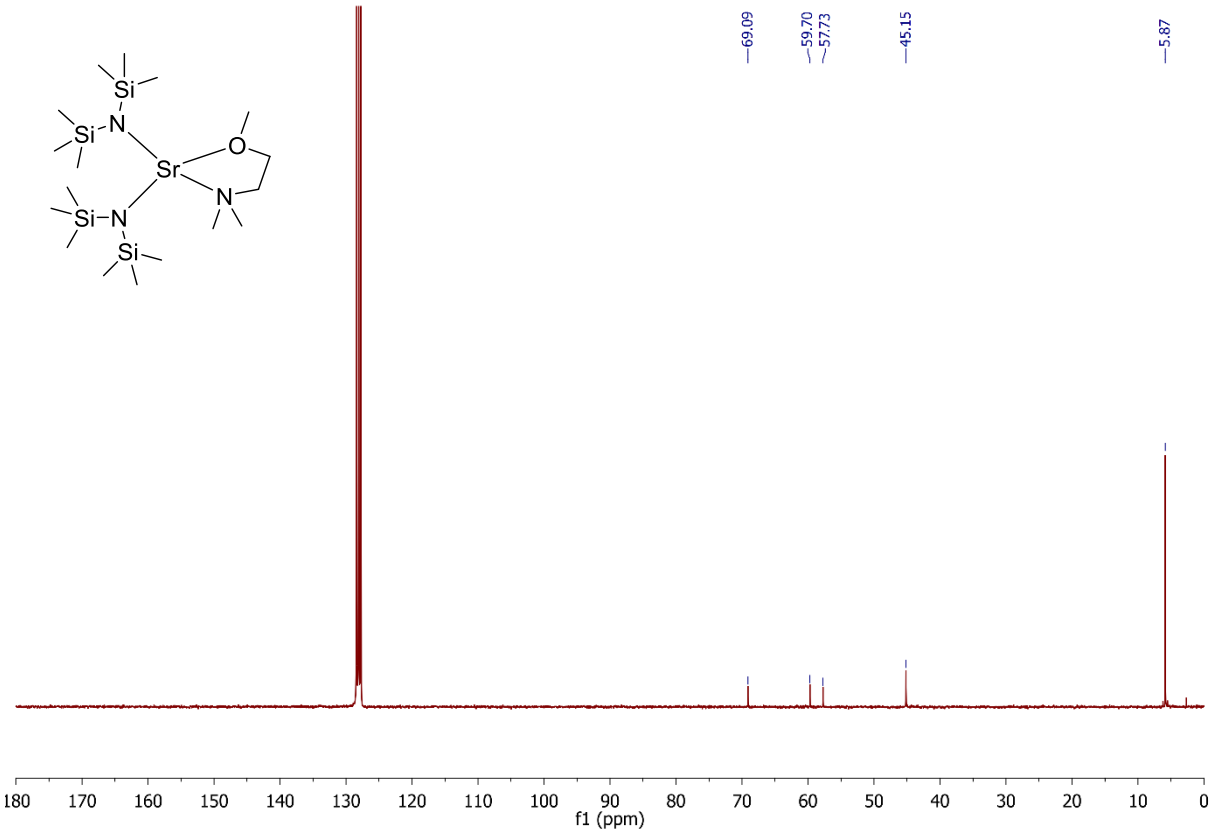

Figure S81: ^{13}C{^{1}H} NMR spectrum (75 MHz, C_6D_6, 298 K) of [(dmmea)Sr(hmds)$_2$] **8b**.

[(dmmea)Ba(hmds)$_2$] **9b**

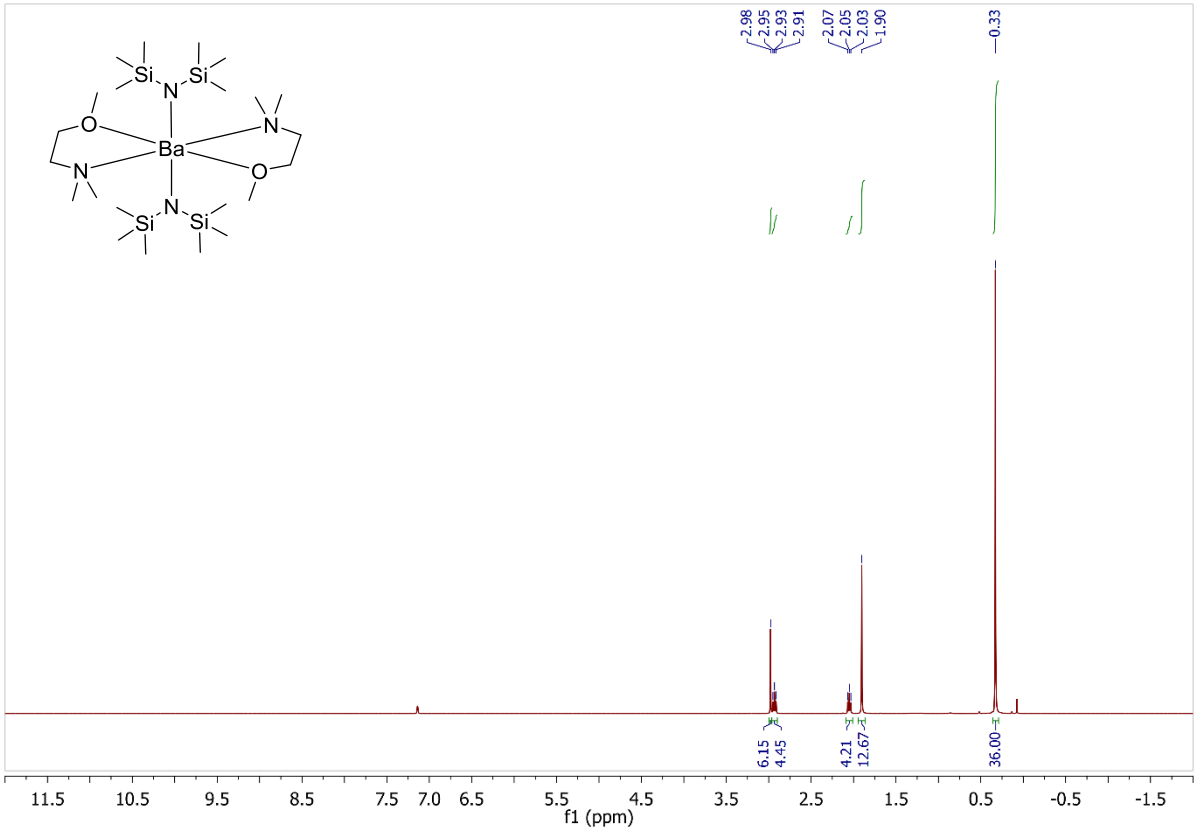

Figure S82: ^{1}H NMR spectrum (300 MHz, C_6D_6, 298 K) of [(dmmea)$_2$Ba(hmds)$_2$] **9b**.

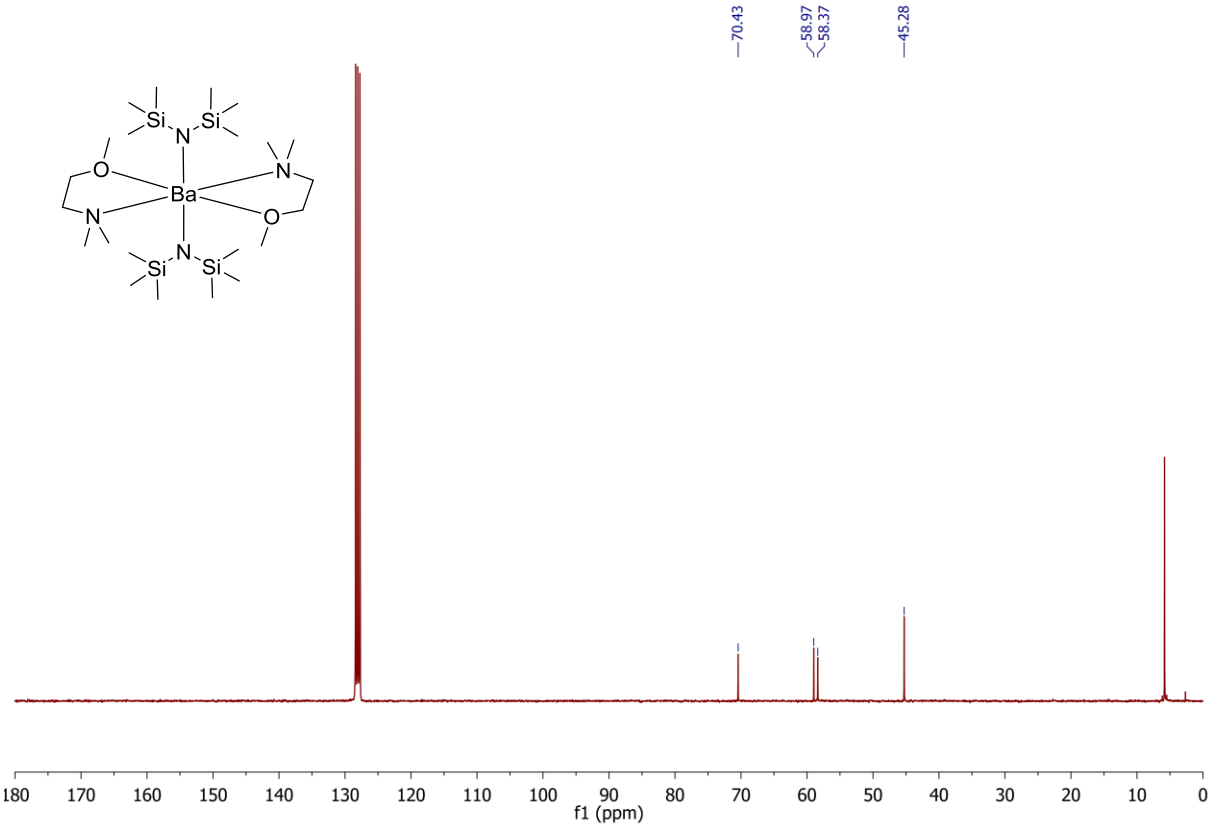

Figure S83: ^{13}C{^{1}H} NMR spectrum (75 MHz, C_6D_6, 298 K) of [(dmmea)$_2$Ba(hmds)$_2$] **9b**.